DETERIORATION OF RAILWAY TRACK DUE TO DYNAMIC VEHICLE LOADING AND SPATIALLY VARYING TRACK STIFFNESS

Robert Desmond FRÖHLING

A thesis submitted in partial fulfilment of
the requirements for the degree of

PHILOSOPHIAE DOCTOR (ENGINEERING)

in the

FACULTY OF ENGINEERING

UNIVERSITY OF PRETORIA, PRETORIA

October 1997

THESIS SUMMARY

DETERIORATION OF RAILWAY TRACK DUE TO DYNAMIC VEHICLE LOADING AND SPATIALLY VARYING TRACK STIFFNESS

Robert Desmond FRÖHLING

Supervisor:	Professor W Ebersöhn
Co-Supervisor:	Doctor H Scheffel
Department:	Civil Engineering
University:	University of Pretoria
Degree:	Philosophiae Doctor (Engineering)

In this thesis a Dynamic and a Static Track Deterioration Prediction Model are developed to predict track deterioration due to dynamic vehicle loading and nonlinear spatially varying track stiffness. The research also contributes to a better understanding of the relationship between spatially varying track stiffness and track deterioration.

Preceding the development of the Track Deterioration Prediction Models, experimental work was done to simultaneously measure the dynamic behaviour of a rail vehicle and the corresponding response of the track. On-track measurements were made as a function of vehicle speed, axle load, track condition, and accumulating traffic. In this process a new technique to measure the dynamic track stiffness was developed.

Track Deterioration Prediction Models were developed systematically to gain a better understanding of the relative influence of vehicle and track parameters. The

dynamic prediction model consists of two elements, an eleven degree-of-freedom dynamic vehicle/track model and a modified track settlement equation, while the static prediction model is based only on the modified settlement equation. The modified settlement equation is based on measurable parameters of the track super-structure, substructure layer properties, the spatial variation of the track stiffness, and the prevailing wheel loading. Using the dynamic interaction between the vehicle and the track, dynamic track loading and differential track settlement are predicted. After validating the model against test results, two applications of the model are given. In the first application void forming is predicted and in the second application the length of a tamping cycle is predicted.

Research presented in this thesis shows that the spatial variation of the track stiffness contributes significantly to track deterioration, both in terms of differential track settlement and increased dynamic vehicle loading. It is thus recommended that track maintenance procedures should be used to reduce the variation of the spatial track stiffness.

Keywords: Track deterioration, track stiffness, track settlement, prediction model, dynamic interaction.

SAMEVATTING VAN PROEFSKRIF

DETERIORATION OF RAILWAY TRACK
DUE TO DYNAMIC VEHICLE LOADING AND
SPATIALLY VARYING TRACK STIFFNESS

Robert Desmond FRÖHLING

Promotor:	Professor W Ebersöhn
Medepromotor:	Doctor H Scheffel
Departement:	Siviele Ingenieurswese
Universiteit:	Universiteit van Pretoria
Graad:	Philosophiae Doctor (Ingenieurswese)

In hierdie proefskrif is 'n Dinamiese en 'n Statiese Spoorbaanagteruitgang-voorspellingsmodel ontwikkel om spoorbaanagteruitgang te voorspel as gevolg van dinamiese voertuigbeladings en nie-liniêre afstandgebaseerde variasies in spoorbaanstyfheid. Die navorsing dra ook by tot 'n beter begrip van die verwandskap tussen afstandgebaseerde variasies in spoorbaanstyfhede en spoorbaanagteruitgang.

Voordat met die ontwikkeling van die spoorbaanagteruitgangvoorspellingsmodelle begin is, is eksperimentele werk gedoen om gelyktydig die dinamiese gedrag van die spoorvoertuig en die gepaardgaande reaksie van die spoorbaan te meet. Hierdie meetings is gedoen as 'n funksie van voertuigspoed, asbelasting, spoorbaantoestand, en toenemende verkeer. In dié proses is 'n nuwe tegniek ontwikkel om die dinamiese spoorbaanstyfheid te meet.

Na voltooiing van die toetse is die spoorbaanagteruitgangvoorspellingsmodelle ontwikkel. Die ontwikkeling is stapsgewys gedoen om 'n beter begrip van die relatiewe invloed van voertuig- en spoorbaanparameters te ondersoek. Die dinamiese voorspellingsmodel bestaan uit twee komponente, 'n elf vryheidsgraad dinamiese voertuig/spoorbaanmodel en 'n gemodifiseerde vergelyking vir spoorbaanversakking, terwyl die statiese model slegs van die gemodifiseerde vergelyking vir spoorbaanversakking gebruik maak. Die gemodifiseerde vergelyking vir spoorbaanversakking is gebaseer op meetbare parameters van die spoorbaanstruktuur, die eienskappe van die substruktuur, die afstandsgebaseerde variasie van die spoorbaanstyfheid, en die heersende wielbelasting. Deur gebruik te maak van die interaksie tussen die voertuig en die spoorbaan, word die dinamiese wielbelasting en die variërende spoorbaanversakking voorspel. Nadat die modelle geverifeer is teen toetsresultate, is twee toepassings van die model gegee. In die eerste toepassing word die vorming van 'n slapte in the spoorbaan voorspel en in die tweede toepassing word die lengte van 'n onderstopsiklus voorspel.

Die navorsing wat gedoen is toon aan dat die afstandgebaseerde variasie in die styfheid van die spoorbaan beslis bydra tot spoorbaanagteruitgang in terme van variërende spoorbaanversakking en toenemende dinamiese wielbelasting. Meer effektiewe spoorbaanonderhoud behoort dus die afstandsgebaseerde variasie van die spoorbaanstyfheid te verminder.

Sleutelwoorde: Spoorbaanagteruitgang, spoorbaanstyfheid, spoorbaanversakking, voorspellingsmodel, dinamiese interaksie.

ABSTRACT

Title:	Deterioration of railway track due to dynamic vehicle loading and spatially varying track stiffness
Author:	R D Fröhling
Supervisor:	Professor W Ebersöhn
Co-Supervisor:	Doctor H Scheffel
Department:	Civil Engineering
University:	University of Pretoria
Degree:	Philosophiae Doctor (Engineering)

In this thesis a Dynamic and a Static Track Deterioration Prediction Model are developed to predict track deterioration due to dynamic vehicle loading and nonlinear spatially varying track stiffness. The dynamic prediction model consists of an eleven degree-of-freedom dynamic vehicle/track model and a modified track settlement equation, while the static prediction model consists only of the modified track settlement equation.

Preceding the development of the Track Deterioration Prediction Models, experimental work was done to simultaneously measure the dynamic behaviour of a rail vehicle and the corresponding response of the track. On-track measurements were made as a function of vehicle speed, axle load, track condition, and accumulating traffic.

Research presented in this thesis shows that the spatial variation of the track stiffness contributes significantly to track deterioration, both in terms of differential track settlement and increased dynamic vehicle loading. It is thus recommended that track maintenance procedures should be used to reduce the variation of the spatial track stiffness.

ACKNOWLEDGEMENT

I wish to express my appreciation to the following organisations and persons who made this thesis possible:

- Professor W Ebersöhn, my supervisor, and Doctor H Scheffel, my co-supervisor for their guidance and support.
- The management of Spoornet, and in particular Mr H Tournay, for giving me the opportunity to do and complete the required research work.
- M Howard, C Kayser, H Maree, and M Tomas for their assistance during the extensive on-track tests.
- My wife Elke, and children Conrad and Claudia, for their continuous encouragement and support.

TABLE OF CONTENTS

iii

LIST OF FIGURES

LIST OF TABLES

LIST OF SYMBOLS

$B_{e'}$: Effective resolution bandwidth

b : Half distance between the secondary suspension on one bogie

b_{cc} : Half bogie centre distance

C : Ballast material constant

C_f : Foundation modulus

C_{slope} : Friction wedge stick slope

d_i : Difference between the elevation at the point of measurement and the mean filtered elevation

E : Young's modulus

F_{ff} : Wedge friction force

I : Rail moment of inertia about its horizontal axis

I_1 : Vehicle body moment of inertia in roll

I_2 : Bogie frame moment of inertia in roll

I_p : Vehicle body moment of inertia in pitch

I_w : Wheelset moment of inertia in roll

K_1 : Settlement constant

K_2 : Settlement constant

K_3 : Track stiffness correction factor

k : General vertical track stiffness

k_1 : Vertical stiffness of secondary suspension

k_2 : Effective linearised vertical track stiffness

k_{2i} : Calculated track stiffness at a particular sleeper

k_{2mi} : Measured track stiffness at a particular sleeper

k_{2BL} : Vertical track stiffness under the left wheel of the trailing wheelset

k_{2BR} : Vertical track stiffness under the right wheel of the trailing wheelset

k_{2FL} : Vertical track stiffness under the left wheel of the leading wheelset

k_{2FR}	:	Vertical track stiffness under the right wheel of the leading wheelset
k_p	:	Vertical stiffness of primary suspension
k_{ss}	:	Stiffness of one stabiliser spring
L_c	:	Characteristic length
l	:	Half distance between the wheel and rail contact points
m_1	:	Mass of vehicle body
m_2	:	Mass of wheel or bogie frame
m_w	:	Mass of wheelset
N	:	Number of load cycles
n	:	Number of measurement in the length of the track under consideration
n_p	:	Ballast porosity
P	:	Concentrated force applied to the rail
P_{dyn}	:	Prevailing dynamic vertical wheel load
P_{ref}	:	Static reference vertical wheel load
P_s	:	Static wheel load
q	:	Vertical force in rail foundation per unit length
R	:	Track roughness
T	:	Total measuring time
u	:	Track modulus
V	:	Vehicle speed
x	:	Distance in direction of vehicle travel
x_{ss}	:	Static deflection of the stabiliser spring from its free height
y	:	Local deflection of the track support
y_0	:	Vertical track profile variation
y_1	:	Vertical displacement of vehicle body
y_2	:	Vertical displacement of wheel or wheelset
y_B	:	Vertical displacement of trailing bogie frame
y_F	:	Vertical displacement of leading bogie frame
y_s	:	Static track deflection
y_{BL}	:	Vertical track profile variation under the left wheel of the trailing wheelset

y_{BR}	:	Vertical track profile variation under the right wheel of the trailing wheelset
y_{FL}	:	Vertical track profile variation under the left wheel of the leading wheelset
y_{FR}	:	Vertical track profile variation under the right wheel of the leading wheelset
z_B	:	Vertical displacement of trailing wheelsets
z_F	:	Vertical displacement of leading wheelsets
ΔP	:	Dynamic wheel load component
α	:	Pitching angle of vehicle body
α_w	:	Angle of friction wedge
δ	:	Ratio of dynamic wheel load component to static wheel load
ϵ_N	:	Permanent axial strain in ballast after N cycles
ϵ_1	:	Permanent axial strain in ballast caused by the first load cycle
ϵ_r	:	Normalized standard error
θ	:	Rolling angle of vehicle body
μ	:	Coefficient of friction
ρ_1	:	Vertical damping of secondary suspension
ρ_{1BL}	:	Vertical damping of the secondary suspension on the left side of the trailing bogie
ρ_{1BR}	:	Vertical damping of the secondary suspension on the right side of the trailing bogie
ρ_{1FL}	:	Vertical damping of the secondary suspension on the left side of the leading bogie
ρ_{1FR}	:	Vertical damping of the secondary suspension on the right side of the leading bogie
ρ_2	:	Vertical track damping
ρ_P	:	Vertical damping of primary suspension
σ	:	Local compressive stress on the track support
σ_1	:	Major principle stress
σ_3	:	Minor principle stress

ϕ_B : Rolling angle of trailing bogie frame

ϕ_F : Rolling angle of leading bogie frame

ω_B : Rolling angle of trailing wheelsets

ω_F : Rolling angle of leading wheelsets

CHAPTER 1

INTRODUCTION

In the quest to survive in a competitive transport market railway organisations have to, amongst others, minimise maintenance expenditure while still maintaining the track and the vehicle in a functionally acceptable condition. To become more efficient in maintaining track, the maintenance approach has changed with time. Initially subjective track inspections were used to assess the condition of the track. This approach was replaced by more objective measurements, evolving into the philosophy of "what gets measured gets managed". By correlating the deterioration of track geometry with accumulating traffic, researchers have produced empirical models for predicting the need for track maintenance so that planning can be done well in advance. But to support these empirical models, further insights are required into the physical processes by which vehicle/track interaction can cause track geometry to deteriorate. For this reason a lot of research is presently being conducted to develop experimentally verified mathematical models that can predict track deterioration under changing circumstances such as axle load, vehicle speed and track structure variations and degradation.

Although there was an early interest to model the dynamic loading and the subsequent deterioration of the track in order to solve practical problems, only a few papers in this respect were published before 1980. Since then the situation has changed largely due to the availability of modern computers. Some of the relevant research on problems due to vehicle/track interaction, modelling of the vehicle/track system, and track settlement in general is given in Appendix A.

Following recent research (Ebersöhn and Selig, 1994), indications are that track maintenance is amongst others a function of the track support characteristics. It was found that due to the varying condition of the track support, track settlement is not uniform and the resultant differential settlement causes a loss of track geometry requiring costly regular maintenance to return the track to the required smoothness. Hence certain maintenance operations are required to minimise or at least contain induced dynamic load variations on the track. These findings have raised the question as to what is the influence of the nonlinear and spatially varying track stiffness on the dynamic loading between the wheel and the track and the subsequent differential track settlement.

1.1 OBJECTIVE

The objective of this thesis is to develop a validated mathematical model to predict track deterioration due to dynamic vehicle loading and nonlinear spatially varying track stiffness, and to contribute to a better understanding of the relationship between spatially varying track stiffness and track deterioration.

In this thesis the influence of the vertical surface profile of the track, the nonlinear and spatially varying vertical track stiffness, vehicle speed and axle load on the vertical dynamic response of the vehicle/track system and subsequent deterioration of the vertical space curve of the track due to differential track settlement, is investigated. Both on-track measurements and mathematical simulations are used to analyse the current and to predict the future performance of the vehicle/track system.

1.2 SCOPE

The scope of this thesis is given in the following brief outline of the contents of the remaining chapters. The main part of the document describes the development, validation and application of the Track Deterioration Prediction Model (TDPM),

while a number of appendixes give additional information relevant to the research that was conducted.

In Chapter 2, a review is given with respect to literature closely related to the present work. The literature review thus deals with the topic of modelling the influence of spatial track stiffness variations on track deterioration. A further literature review covering problems related to vehicle/track interaction, vehicle/track interaction models, and research with respect to track settlement is given in Appendix A.

The experimental work that was done to support the development of the validated Track Deterioration Prediction Model is summarised in Chapter 3. A comprehensive description of the rolling stock used, the infrastructure at the test site, the instrumentation, and a representative part of the results is, given in Appendix B. Attention is also given to the measured influence of axle load, vehicle speed, and accumulating traffic on the performance of the vehicle/track system.

Chapters 4, 5 and 6 deal with the development of the Dynamic and the Static Track Deterioration Prediction Model. In Chapter 4, the basic methodology of predicting track settlement and the development of a modified track settlement equation is described. Chapter 5 presents the development of the mathematical model of the vehicle/track system. In this chapter a chronological overview of the development of the model is given together with a discussion of relevant assumptions. In Chapter 6 the Dynamic Track Deterioration Prediction Model (DTDPM) and the Static Track Deterioration Prediction Model (STDPM) are presented. The Dynamic Track Deterioration Prediction Model makes use of the vertical space curve of the track, the spatial variation of the track stiffness, and engineering parameters of the rail vehicle to be used. The Static Track Deterioration Prediction Model on the other hand only requires information about the spatial variation of the track stiffness and the nominal wheel load.

In Chapter 7, the developed models are verified against experimental results and a discussion about the assumptions and simplifications that were made in the development of the models is given. Chapter 8 deals with the prediction and evaluation of track deterioration. After listing track evaluation criteria as used by Spoornet, two applications of the developed models are given. In the first application void forming is simulated and in the second application a tamping cycle is predicted. Finally a conclusion, together with references to further recommended research and development work, is given in Chapter 9.

CHAPTER 2

LITERATURE REVIEW

This chapter gives a review of literature concerned with the present subject under investigation. A more comprehensive literature review on topics related to the interaction between the vehicle and the track, various approaches to vehicle/track system modelling, and research with respect to track settlement is given in Appendix A.

Although nonlinear and spatially varying track stiffness was measured as early as 1918 (Talbot, 1980), only a few researchers have attempted to model its effect on track deterioration. In 1982, Lane started to study the effect of ballast stiffness variations on track roughness. Lane showed that "static effects" caused by the variability in the ballast and the sub-grade properties make a significant contribution to the development of track roughness. The research work also showed that if larger freight cars are used to reduce unit costs, considerable benefit can be realised if the specification of the ballast is tightened to reduce its variability.

Realising the possible consequences of spatial track stiffness variations, Shenton (1985) used the computer programs developed by British Rail (Lane, 1982) to simulate the deterioration of a section of track. The dynamic wheel loads were calculated, and from the maximum load seen by a particular sleeper its settlement was in turn calculated, taking into account the variation in the track stiffness. The resulting deteriorated shape of the track was then used to re-calculate new dynamic loads and by repetitive cycling of this procedure track deterioration was simulated. Shenton observed that it is the top ballast layer which is subjected to the highest

stress and it is also this particular layer which is constantly disturbed by track maintenance and traffic. Furthermore, Shenton observed that the rate of track deterioration decreases with accumulating traffic or time. This stable condition is reached once the loads have been re-distributed among the sleepers. Shenton claimed that after this re-distribution the settlement of all sleepers is uniform.

A few years later, simulation runs with inhomogeneous track beds were carried out by Schwab and Mauer (1989) to gather more insight into the settlement behaviour at points where the track stiffness varied. Two sections of different track stiffness but equal damping were used in their investigations. In the model, the wheel/rail forces were distributed through the rails and sleepers, resulting in sleeper/ballast forces to be lower in the region of lower track stiffness. This indicated a better distribution of the vehicle forces to track in a softer region. As a result, higher track settlement was predicted in the stiffer region where the vehicle forces are poorly distributed and higher sleeper/ballast forces occur. It should be noted that Schwab and Mauer predicted track settlement using an identical settlement rate in the two different stiffness regions.

In a workshop devoted to "Interaction of Railway Vehicles with the Track and its Substructure" (Knothe *et al.*, 1995) three papers concerned with the influence of spatial track stiffness variations were presented (Li and Selig, 1995; Sato, 1995; Ford, 1995). In the paper presented by Li and Selig (1995), two mathematical models are discussed. The more comprehensive model is a finite element model which is used to determine the vertical dynamic deflection and acceleration of the rail and the sleepers as a function of spatial track stiffness variations. The other model is a simplified lumped-parameter model in which conversion equations are used to determine values for the lumped-mass and the lumped-stiffness of the vehicle/track system. In these equations the spatial track stiffness variations are represented by a single factor. Using these models the authors predicted track settlement using an equivalent number of maximum wheel loads. The work done by Li and Selig showed that the factor most affecting the track modulus is the

characteristic of the subgrade, including both the resilient modulus and the thickness of the subgrade layer. They stated that the influence of the subgrade condition on track modulus is further enhanced by the fact that the subgrade resilient modulus is the most variable quantity among all the track parameters. The next most important factor effecting the track modulus is the thickness of the granular layer which consists out of a ballast and a sub-ballast layer.

The paper by Sato (1995) described Japanese studies with respect to the settlement of ballast and the growth of track irregularities. An average growth of track irregularities was defined.

Ford (1995) describes research done to evaluate the influence of differential ballast settlement on the growth of track irregularities. Assuming an initially continuous sinusoidal perturbation in the vertical profile of the track, and assuming that the vertical response of the vehicle is in phase with the wave in the track, the deterioration of the track geometry was investigated in terms of changes in vehicle load and ballast parameters. Although the model is essentially qualitative, it offers a greater understanding of the physical phenomena underlying the way that vehicle/track interaction contributes to the deterioration of track geometry.

Recent research work done by Hunt (1996) on track settlement adjacent to bridge abutments shows that settlement near an abutment can be controlled to some extent by a careful selection of the subgrade stiffness profile. Considering the variation of subgrade stiffness between the ballast and the abutment, numerical computations were carried out in the time domain using linear track and vehicle models. A logarithmic deformation law was used to adjust the track geometry with accumulating traffic.

Summary

The literature review shows that although several attempts have been made to model the effect of nonlinear and spatially varying track stiffness on track

deterioration there are always limitations. However, having realised the possible consequences of spatial track stiffness variations on track deterioration, the research work done to date has already contributed significantly towards understanding the qualitative influence of various vehicle and track parameters. Research in this field is still ongoing.

CHAPTER 3

ON-TRACK TESTING

In this chapter, the on-track tests that were conducted to simultaneously measure the behaviour of the vehicle and the track are described in terms of measurements taken and the test methodology. The purpose of the on-track tests was:

- To gain an improved understanding of the dynamic interaction between the vehicle and the track, and the degradation of the track, as a function of vehicle speed, axle load, track condition and accumulating traffic.
- To validate the Track Deterioration Prediction Models in terms of the predicted dynamic behaviour and the predicted differential track settlement.
- To have measured track geometry and track stiffness values available to be used as excitation input in the Track Deterioration Prediction Models to be developed.

The tests were conducted on the Heavy Haul Coal Export Line in South Africa. This line links the coal fields in the Witbank area with the export harbour in Richards Bay on the East coast of South Africa. Presently the line carries 60 million tons of coal per annum. The line was selected for this investigation due to its high annual tonnage and heavy, that is 26 ton per axle, load carrying capacity.

For the on-track tests a 150 sleeper long section of straight track with a uniform ballast layer thickness was selected. Figure 3.1 shows the middle thirteen sleepers of the test section which were instrumented to measure their dynamic behaviour as caused by passing vehicles.

To conduct controlled simultaneous measurements of vehicle and track behaviour a loaded CCL-5 gondola coal wagon, as shown in Figure 3.2, was selected as the test vehicle and placed in the test train. The CCL-5 wagon has a loaded mass of 104 tons and is the most common vehicle running on this particular line. Further detail on both the track and the vehicle is given in Appendix B.
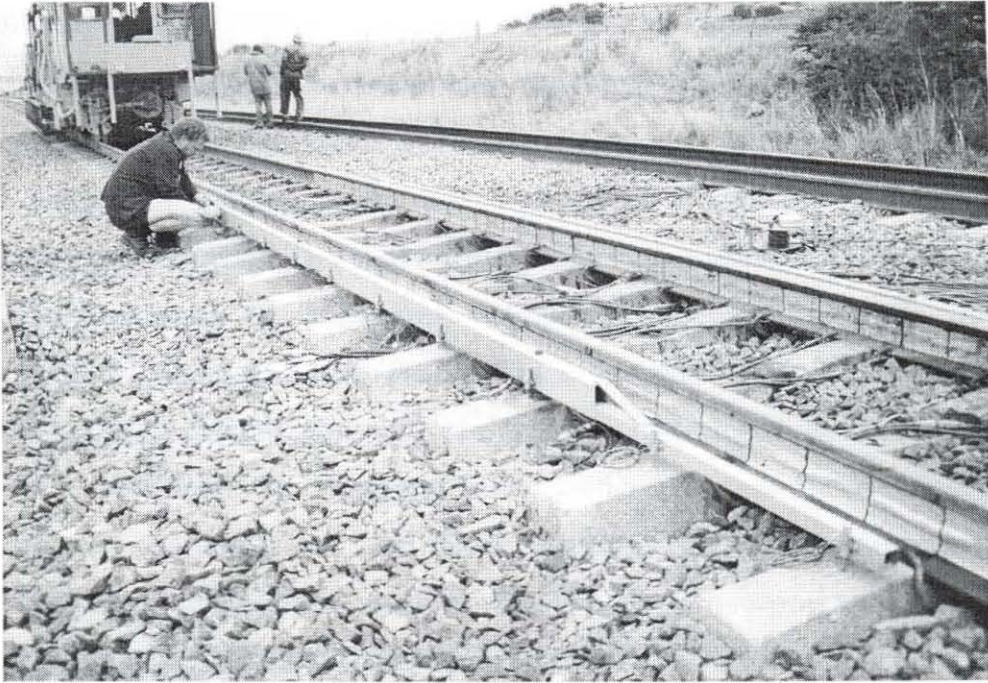
Figure 3.1: Instrumented test site.
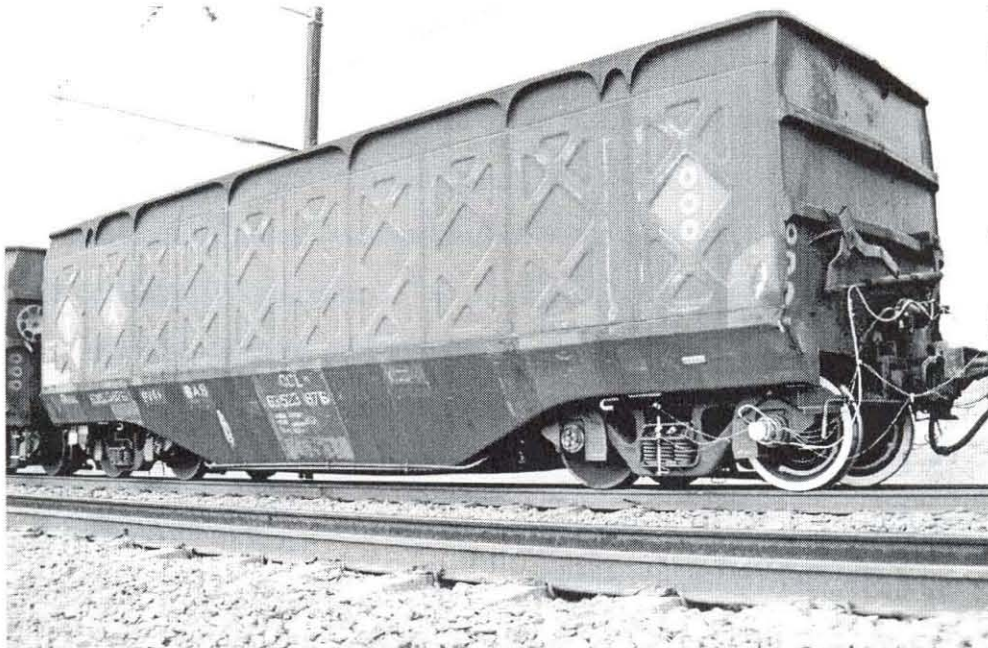
Figure 3.2: Instrumented CCL-5 gondola coal wagon.

3.1 MEASUREMENTS

In this section the general measurements that were taken during the tests are listed together with a short description of their specific purpose and the measurement method used. The measurements taken are:

- *Vertical space curve.* The vertical space curve of the track was measured at regular intervals to determine the unloaded track geometry as well as differential and overall track settlement with accumulating traffic. A digital level was used for this purpose.

- *Vertical track stiffness.* The spatial variation in the vertical track stiffness was measured using a track loading vehicle. These measurements were done repeatedly with accumulating traffic. The measured track stiffness was used as input to, and in the development of the Track Deterioration Prediction Model.

- *Dynamic wheel load.* The dynamic wheel load was measured to investigate the influence of vehicle speed and track condition on the dynamic interaction between the vehicle and the track. On the vehicle measurement were done using a load measuring wheelset in the leading position of the leading bogie of the test vehicle, and on the track by strain gauges on the rail between fourteen consecutive sleepers.

- *Sleeper reaction force.* The reaction force between the sleeper and the ballast was measured to determine the dynamic track stiffness as well as changes in sleeper support conditions due to vehicle speed, axle load and accumulating traffic. To measure this parameter, strain gauges were placed on the rail directly above thirteen consecutive sleepers.

- *Sleeper deflection.* The dynamic deflection of thirteen consecutive sleepers was measured relative to a reference frame anchored 3.15m below the rail. These measurements were essential in obtaining the dynamic track stiffness at each of the thirteen sleepers. Furthermore, changes in the sleeper deflection due to vehicle speed, axle load and accumulating traffic were also recorded.

- *Substructure layer deflection.* Using a Multi Depth Deflection Meter, the deflection of the various sub-structure layers was measured to establish

substructure layer properties with accumulating traffic.

- *Vehicle behaviour.* The dynamic behaviour of the test vehicle was measured in terms of the dynamic displacement across the secondary suspension of the leading bogie of the test vehicle. Again changes in the dynamic behaviour due to vehicle speed and changing track conditions were observed.

A more comprehensive description and discussion of the experimental work that was done as part of this research, is given in Appendix B. In Appendix B, the rolling stock used and the infrastructure at the test site is described in detail. Further detail on the instrumentation that was used on both the test vehicle and the test track is also given. Finally, Appendix B also presents and discusses some test results that show the measured influence of axle load, vehicle speed and accumulating traffic on the performance of the vehicle/track system.

3.2   METHODOLOGY

The following is a brief outline of the test methodology that was followed.

- After instrumenting the track and the vehicle, initial measurements were taken to assess whether meaningful results are obtained, and to establish correctness, consistency and repeatability of the readings.
- The next step was to tamp the selected section of track. This was done to be able to monitor track deterioration starting directly after track maintenance through tamping had been done. No dynamic track stabilisation was done.
- Immediately after tamping, the vertical space curve and the vertical stiffness of the track were measured and recorded.
- This was followed by conducting the first series of controlled tests. In these tests the test train which had several wagons with varying axle load passed over the test section at speeds varying between 10km/h and 70km/h while simultaneously measuring track and vehicle behaviour. Dynamic measurements included wheel loads, sleeper reaction forces, sleeper deflections, and vehicle suspension behaviour.

CHAPTER 4

TRACK SETTLEMENT MODELLING

Although it is known that track geometry generally deteriorates due to repetitive loading from passing traffic, the mechanism governing this phenomenon is rather complex. If every point of the track were to settle by the same amount, no irregularities in the vertical space curve would develop. However, these settlements are generally far from uniform due to variations in the track support and the wheel load distribution. These deviations cause differential track settlement due to plastic deformation of the support in the wavelengths experienced by rolling stock.

Various approaches to predict such track settlement are discussed in literature. The most common approach to predict track settlement is the use of the logarithmic track settlement law. Some research work however looks at simplified predictions using a statistical distribution of track properties or a so-called damage factor. More comprehensive approaches consider localised discrete irregularities or extended spatially distributed irregularities. A review in this respect is given in Appendix A. Although a large portion of the research reviewed, focuses on laboratory and field tests intended to determine the rate of track deterioration, very few authors have considered differential track settlement due to dynamic wheel loads and spatially varying nonlinear track stiffness. References in this respect have already been given in Chapter 2.

In this chapter a new approach to determine differential track settlement due to dynamic wheel loading and spatially varying track support conditions is formulated. The first section of this chapter outlines the basic assumptions that were made. The

second section describes the basic methodology used to predict track settlement and in the last section a validated Modified Settlement Algorithm is developed for later implementation into the Track Deterioration Prediction Model.

4.1 ASSUMPTIONS

As the objective of this research is to predict and analyse track settlement due to dynamic wheel loads and spatial track stiffness variations alone, numerous factors which could also influence track deterioration are not accounted for. The basic assumptions are:

- Only settlement in the ballast layer is considered. It is assumed that the sub-ballast and subgrade stays undisturbed and continues on its relatively low settlement trend, while the top ballast layer is loosened by tamping. The contribution of ballast settlement is thus more significant. This assumption would for example be invalid if the moisture content of the subgrade would change.
- The ballast layer thickness is constant over the test section.
- No ballast degradation is considered.
- Track settlement due to vibrations, transmitted by the track superstructure to the ballast, is not included in the settlement model. These vibrations are typically caused by rail joints, rail corrugations and wheel flats.
- Environmental changes due to the weather are not included.

4.2 PREDICTION OF TRACK SETTLEMENT

A schematic of the basic methodology to predict track settlement is shown in Figure 4.1. Figure 4.1 shows the various components and the feedback mechanism of the proposed interactive dynamic track settlement model. Using the initial vertical track profile, the spatial track stiffness variations and the static wheel load, the track definition module calculates the loaded vertical track profile and the effective linearised track stiffness under the given static wheel load. The initial loaded track

profile together with the spatial track stiffness variations are then used as input into the vertical vehicle/track model, where the vertical dynamic wheel/rail interaction forces are calculated. Together with the effective linearised track stiffness, the dynamic forces between the wheel and the rail are used as input into the track settlement model. The predicted track settlement is then added to the loaded track profile which is then used as a new excitation input into the vehicle/track model where a different dynamic reaction will result in different dynamic loads and subsequently a change in the differential settlement of the track.
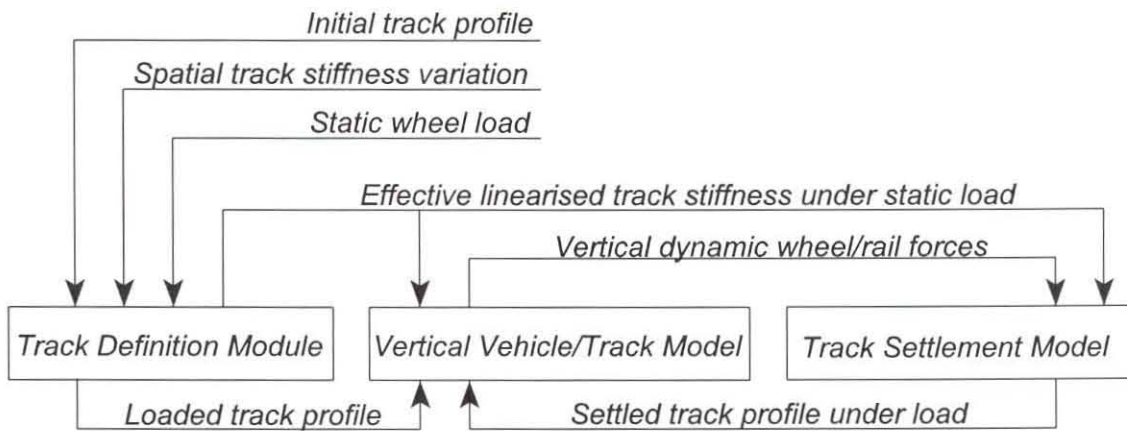
Figure 4.1: Interactive dynamic settlement methodology.

Before describing the development of the Modified Settlement Algorithm, some detail with respect to the mechanisms of track settlement is given. In principle, the methodology as developed by Stewart and Selig (1982) was used as the foundation on which to build the proposed interactive dynamic settlement model. The sequence to determine the permanent differential settlement of the ballast due to dynamic wheel loads and spatial track stiffness variations is given in Figure 4.2. The main components of the dynamic track settlement model are now discussed in detail.

Vertical dynamic wheel/rail forces

Effective linearised track stiffness
under static load

Stresses in ballast

Strain in ballast

Superposition of strains

Permanent deformation of ballast layer

Settled loaded track profile
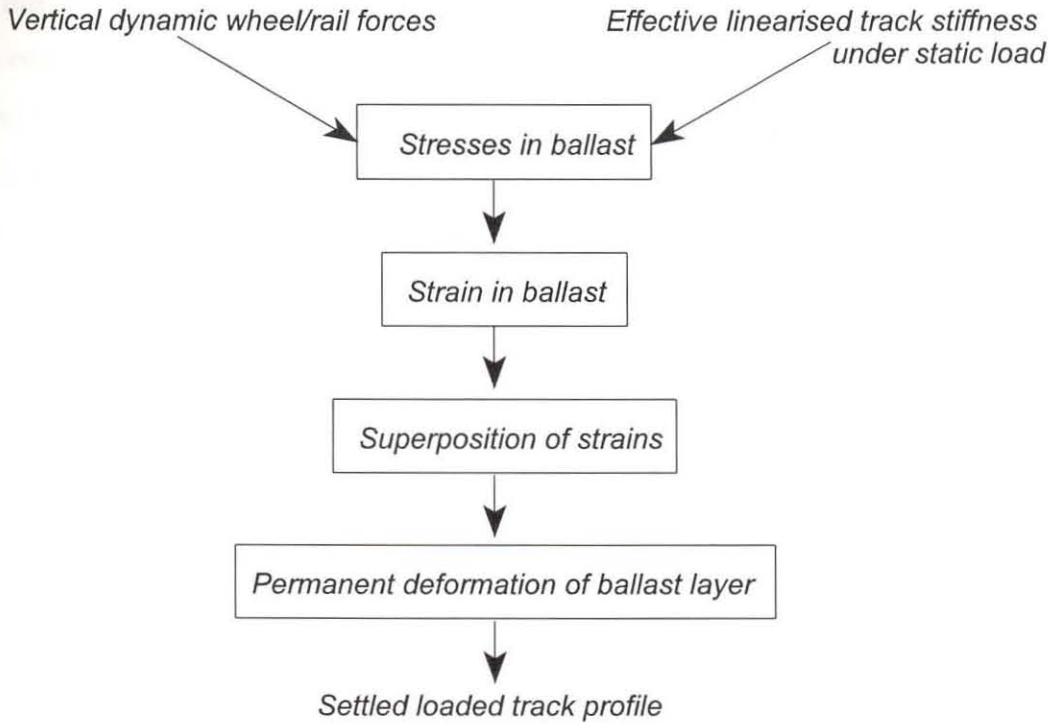
Figure 4.2: Dynamic track settlement model.

Stresses in the ballast. The methodology for predicting permanent track deformation starts by determining the stress state at the top of the ballast layer. These stresses comprise the initial vertical geostatic stresses that are due to the weights of the track superstructure and the soil, as well as the incremental stresses, that is those due to the imposed wheel loads. The incremental stresses are determined using the three-dimensional elastic multi-layer computer model GEOTRACK (Chang *et al.*, 1980) and are added to the initial geostatic stresses to determine the final three-dimensional stress state. These three-dimensional stresses are then converted into an equivalent triaxial stress state. The axial stress is defined by the difference between the major principle stress, σ_1, and the confining stress that is the minor principle stress, σ_3, in the loaded state, and is used to determine permanent track deformation under the instantaneous dynamic wheel load. The axial or vertical stress is also known as the principle stress difference, $(\sigma_1 - \sigma_3)$, or deviator stress.

The major principle stress and the minor principle stress of the loaded track are both computed using the GEOTRACK program. An extract out of a GEOTRACK output file is given in Appendix C. The slope of a measured axial stress-strain curve is defined as Young's modulus as long as the lateral stress is constant. One of the most versatile and useful laboratory tests for soil stress-strain and strength properties is the triaxial compression test (ORE Q C116 (Report 8), 1977).

Strain in the ballast. Once the stress in the ballast has been computed for the various dynamic wheel loads, the next step is to determine the permanent strains that would be expected to develop under the applied loads. This is generally done by using the following equation for permanent ballast strain as derived by British Rail from laboratory test results (ORE Q D71 (Report 10), 1970).

$$\epsilon_N = \epsilon_1(1 + C \log N) \tag{4.1}$$

In this equation ϵ_N is the permanent axial strain after N load cycles, ϵ_1 is the permanent strain caused by the first load cycle, and C is a material constant between 0.2 and 0.4 (Selig and Waters, 1994). Although based on a limited number of tests, the following relationship between the deviator stress (given in terms of [kgf]), the porosity of the ballast n_p and the deformation produced by the first load cycle ϵ_1, was proposed.

$$\epsilon_1 = 0.082(100 n_p - 38.2)(\sigma_1 - \sigma_3)^2 \tag{4.2}$$

Equation (4.2) can thus be used to relate the permanent axial strain to the ballast condition (porosity) and the number and magnitude of the applied axial load cycles. Typical values for porosity are between 0.4 and 0.5. For slag the porosity value is 0.34, for granite it is 0.26 and for limestone it is 0.40 (Stewart and Selig, 1982). The law governing the settlement of ballast is thus based on the assumption that the settlement of the track is proportional to the logarithm of the total tonnage moving over the section.

Superposition of strains. The cumulative strains due to a mix of wheel loads is based on a cumulative relationship similar to Miner's rule for structural fatigue analysis.

The procedure for superimposing strains to account for a mix of wheel loads at a particular sleeper is illustrated in Figure 4.3 for a two-load-level case. For each load level, the stresses in the ballast and the equivalent triaxial stress paths lead to different first cycle strains, ϵ_1. The higher load will cause a higher first cycle strain than the lower load. Knowing the respective first cycle strains and the material constant, C, the permanent strain, ϵ_N, that is expected to develop after N constant magnitude load cycles can be determined using Equation (4.1).
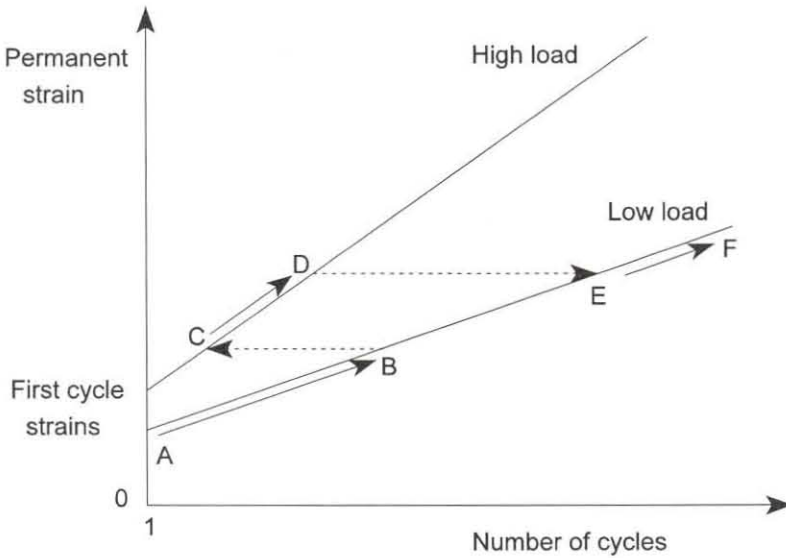
Figure 4.3: Ballast strain superposition for mixed loading.

The permanent strains due to the low load applications are determined by moving along the low load curve, Point A to Point B, in Figure 4.3 using the first cycle strain and the given number of low load cycles. Additional strains due to higher loads are calculated by first finding an "equivalent" number of cycles on the high load curve that would have caused the same strain as developed by the lower load. The equivalent number of high load cycles are found at Point C on the high load curve. The next step is to add the additional cycles at the higher load to these "equivalent" number of load cycles. The superimposed strain is then calculated by effectively following the high load curve, that is Point C to Point D. For subsequent lower

loading, a similar procedure is used to return to the low load deformation curve, that is Point D to Point E for the equivalent number of load cycles, and then Point E to Point F for the increase in strain after an additional number of low load cycles. Finally the calculated strain in the ballast layer is multiplied by the thickness of the ballast layer to get the actual permanent settlement of the ballast layer.

4.3 MODIFIED SETTLEMENT EQUATION

As part of the research a model for the complex relationship between vehicle and track parameters, the dynamic response of the vehicle, and the track settlement behaviour had to be found. It was soon realised that the basic settlement equation as given in Equation (4.1) did not give results that could be compared to the measured differential track settlement. The reason for this was that Equation (4.1) was developed from controlled laboratory results. A new approach thus had to be taken.

Finding a relationship between the dynamic wheel loads, the spatial variation of the track stiffness and the resulting differential track settlement was difficult. To determine whether the dynamic wheel load, or the spatial variation of the track stiffness was dominant, and by how much, or to determine whether an average stiffness, the seating stiffness or the contact stiffness should be used and how the measured track modulus of elasticity relates to stress in the track was a challenge. An example of the measured dynamic wheel load, track settlement, track geometry and track stiffness over the 150 sleeper test section is given in Figure 4.4. From Figure 4.4 it can be seen that there is no dominant relationship between the measured parameters. Filtering over a certain number of sleepers was also tried as a means to identify possible correlations between measured vehicle and track parameters.
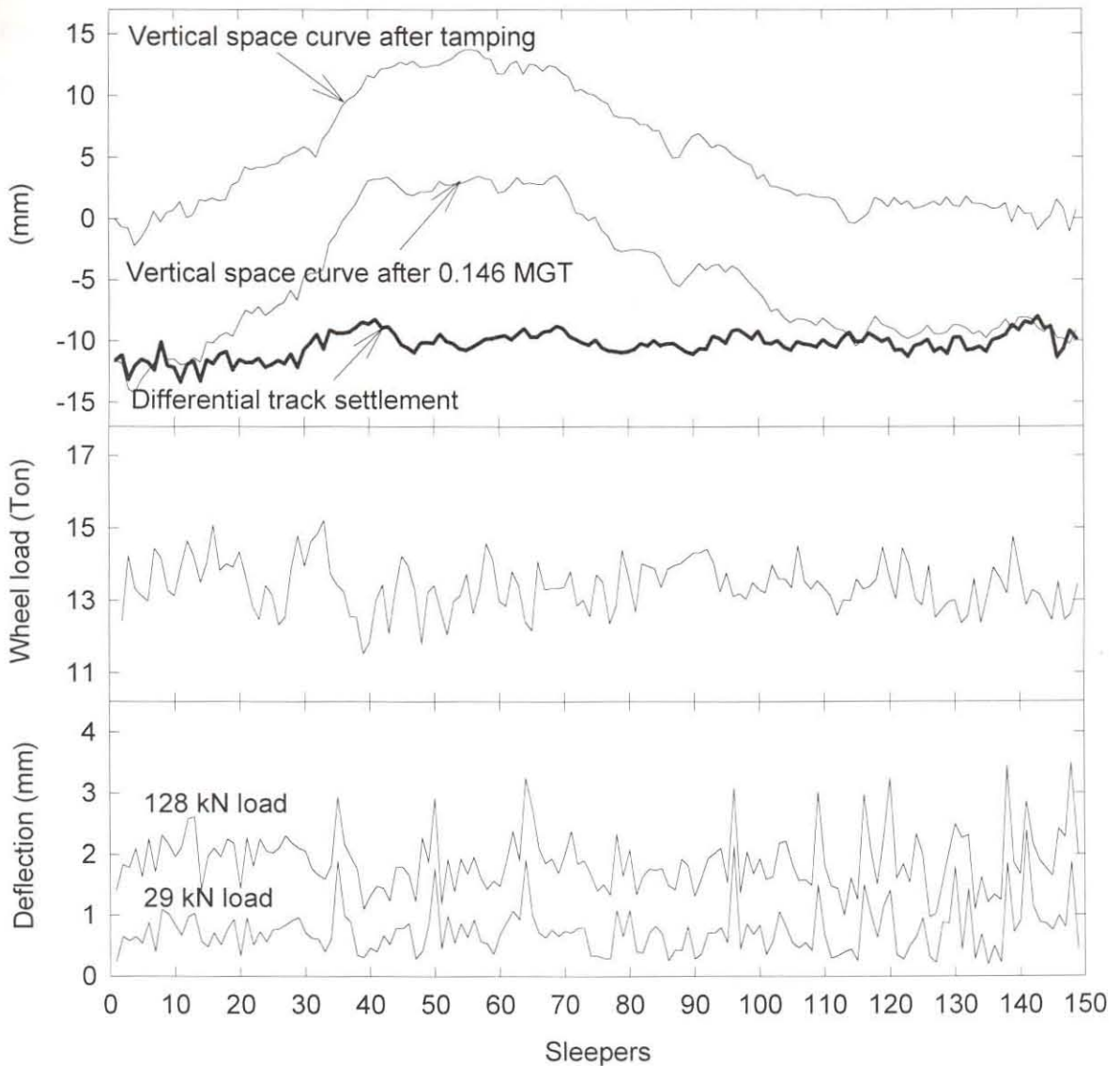
Figure 4.4: Measured vertical track space curve, differential track settlement, wheel load and track deflection.

Eventually it was realised that the differential settlement of the track is dominated by the spatial variation of the track stiffness and the modified settlement equation was developed. The remaining part of this section gives a chronological discussion of the development of the modified settlement equation. In principle the permanent deformation of the ballast is still modelled along the lines set out in the literature (Selig and Alva-Hurtado, 1982; Stewart and Selig, 1982; Fröhling *et al*, 1996a) and

as discussed in the previous section. Before outlining the development of the modified settlement equation, the assumptions and simplifications that were made are listed.

- As a method for continuously measuring the spatially varying dynamic track stiffness is not yet available, the discretely measured static track stiffness values were used.
- It was assumed that the track stiffness as measured after the rate of settlement had decreased significantly, is a representative signature of the spatially varying track stiffness.
- As structural damping can only be determined from dynamic track stiffness measurements, the track damping was assumed to be linear and constant over the entire test section.
- Although there is a mixture of freight traffic on the line, the dominant 26 ton axle loading was used in the development of the model.
- Although the modulus of elasticity of the various sub-structure layers was measured only at one particular sleeper, this set of values was used to estimate the permanent strain behaviour of the entire test section. It was thus assumed that the modulus of elasticity of the top layer, that is that of the ballast, changes as a function of the measured static track stiffness.
- An equivalent linear but spatially varying track stiffness was used in the program GEOTRACK (Chang et al, 1980; Li and Selig, 1995) to be able to calculate the deviator stress in the track structure for each individually measured track stiffness. The equivalent linear track stiffness is defined as the prevailing wheel load divided by the prevailing track deflection.
- Only loading in the vertical direction was considered and the actual dynamic wheel loads were represented by equivalent quasi-static loads in GEOTRACK.

Having defined the relevant assumptions, the development of the modified settlement equation is described in more detail. The first step in the development of the modified settlement equation was to take the statically measured spatially

varying nonlinear track stiffness and linearise it to obtain the effective linearised track stiffness under the dominant wheel load. The linearised track stiffness is defined as the static wheel load divided by the prevailing track deflection. As the track stiffness randomly varies at a particular sleeper with accumulating traffic, the track stiffness as measured after the rate of track settlement had reduced considerably, that is after 2.84 Million Gross Ton (MGT), was used. It was found that this spatially varying track stiffness gives a better prediction with respect to the differential track settlement than if the track stiffness as measured directly after tamping would be used.

To be able to use GEOTRACK to calculate the stress state in the track substructure, in particular the stress state in the ballast layer, the varying modulus of elasticity of the various substructure layers are required. These moduli can be determined using GEOTRACK, but the differential deflections of the substructure layers are required. As the measurement of the differential deflection in the substructure layers is a costly and time consuming exercise only two Multi Depth Deflection Meters (MDDs), that is one on either side of Sleeper 76, were placed in position. See Figure B18 in Appendix B. Hence, only the deflection values in the various substructure layers at this particular sleeper were available to be used in GEOTRACK. The method of how to obtain the modulus of elasticity for the substructure layers is described in more detail in Appendix B Section 2.4.1 and calculated values are given in Table B4.

The next step was to use the modulus of elasticity values as determined at Sleeper 76 as input into GEOTRACK and determine the effective linear track stiffness and deviator stress. The relevant GEOTRACK input and an extract out of a typical output file are given in Appendix C. During the computations with GEOTRACK, it was found that the calculated track stiffness was on average 1.34 times lower than the actually measured linearised track stiffness at this particular sleeper. Subsequently this factor was incorporated into the settlement equation to relate measured track stiffness to the calculated deviator stress in the ballast layer.

As the modulus of elasticity values were only available at Sleeper 76, the assumption was made that the change in the elasticity of the top ballast layer from sleeper to sleeper is directly proportional to the change in the equivalent linear track stiffness. Using this assumption, the modulus of elasticity of the top layer was varied until a whole set of track stiffness values were determined, effectively covering the whole spectrum of measured track stiffness values. The stiffness factor of 1.34 between measured and calculated track stiffness was taken into consideration.

The result was that the deviator stress could now be calculated with GEOTRACK as a function of track stiffness by using different modulus of elasticity values. The relationship between the deviator stress and the track stiffness is shown in Figure 4.5 for the left and right hand side of the track. The fact that there is a dropping off of the curve below a track stiffness of 60MN/m means that the stress and thus effectively the differential plastic strain in the ballast layer is such that there would be no significant differential settlement at these low stiffness values. Hence, this part of the curve was ignored and a straight line was fitted through the data. It is assumed that this behaviour is due to the fact that actual changes in the properties of the other substructure layers were not considered. As the deflections of the substructure layers at only one sleeper are used for a given test site, there is no value in differentiating between the stress properties of the left and the right hand side of the track. Therefore the equation describing the relationship between the deviator stress and the track stiffness is the average curve fitted through both graphs in Figure 4.5. The resulting equation for the deviator stress [in kPa] is

$$\sigma_1 - \sigma_3 = K_1 + K_2 \, (k_{2i}) \tag{4.3}$$

where k_{2i} [in kN/m] is the track stiffness at a particular sleeper as calculated by GEOTRACK. For the particular case under investigation K_1 is 194 kPa and K_2 is -1.96×10^{-3} m^{-1}. These values are site specific. Using the measured track stiffness, Equation (4.3) becomes

$$\sigma_1 - \sigma_3 = K_1 + K_2 \left(\frac{k_{2mi}}{K_3}\right) \tag{4.4}$$

where k_{2mi} is the measured track stiffness at a particular sleeper and K_3 is 1.34.
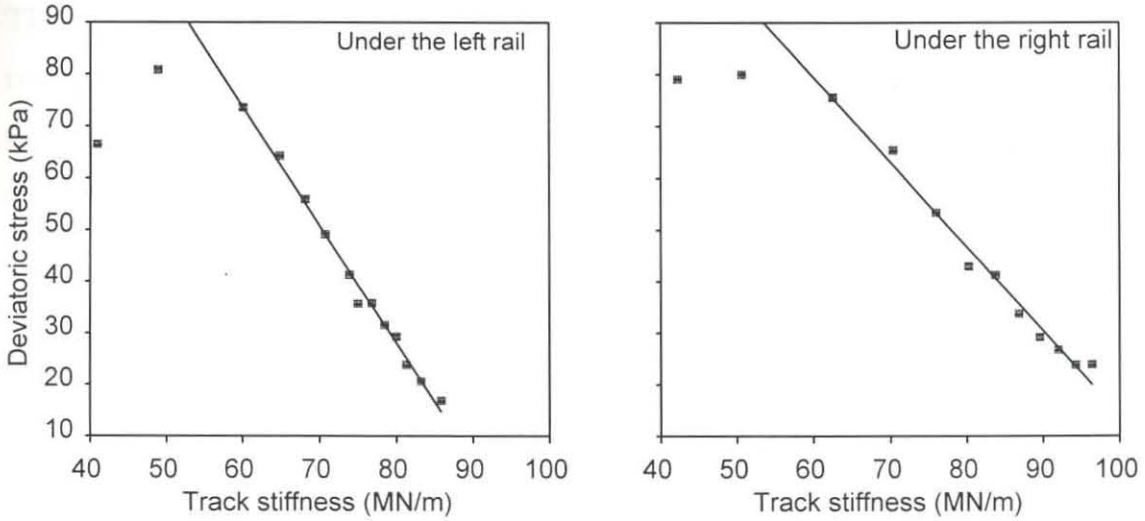
Figure 4.5: Deviator stress versus track stiffness.

To obtain the relationship between the dynamic wheel load and the settlement of the track, GEOTRACK was used once again. The procedure was to use a particular modulus of elasticity value and only change the static wheel load. The relationship between the resulting change in the deviator stress was approximately equal to the change in the dynamic wheel load relative to the static wheel load. The relationship between the deviator stress and the prevailing dynamic wheel load, P_{dyn}, is given as:

$$\sigma_1 - \sigma_3 = \left[K_1 + K_2 \left(\frac{k_{2mi}}{K_3}\right)\right] \frac{P_{dyn}}{P_{ref}} \tag{4.5}$$

where P_{ref} is a static reference wheel load. For this analysis the static reference wheel load was 13 tons.

It should be noted that Equation (4.5) is only valid for a measured linearised track stiffness below 132.6MN/m. In a section of track with a different stiffness range, the

parameters K_1, K_2 and K_3 would change and could be re-determined using the procedure described above. It was however found, that Equation (4.5) can be used successfully for average track stiffness values between 60 and 132MN/m.

The next step was to obtain the logarithmic settlement behaviour as well as the relative differential settlement as a function of the dynamic wheel load and the spatial variation of the track stiffness after a number of load cycles. The final differential settlement equation [in mm] is thus given as

$$\epsilon_{N_i} = (\sigma_1 - \sigma_3)^w \log N \tag{4.6}$$

that is

$$\epsilon_{N_i} = [[K_1 + K_2 \, (\frac{k_{2mi}}{K_3})] \, \frac{P_{dyn}}{P_{ref}}]^w \log N \tag{4.7}$$

where w is the settlement exponent to give the best fit to the measured overall track settlement. For the chosen test site w is 0.3. Validated results and further analysis are given in Chapters 7 and 8.

Summary

In this chapter the assumptions and methodology to predict track settlement have been presented. The most important contribution is the development of the modified settlement equation. The constants of this settlement equation are dependent on the basic properties of a certain section of track and can systematically be determined for any typical section of track using the procedure as described in this chapter.

CHAPTER 5

MODEL OF VEHICLE/TRACK SYSTEM DYNAMICS

In this chapter the development of the vehicle/track model to be used in the Dynamic Track Deterioration Prediction Model is described. Firstly, the rail support model is described, followed by a detailed description of the excitation model which consists out of the vertical space curve as well as spatial track stiffness variations. As the choice of assumptions and simplifications in the mathematical model of the vehicle is important in the development of the model, the basic philosophy in this respect is outlined before describing the development of the mathematical vehicle/track model.

The first model that is described is a two degree-of-freedom model. This model was used to do a basic analysis of the influence of spatial track stiffness variations on the dynamic behaviour of such a model. After considering a number of alternative vehicle/track models the reasons for arriving at the eleven degree-of-freedom model become apparent. The validation of the eleven degree-of-freedom model is given in Chapter 7.

5.1 TRACK SUPPORT MODEL

Although a discrete support appears to be more representative of track supported by discrete sleepers on a nonlinear and spatially varying flexible foundation, continuous support models are valid for calculating the dynamic response of the track at frequencies below 500 Hz (Knothe and Grassie, 1993). The simplest representation of a continuous elastic foundation is the Winkler foundation model.

In this model the rail is represented by an infinite, uniform, Euler-Bernoulli beam supported by a continuous damped, elastic Winkler foundation. The effective mass of the sleepers is distributed uniformly and added to the mass of the rail (Winkler, 1867; Winkler, 1875; Hetényi, 1946; Fastenrath, 1977; Esveld, 1989; Li and Selig, 1995). Winkler's hypothesis states that at each rail support the compressive stress is proportional to the local compression, that is

$$\sigma = C_f\, y \tag{5.1}$$

where

σ = local compressive stress on the support,

y = local deflection of the support, and

C_f = foundation modulus [N/m^3].

Based on the Winkler theory, the track modulus, u, which represents the overall stiffness of the rail foundation (that is sleepers, rail pads, ballast, sub-ballast, and subgrade), is defined as the supporting force per unit length of rail per unit deflection. Thus

$$u = \frac{q}{y} \tag{5.2}$$

with q the vertical rail foundation force per unit length.

The track stiffness itself is defined as

$$k = \frac{P}{y} \tag{5.3}$$

with P the concentrated force applied to the rail.

The difference between the track stiffness and the track modulus is that the track stiffness includes the rail stiffness, EI, whereas the track modulus represents only the remainder of the superstructure and the substructure. The various components of ballasted track are shown in Figure 5.1.
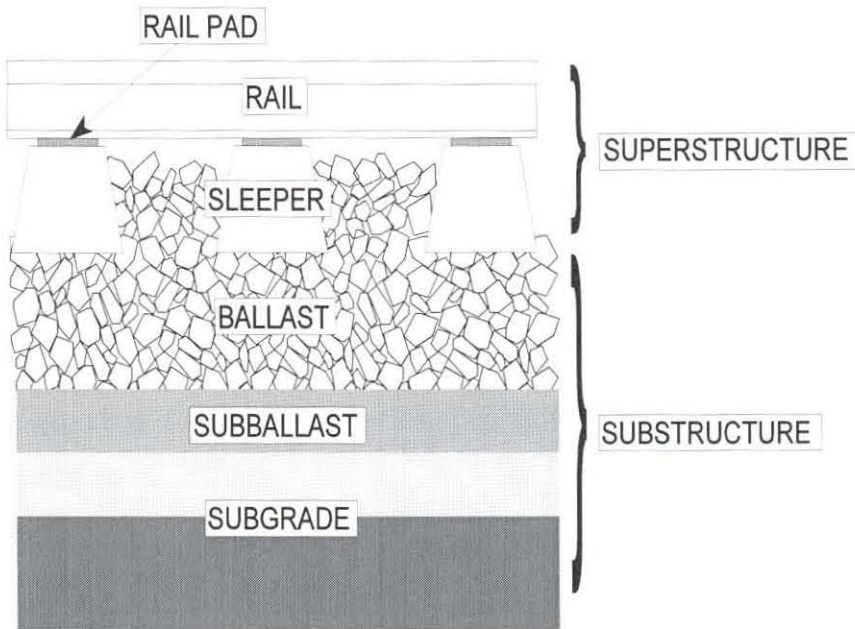
Figure 5.1: Components of ballasted track.

The linear differential equation of the beam-on-elastic foundation model is given as:

$$EI \frac{d^4 y}{d x^4} + uy = 0 \tag{5.4}$$

where

E = Young's modulus of rail steel,

I = rail moment of inertia about the horizontal axis,

y = incremental track deflection, and

x = distance from the applied load.

Solving Equation (5.4), the deflected shape of the track is

$$y = \frac{P}{2 u L_c} e^{-x/L_c} [\cos(x/L_c) + \sin(x/L_c)] \tag{5.5}$$

The characteristic length, L_c, is defined as

$$L_c = \sqrt[4]{\frac{4EI}{k}} \tag{5.6}$$

Substituting Equation (5.3) and (5.6) into Equation (5.4), the relationship between the track modulus and the track stiffness is given as

$$u = \frac{(k)^{4/3}}{(64EI)^{1/3}} \tag{5.7}$$

Re-writing Equation (5.7), the relationship between track stiffness and track modulus is found to be

$$k = \frac{2u}{\sqrt[4]{\dfrac{u}{4EI}}} \tag{5.8}$$

As illustrated in Figure 5.2, the rail support can also be nonlinear. The slope of the line between 0 and 32.5kN gives an indication of the voids between the sleepers and the ballast in the influence length of the wheel load (Ebersöhn *et al.*, 1993). The 32.5kN load is referred to as the seating load. For higher wheel loads the load deflection relationship is linear in most cases although in some cases stiffening of the track is found. This phenomenon makes it more complex to determine the deflection basin especially if the track stiffness also varies from point to point along the track.

To analyse the effect of wheel loads on the shape of the track deflection basin, and on the distribution of the wheel loads across a number of adjacent sleepers when the track has a spatially varying nonlinear support stiffness, a track model using elastic Euler-Bernoulli beams supported on a nonlinear discrete support has to be used. The rail in such a model is thus modelled by a finite element flexible beam and the structure is approximated as an assemblage of discrete elements interconnected at their nodal points. To find the solution to the nonlinear structural response, a load stepping procedure like the Newton-Raphson iteration procedure can be used. This

procedure is stable and converges quadratically although the stiffness matrix has to be inverted during each iteration.
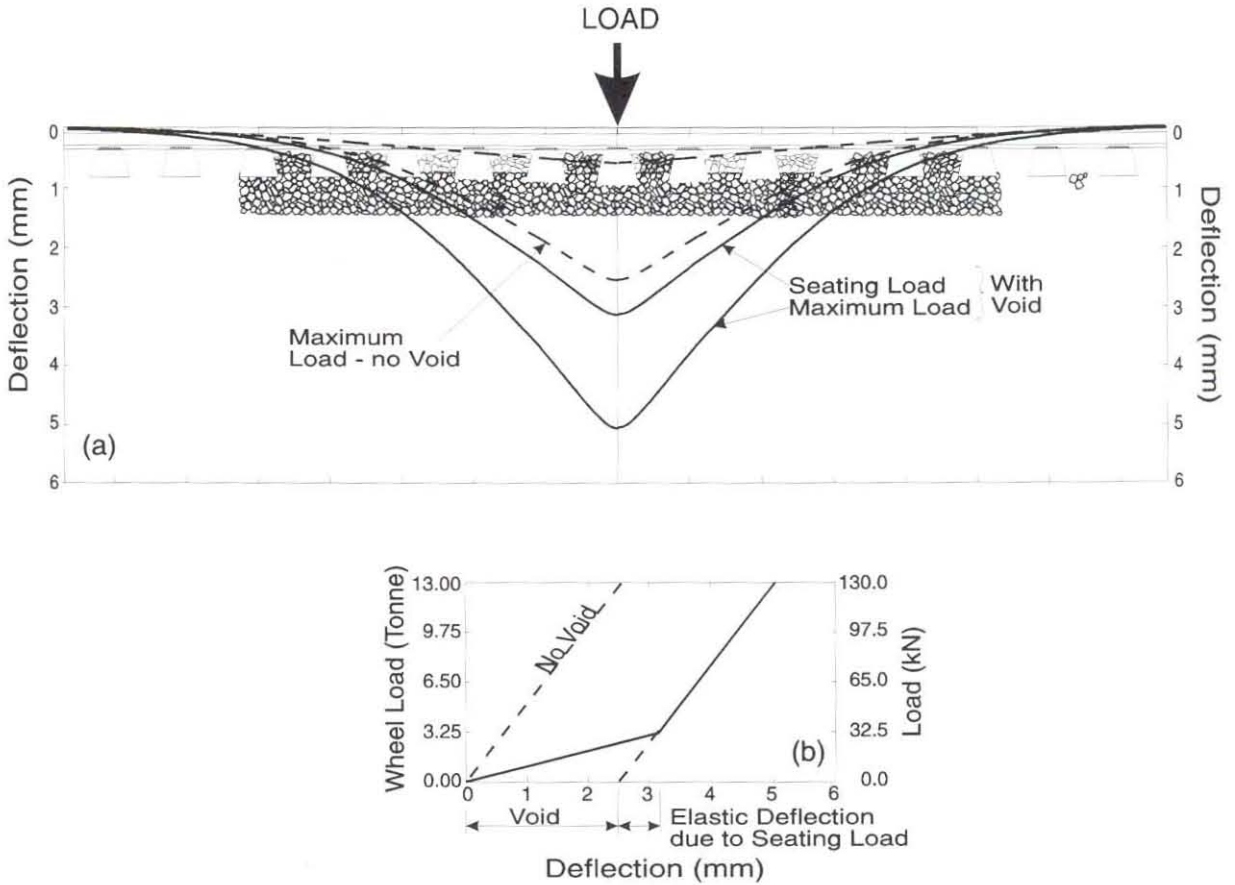
Figure 5.2: Track deflection basin.

In 1995, Moravčík made an analysis of rail on nonlinear discrete elastic supports. According to Moravčík the theoretical model of the rail as a beam on a continuous elastic foundation provides a basis for track design and stress analysis of the track components. However, due to on-track tests which revealed that the relationship between the vertical rail deflection and the wheel load is generally nonlinear, a different approach was required and a nonlinear finite element program was used to solve the problem. The nonlinear relationship between the wheel load and the vertical displacement of the sleeper was approximated by a bilinear spring, supports

with gaps, or a piecewise linear spring characteristic. Such a nonlinear analysis of the deflection basin provided a better picture of the rail behaviour, specially under locally poor track conditions where a large reduction in support resistance could be the major cause of overstressing in the track structure. A standard linear analysis generally underestimates the stresses in the track structure.

In this research a continuous one-layer pseudo-static track support model is used, but allowing the track stiffness to vary with time according to the instantaneous local track stiffness values underneath each wheel on both the left and the right hand rail of the track. Track damping is assumed to be constant along the track.

5.2 TRACK INPUT

The vehicle/track model is excited by the vertical space curve of the track as well as spatial vertical track stiffness variations. The excitation model is a moving excitation model, that is the vertical space curve and the stiffness variations are effectively pulled through under the wheelset.

If the track stiffness is linear, the vertical track profile variations can simply be multiplied by the track stiffness to determine the effective force input. However, if the track stiffness is nonlinear, an effective linearised loaded track stiffness, k_2, and an effective loaded track deflection, y_s, as shown in Figure 5.3 has to be used. Using the nonlinear track stiffness as measured at each sleeper, the following procedure is used to derive the effective linearised loaded track stiffness.

Let P_s be the static wheel load and

$$\Delta P = \delta P_s \qquad (5.9)$$

where δ is the dynamic wheel load increment. The wheel load increment is obtained from the prevailing dynamic wheel load as measured by the load measuring wheelset. If such a value is not available a good estimate is 0.3.

Using cubic-polynomial interpolation, the values y_{s1} and y_{s2} are found at $(P_s - \Delta P)$ and $(P_s + \Delta P)$ respectively. With these values available, the effective linearised loaded track stiffness is defined as

$$k_2 = \frac{P_s}{y_{s2} - y_{s1}} \tag{5.10}$$

and the static track deflection is defined as

$$y_s = \frac{y_{s2} + y_{s1}}{2} \tag{5.11}$$
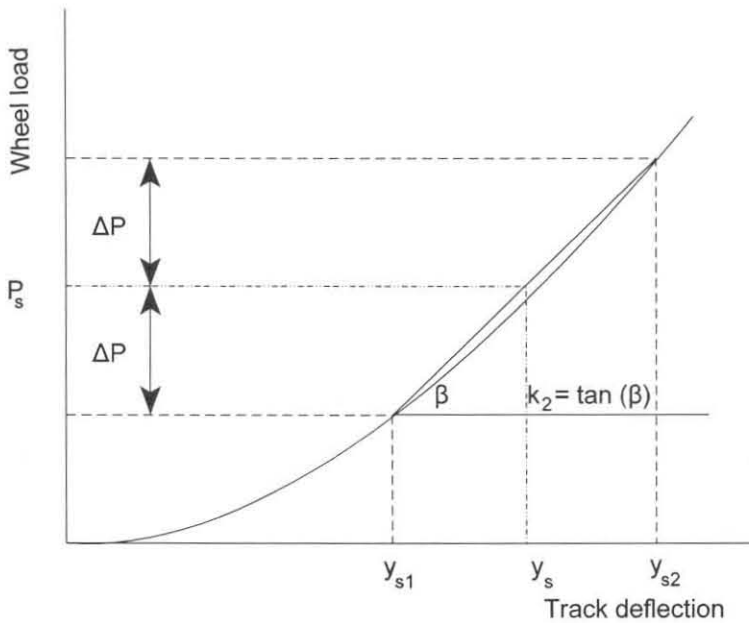
Figure 5.3: Effective linearised loaded track stiffness.

Linearisation is thus done over a range of static wheel load plus the dynamic increment. Figure 5.3 clearly shows that only a minimal deviation occurs between the linear approximation and the measured nonlinear stiffness. Note that due to the static load at a particular sleeper that is supported by a nonlinear track stiffness, the sleeper is deflected by a certain amount y_s. Would there be no spatial variation in the track stiffness, this would not be important, but as there are continuous

variations in the track stiffness, these deflections due to static or dynamic loading, vary as a function of the specific spatially varying load-deflection curve. An example is given in Figure 5.4. These varying deflections are added to the unloaded vertical space curve to obtain the effective loaded track geometry profile. This profile is then multiplied by the effective linearised loaded track stiffness at a particular point in the track to give the required input force to the mathematical model of the vehicle/track system. An effective linearised loaded track stiffness and loaded geometry profile which depends on the static and dynamic wheel load is thus obtained.
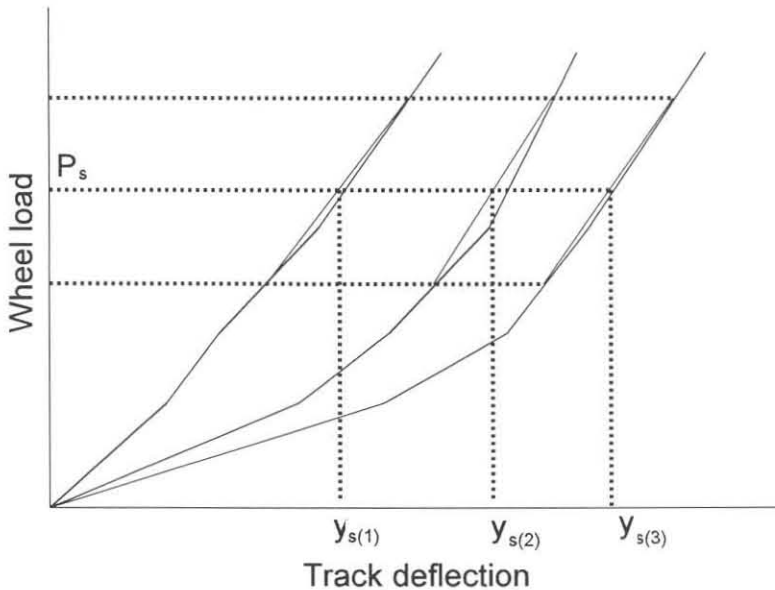
Figure 5.4: Varying static track deflections.

5.3 VEHICLE MODEL

Although a range of vehicle models are available to the rail vehicle dynamicist, unique requirements make it necessary to develop more suitable models from time to time. Such a unique application is the development of the Dynamic Track Deterioration Prediction Model that is to be used to predict and show the important relationship between spatially varying track stiffness and track deterioration.

Before proceeding with the development of the vehicle/track model that is to be incorporated in the Dynamic Track Deterioration Prediction Model, the basic philosophy behind the assumptions and simplifications in the development of vehicle models is given.

When developing a mathematical model of a railway vehicle it is important to have accurate data for parameters such as masses, stiffnesses, damping rate, friction levels etc. Furthermore it is up to the experienced railway vehicle dynamicist to make an informed judgement as to what level of detail to include in the model. Provided that realistic sensitivity studies have been done during the development of a new model to ensure that the parameters used are either not critical or at least reasonably realistic, calculated trends and comparisons can give a good insight into dynamic rail vehicle behaviour.

As the objective of this thesis is to predict the dynamic interaction between the vehicle and the track, and not the dynamic behaviour of the vehicle alone, the development of the vehicle model is done in terms of the development of the total vehicle/track system model.

5.4   VEHICLE/TRACK MODEL DEVELOPMENT

This section discusses the development of the vehicle/track model. The first model that is described is a two degree-of-freedom model. This is followed by a set of alternative models which systematically strive to adequately simulate the dynamic behaviour in the vehicle/track system. Finally, an eleven degree-of-freedom vehicle/track model is described. This model is sufficient for investigating the relationship between spatial track stiffness variations and track deterioration. For the interested reader some background information on dynamic modelling of a simple one degree-of-freedom system is given in Appendix D.

5.4.1 Two Degree-of-Freedom Vehicle/Track Model

To be able to gain a better understanding of the dynamic interaction between a vehicle and the track, a *two degree-of-freedom model* as shown in Figure 5.5 was initially developed. The two degree-of-freedom model was used to determine the dynamic wheel loads in the vehicle/track system due to a nonlinear and spatially varying track stiffness (Fröhling *et al.*, 1996a). By restricting the number of degrees of freedom to be investigated, a simpler understanding of the problem was formed and the emphasis was placed on effects due to the nonlinear spatially varying track stiffness.
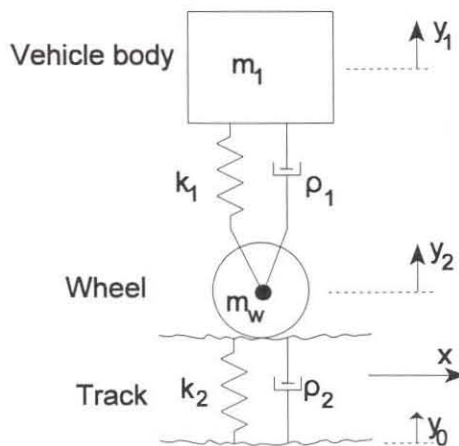
Figure 5.5: Two Degree-of-Freedom Vehicle/Track Model.

In this simplified model the following assumptions were made:
- The effect of the primary suspension of the vehicle was neglected.
- The stiffness and damping of the secondary suspension of the vehicle was assumed to be linear.
- A continuous one-layer track support model was used.
- The mass of the vehicle body represents one eighth of the sprung mass of the vehicle as this is the mass that is effectively carried by each of the eight wheels of the vehicle.
- Both the vehicle and the wheel are assumed to be rigid bodies.

The following nonlinear equations of motion describe the dynamic behaviour of the two degree-of-freedom vehicle/track model.

$$m_1 \ddot{y}_1 + \rho_1 \dot{y}_1 + k_1 y_1 - \rho_1 \dot{y}_2 - k_1 y_2 = 0 \qquad (5.12)$$

$$m_w \ddot{y}_2 + (\rho_1 + \rho_2)\dot{y}_2 + (k_1 + k_2(y_2,x))y_2 - \rho_1 \dot{y}_1 - k_1 y_1 - k_2(y_2,x)y_0 = 0 \qquad (5.13)$$

$$k_2(y_2,x) = f(y_2,x) \qquad (5.14)$$

The instantaneous value for the track stiffness, k_2, is obtained from a bi-variant cubic polynomial interpolation in the two-dimensional data set of measured track stiffness values. The value of the track stiffness is also dependant on the prevailing static wheel load.

To solve the system of equations as given by Equations (5.12) to (5.14), the derivatives in the differential equations are replaced by finite central difference approximations (Levy and Wilkinson, 1976). In the approximation the derivative of y with respect to t is defined at $t=t_0$ by

$$\left(\frac{dy}{dt} \right)_{t=t_0} = \frac{\Delta y}{\Delta t} = \frac{y_1 - y_{-1}}{t_1 - t_{-1}} = \frac{y_1 - y_{-1}}{2\Delta t} \qquad (5.15)$$

Likewise, a similar approximation can be made for the acceleration which is the second derivative:

$$\left(\frac{d^2 y}{dt^2} \right)_{t=t_0} = \frac{y - 2y_0 + y_{-1}}{(\Delta t)^2} \qquad (5.16)$$

By introducing these approximations, the derivatives in the equations of motion can be replaced by the differences between successive positions taken by the mass at successive increments in time. These differences are known as finite differences because they are separated by finite time increments.

Equations (5.12) and (5.13) are thus re-written as:

$$m_1\left(\frac{y_{1(1)}-2y_{1(0)}+y_{1(-1)}}{(\Delta t)^2}\right)+\rho_1\left(\frac{y_{1(1)}-y_{1(-1)}}{2\Delta t}\right)+k_1 y_{1(0)}-\rho_1\left(\frac{y_{2(1)}-y_{2(-1)}}{2\Delta t}\right)-k_1 y_{2(0)}=0 \tag{5.17}$$

$$m_w\left(\frac{y_{2(1)}-2y_{2(0)}+y_{2(-1)}}{(\Delta t)^2}\right)+(\rho_1+\rho_2)\left(\frac{y_{2(1)}-y_{2(-1)}}{2\Delta t}\right)+(k_1+k_2(y_{2(0)},x)))y_{2(0)}-\rho_1\left(\frac{y_{1(1)}-y_{1(-1)}}{2\Delta t}\right)-k_1 y_{1(0)}-k_2(y_{2(0)},x)y_0=0 \tag{5.18}$$

The three simultaneous nonlinear equations are solved at each time step, using the Newton-Raphson algorithm. Having obtained the displacement values $y_{1(1)}$ and $y_{2(1)}$, and the instantaneous track stiffness, the values $y_{1(2)}$ and $y_{2(2)}$ are found in terms of the already calculated values. This process of finding the new displacement based on knowledge of the two previous displacements is known as a step-by-step process of integration. The procedure is simple in concept, but can, with repetitive application, yield the complete time history of the behaviour of the system. By adjusting the size of the time step Δt, the desired accuracy can be obtained. Convergence with a nonlinear set of equations is readily obtained using this approach. This numerical solution technique was used in a computer program which was developed to solve the system of equations of the two degree-of-freedom vehicle/track model at each consecutive time step using the instantaneous information on track geometry and track stiffness variations.

The two degree-of-freedom model was used to simulate both an empty and a loaded vehicle, both alternatively equipped with a low and a high secondary damping, running over a section of irregular track (Fröhling et al., 1996a). Under these conditions, the vertical acceleration of the vehicle body and the dynamic loading of the track was analysed as a function of the vertical space curve of the track and an infinite track stiffness, the vertical space curve of the track and a constant track stiffness, no track geometry irregularities and only a spatially varying track stiffness, and spatially varying track stiffness superimposed on the vertical space curve of the track. From simulations over single vertical track geometry irregularities, it was found that it is not the nonlinearity of the track stiffness in itself that causes a dynamic input, but the spatial change in track deflection under a given load.

Using the two degree-of-freedom model and comparing the results to those measured during on-track tests, it became clear that the model is not able to simulate the low frequency dynamic behaviour that originates from the rolling motion of the wagon body. These motions were dominant in the measured results. Furthermore, the model was not able to simulate the difference in track input between the left and the right rail. Hence, further model development was required.

5.4.2 Alternative Vehicle/Track Models

After realising the limitations of the two degree-of-freedom vehicle/track model, the search for a more appropriate vehicle/track model started. The first step was to *incorporate the load sensitive damping of the secondary suspension* into the two degree-of-freedom model by using Equations (B1) to (B3) given in Appendix B. This was done because of the nonlinear displacement that was measured across the secondary suspension during the on-track tests, and its influence on the force transmitted through the secondary suspension and thus also the resultant force between the wheel and the rail.

The next step was to *include the rolling motion* of the wheelset and the vehicle body. This was done using a two dimensional four degree-of-freedom model with varying track input between the left and the right rail. This model was tested with and without load sensitive frictional damping. Comparing its results to those measured on track, it became clear that this model was unable to simulate the coupling between the dynamic wheel load in the front of the vehicle and that at the trailing end that occurs due to the distance based track input. To include this effect, the *pitching motion* of the vehicle was included. This resulted in a seven degree-of-freedom model.

At this stage the magnitude of the dynamic wheel load and the vertical displacement across the secondary suspension was still not representative of the measured results. Patterns were however becoming similar.

5.4.3 Eleven Degree-of-Freedom Vehicle/Track Model

The next step was to include the *vertical stiffness and damping of the primary suspension*, increasing the degrees-of-freedom of the model to eleven. At this stage the vehicle/track model was still simulating a two-axle vehicle and not a two-bogie vehicle as used during the on-track tests. The following was however done to include some influence due a bogie with two wheelsets on the dynamic behaviour of the vehicle/track system.

- To get the correct dynamic track deflection, the mass and the inertia of the two wheelsets of the bogie were added together to create a wheelset with twice the mass of the actual wheelset. The two wheelsets were thus seen to be close enough to one another to act as one inertial system and the exact behaviour of the unsprung mass was thus of secondary importance.

- To simulate the vertical space curve of the track as seen by a bogie, the average between the vertical space curve at the leading and the trailing axle on one side of the bogie was calculated at any point in time and used as excitation input. This made it possible simulated the effect the side frames have on averaging the force input to the secondary suspension.

- To compensate for the fact that only one and not two wheels are in contact with the track on one side of the bogie, the track stiffness as observed at any point in time at the leading and the trailing wheel on one side of the bogie was added together to simulate the fact that a quarter of the vehicle is effectively being supported by two times the track stiffness.

The simulated results were checked against results obtained with the multi-body simulation program MEDYNA (Schielen, 1990). In the MEDYNA model the side frames of the bogies were modelled as separate bodies. The results showed that the approximation described above was sufficient to predict the magnitude of the dynamic wheel load, the vertical displacement across the secondary suspension, and the dominant frequencies in the system. The validation of the eleven degree-of-

freedom vehicle/track model is done in Chapter 7. A complete list of assumptions and the overall motivation for these assumptions is also given in Chapter 7.

The vehicle/track model was thus developed in close conjunction with experimental results. In particular the patterns and the magnitudes of the vertical displacement across the secondary suspension and the dynamic wheel loads were used for this purpose. Fault finding and sensitivity studies were also part of the development process. A schematic of the eleven degree-of-freedom vehicle/track model is shown in Figure 5.6. Note that the mathematical procedure to include the effect of the bogie on the excitation of the model is not shown in the figure.

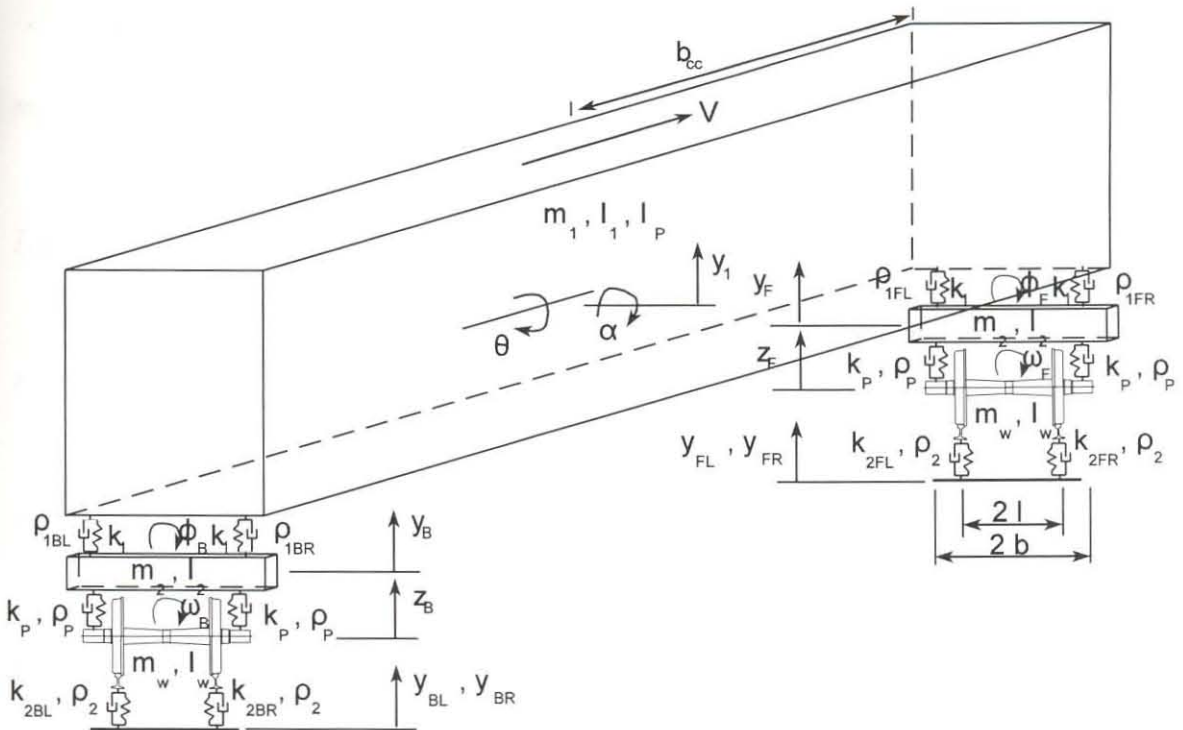
Figure 5.6: Eleven degree-of-freedom vehicle/track model.

As mentioned, all the major body modes of vibration were included to simulate the influence of track input being different at the front and the rear of the vehicle at any point in time as this has a significant influence on the dynamic behaviour of the vehicle, in particular its rolling motion, and the subsequent dynamic loading of the

track. Furthermore, the nonlinearity of the secondary suspension was included as it significantly influences the magnitude and frequency of the loading between the vehicle and the track. Equations (5.19) to (5.29) below describe the model in terms of its *equations of motion*. Note that k_2 is defined by Equation (5.10) and is a function of the static load and its position along the track.

$$m_1 \ddot{y}_1 + F_{ff_{1FL}} + F_{ff_{1FR}} + F_{ff_{1BL}} + F_{ff_{1BR}} \\ + 4k_1 y_1 - 2k_1 y_F - 2k_1 y_B = 0 \tag{5.19}$$

$$I_1 \ddot{\theta} + b F_{ff_{1FL}} - b F_{ff_{1FR}} + b F_{ff_{1BL}} - b F_{ff_{1BR}} \\ + 4b^2 k_1 \theta - 2b^2 k_1 \phi_F - 2b^2 k_1 \phi_B = 0 \tag{5.20}$$

$$I_p \ddot{\alpha} - b_{cc} F_{ff_{1FL}} - b_{cc} F_{ff_{1FR}} + b_{cc} F_{ff_{1BL}} + b_{cc} F_{ff_{1BR}} \\ + 4b^2_{cc} k_1 \alpha + 2b_{cc} k_1 y_F - 2b_{cc} k_1 y_B = 0 \tag{5.21}$$

$$m_2 \ddot{y}_F - F_{ff_{1FL}} - F_{ff_{1FR}} \\ + 2\rho_p \dot{y}_F - 2k_1(y_1 - y_F) + 2k_p(y_F - z_F) + 2k_1 b_{cc} \alpha - 2\rho_p \dot{z}_F = 0 \tag{5.22}$$

$$I_2 \ddot{\phi}_F - b F_{ff_{1FL}} + b F_{ff_{1FR}} \\ + 2b^2 \rho_p \dot{\phi}_F - 2bk_1(b\theta - b\phi_F) + 2b^2 k_p \phi_F - 2b^2 \rho_p \dot{\omega}_F - 2b^2 k_p \omega_F = 0 \tag{5.23}$$

$$m_2 \ddot{y}_B - F_{ff_{1BL}} - F_{ff_{1BR}} \\ + 2\rho_p \dot{y}_B - 2k_1(y_1 - y_B) + 2k_p(y_B - z_B) - 2k_1 b_{cc} \alpha - 2\rho_p \dot{z}_B = 0 \tag{5.24}$$

$$I_2 \ddot{\phi}_B - b F_{ff_{1BL}} + b F_{ff_{1BR}} \\ + 2b^2 \rho_p \dot{\phi}_B - 2bk_1(b\theta - b\phi_B) + 2b^2 k_p \phi_B - 2b^2 \rho_p \dot{\omega}_B - 2b^2 k_p \omega_B = 0 \tag{5.25}$$

$$m_w \ddot{z}_F + 2(\rho_p + \rho_2)\dot{z}_F + 2k_p z_F + k_{2FL} z_F + k_{2FR} z_F - 2\rho_p \dot{y}_F - 2k_p y_F \\ - k_{2FL} y_{FLi} - k_{2FR} y_{FRi} + k_{2FL} l \omega_F - k_{2FR} l \omega_F = 0 \tag{5.26}$$

$$I_w \ddot{\omega}_F + 2(b^2 \rho_p + l^2 \rho_2)\dot{\omega}_F + 2b^2 k_p \omega_F + k_{2FL} l^2 \omega_F + k_{2FR} l^2 \omega_F \\ - 2\rho_p b^2 \dot{\phi}_F - 2k_p b^2 \phi_F - k_{2FL} l y_{FLi} + k_{2FR} l y_{FRi} + k_{2FL} l z_F - k_{2FR} l z_F = 0 \tag{5.27}$$

$$m_w \ddot{z}_B + 2(\rho_p + \rho_2)\dot{z}_B + 2k_p z_B + k_{2BL} z_B + k_{2BR} z_B - 2\rho_p \dot{y}_B - 2k_p y_B \\ - k_{2BL} y_{BLi} - k_{2BR} y_{BRi} + k_{2BL} l \omega_B - k_{2BR} l \omega_B = 0 \tag{5.28}$$

$$I_w \ddot{\omega}_B + 2(b^2 \rho_p + l^2 \rho_2)\dot{\omega}_B + 2b^2 k_p \omega_B + k_{2BL} l^2 \omega_B + k_{2BR} l^2 \omega_B \\ - 2\rho_p b^2 \dot{\phi}_B - 2k_p b^2 \phi_B - k_{2BL} l y_{BLi} + k_{2BR} l y_{BRi} + k_{2BL} l z_B - k_{2BR} l z_B = 0 \tag{5.29}$$

with the friction forces, *Fff*, defined as follows:

$F_{ff_{FL}}$: If $(\dot{y}_1 - \dot{y}_F + b\dot{\theta} - b\dot{\phi}_F - b_{cc}\dot{\alpha}) < 0.0$

then $F_{ff_{FL}} = \dfrac{-(x_{ss} + (y_1 - y_F + b\theta - b\phi_F - b_{cc}\alpha))k_{ss}\mu}{\tan\alpha_w + \mu}$

If $(\dot{y}_1 - \dot{y}_F + b\dot{\theta} - b\dot{\phi}_F - b_{cc}\dot{\alpha}) > 0.0$

then $F_{ff_{FL}} = \dfrac{(x_{ss} + (y_1 - y_F + b\theta - b\phi_F - b_{cc}\alpha))k_{ss}\mu}{\tan\alpha_w - \mu}$ (5.30)

If $|C_{slope}(\dot{y}_1 - \dot{y}_F + b\dot{\theta} - b\dot{\phi}_F - b_{cc}\dot{\alpha})| < |F_{ff_{FL}}|$

then $F_{ff_{FL}} = C_{slope}(\dot{y}_1 - \dot{y}_F + b\dot{\theta} - b\dot{\phi}_F - b_{cc}\dot{\alpha})$

$F_{ff_{FR}}$: If $(\dot{y}_1 - \dot{y}_F - b\dot{\theta} + b\dot{\phi}_F - b_{cc}\dot{\alpha}) < 0.0$

then $F_{ff_{FR}} = \dfrac{-(x_{ss} + (y_1 - y_F - b\theta + b\phi_F - b_{cc}\alpha))k_{ss}\mu}{\tan\alpha_w + \mu}$

If $(\dot{y}_1 - \dot{y}_F - b\dot{\theta} + b\dot{\phi}_F - b_{cc}\dot{\alpha}) > 0.0$

then $F_{ff_{FR}} = \dfrac{(x_{ss} + (y_1 - y_F - b\theta + b\phi_F - b_{cc}\alpha))k_{ss}\mu}{\tan\alpha_w - \mu}$ (5.31)

If $|C_{slope}(\dot{y}_1 - \dot{y}_F - b\dot{\theta} + b\dot{\phi}_F - b_{cc}\dot{\alpha})| < |F_{ff_{FR}}|$

then $F_{ff_{FR}} = C_{slope}(\dot{y}_1 - \dot{y}_F - b\dot{\theta} + b\dot{\phi}_F - b_{cc}\dot{\alpha})$

$F_{ff_{BL}}$: If $(\dot{y}_1 - \dot{y}_B + b\dot{\theta} - b\dot{\phi}_B + b_{cc}\dot{\alpha}) < 0.0$

then $F_{ff_{BL}} = \dfrac{-(x_{ss} + (y_1 - y_B + b\theta - b\phi_B + b_{cc}\alpha))k_{ss}\mu}{\tan\alpha_w + \mu}$

If $(\dot{y}_1 - \dot{y}_B + b\dot{\theta} - b\dot{\phi}_B + b_{cc}\dot{\alpha}) > 0.0$

then $F_{ff_{BL}} = \dfrac{(x_{ss} + (y_1 - y_B + b\theta - b\phi_B + b_{cc}\alpha))k_{ss}\mu}{\tan\alpha_w - \mu}$ (5.32)

If $|C_{slope}(\dot{y}_1 - \dot{y}_B + b\dot{\theta} - b\dot{\phi}_B + b_{cc}\dot{\alpha})| < |F_{ff_{BL}}|$

then $F_{ff_{BL}} = C_{slope}(\dot{y}_1 - \dot{y}_B + b\dot{\theta} - b\dot{\phi}_B + b_{cc}\dot{\alpha})$

$F_{ff_{BR}}$:   If $(\dot{y}_1 - \dot{y}_B - b\dot{\theta} + b\dot{\phi}_B + b_{cc}\dot{\alpha}) < 0.0$

then $F_{ff_{BR}} = \dfrac{-(x_{ss} + (y_1 - y_B - b\theta + b\phi_B + b_{cc}\alpha))\,k_{ss}\,\mu}{\tan\alpha_w + \mu}$

If $(\dot{y}_1 - \dot{y}_B - b\dot{\theta} + b\dot{\phi}_B b_{cc}\dot{\alpha}) > 0.0$

then $F_{ff_{BR}} = \dfrac{(x_{ss} + (y_1 - y_B - b\theta + b\phi_B + b_{cc}\alpha))\,k_{ss}\,\mu}{\tan\alpha_w - \mu}$ (5.33)

If $|C_{slope}(\dot{y}_1 - \dot{y}_B - b\dot{\theta} + b\dot{\phi}_B + b_{cc}\dot{\alpha})| < |F_{ff_{BR}}|$

then $F_{ff_{BR}} = C_{slope}(\dot{y}_1 - \dot{y}_B - b\dot{\theta} + b\dot{\phi}_B + b_{cc}\dot{\alpha})$

To solve this system of equations the derivatives in the differential equations were replaced by finite central difference approximations and solved using the same technique as described in Section 5.4.1. In terms of the force between the wheel and the rail, the average force between the leading and the trailing wheel on either side of each bogie is given as output.

During the development of the vehicle/track model, a parameter variation analysis was done to evaluate the sensitivity of the vehicle/track model to changes in certain suspension parameters. In this study it was found that under the prevailing relatively good track condition, changes in the damping of the primary suspension as well as changes in the stiffness of the secondary suspension have no significant influence on the dynamic wheel load. Changes in the stiffness of the primary suspension only resulted in changes in the frequency of the dynamic wheel load. The most significant changes were observed when changing the coefficient of friction in the load dependent friction damper of the secondary suspension. An increase in the coefficient of friction resulted in a higher dynamic wheel load. From laboratory tests as described in Appendix B Section B.1.2, a realistic coefficient of friction could however be chosen to achieve realistic dynamic wheel loads.

Summary

After considering the track support model to be used and defining the type of track input, a number of alternative vehicle/track models were evaluated. The final eleven degree-of-freedom model is described in terms of its equations of motion. In Chapter 6, this model is implemented in the Dynamic Track Deterioration Prediction Model.

CHAPTER 6

TRACK DETERIORATION PREDICTION MODELS

In this chapter the development of the Dynamic Track Deterioration Prediction Model and the Static Track Deterioration Prediction Model is presented.

6.1   DYNAMIC TRACK DETERIORATION PREDICTION MODEL

In principle, the Dynamic Track Deterioration Prediction Model is simply the joining of the eleven degree-of-freedom vehicle/track model and track settlement as defined by Equation (4.7). Using the measured vertical space curve of the track and the spatial variation in the track stiffness as excitation input, the vehicle/track model is excited into its dynamic motions. These dynamic motions cause a certain dynamic loading of the track and thus the ballast. This causes stresses in the ballast which in turn leads to permanent strain. The resulting settlement varies from sleeper to sleeper causing differential settlement along the track. The different local settlements are then added to the loaded track geometry and the dynamic behaviour of the vehicle can again be simulated while running over the now settled track. This results in a different wheel loading pattern, more stress in the track, more permanent strain in the ballast and subsequent further differential track settlement.

Using the settlement algorithm, the vertical track geometry is thus always changed before the next dynamic simulation is done. This sequence of calculations is repeated until the required gross tonnage of traffic has passed over the selected track while continuously predicting new dynamic wheel loads and a prevailing

differential track settlement. Averaging the settlement of the individual sleepers over three sleepers is done to spread settlement in accordance with deflection basin behaviour.

In reality a variety of track stiffness values are present during the settlement process. As these stiffness values are dependant on measurement accuracy, weather conditions, tamping repeatability, and a complex interrelationship during settlement, stiffness measurement would be required at regular intervals. This is impractical and would defeat the object. Therefore, only one measurement of track stiffness is taken after the initial high rate of track settlement has decreased. This stiffness is then used as a reference stiffness for the prediction of differential track settlement.

To be able to compute and predict the dynamic behaviour of the vehicle and the response of the track, especially in terms of track settlement, the computer program VEHTRAS (Vehicle Track System) was developed. VEHTRAS is based on the Dynamic Track Deterioration Prediction Model and uses the numerical techniques as described in Section 5.4.1.

6.2   STATIC TRACK DETERIORATION PREDICTION MODEL

When assuming that there is no or very little dynamic wheel loading, which would be a good approximation under relatively good track conditions, the ratio between the dynamic wheel load and the static reference wheel load in Equation (4.7) approaches one and the prediction of differential track settlement becomes independent of the dynamic track loading. The advantage of this simplification is that the modified settlement equation can be applied directly to the measured spatial variation of the track stiffness to determine differential track settlement and subsequent changes in track roughness. Note that the three sleeper filter which is applied in the dynamic settlement model still needs to be applied. If however the track geometry or track stiffness variations are high, the dynamic component of the

wheel load has to be included. Furthermore, if the dynamic loading of the track or the dynamic response of the vehicle is required, the Dynamic Track Deterioration Prediction Model has to be used.

CHAPTER 7

MODEL VALIDATION

In this chapter the Dynamic Track Deterioration Prediction Model and the Static Track Deterioration Prediction Model are validated against measured results. The Dynamic Track Deterioration Prediction Model is validated in terms of its dynamic behaviour as well as its ability to predict differential track settlement. The Static Track Deterioration Prediction Model is only validated in terms of its ability to predict differential track settlement. After validating the models the assumptions and simplifications that were made during the development of these models are once again listed and discussed in terms of their overall influence on the calculated predictions.

7.1   DYNAMIC BEHAVIOUR

With respect to the dynamic behaviour of the vehicle/track system the vertical displacement across the secondary suspension and the dynamic wheel load were used to compare simulated and measured results. In the comparative analysis, the vehicle and track parameters as given in Table 7.1 were used. Note that the wheelsets in the model effectively have the mass and rolling inertia of two wheelsets. Furthermore, the vertical stiffness of the primary suspension has been lowered to compensate for deflections in the side frame and the adaptor frame.

In Figure 7.1 and Figure 7.2 simulated and measured wheel loads are compared for vehicle speeds of 30 km/h and 70 km/h respectively. It can be seen that the predicted results agree reasonably well in terms of the frequency content, average

wheel load and the dynamic wheel load range, with measurements taken during on-track tests when both track geometry and track stiffness variations were used as input into the vehicle model. See Table 7.2 for a summary of the dominant wheel load frequencies.

Table 7.1: Vehicle and track parameters.

Description	Symbol	Value
Mass of vehicle body	m_1	93920.0 kg
Mass of bogie frame	m_2	2620.0 kg
Mass of two wheelsets	m_w	2420.0 kg
Vehicle body moment of inertia in roll	I_1	360000.0 kgm^2
Bogie frame moment of inertia in roll	I_2	660.0 kgm^2
Vehicle body moment of inertia in pitch	I_p	1000000.0 kgm^2
Two wheelsets moment of inertia in roll	I_w	732.0 kgm^2
Vertical track damping	ρ_2	1000000.0 N/m/s
Vertical damping of primary suspension	ρ_p	20000.0 N/m/s
Vertical stiffness of secondary suspension	k_1	3881600.0 N/m
Vertical stiffness of primary suspension per bogie side	k_p	30000000.0 N/m
Stiffness of two stabilizer springs	k_{ss}	358120.0 N/m
Stabilizer spring pre-compression	x_{ss}	0.077 m
Wedge damping slope	C_{slope}	30000000.0 N/m/s
Half distance between secondary suspension	b	0.838 m
Distance between axles of one bogie	a	1.83 m
Half distance between wheel/rail contact points	l	0.55 m
Half bogie centre distance	b_{cc}	4.155 m
Wedge friction coefficient	μ	0.35

Table 7.2: Dominant wheel load frequencies.

	30 km/h			70 km/h	
Measured	0.02 Hz	0.1 Hz	0.45 Hz	0.03 to 0.1 Hz	0.23 and 0.45 Hz
Simulated	0.02 Hz	0.1 Hz	0.4 Hz	0.03 and 0.1 Hz	0.25 to 0.45 Hz

In Figure 7.2, the effect of excluding the nonlinear spatially varying track stiffness is illustrated and it can be seen that the spatially varying track stiffness has a significant influence on the dynamic loading of the vehicle on the track. What is even more important is the fact that the spatial track stiffness variations have a significant influence on differential track settlement. This is shown in Section 7.2.

In Figure 7.3 and Figure 7.4, a comparison between the simulated and measured vertical displacement across the secondary suspension is given. From these two figures it can be seen that the overall vertical displacement across the secondary suspension is approximately 3mm in both the measured and simulated cases. Although the patterns are different, higher simulated displacement generally occurs at the same point in time as in the measured results.

From the comparison between the measured and the simulated results it can be seen that the dynamic magnitude of both the dynamic wheel load and the vertical displacement across the secondary suspension compares very well with measured values. Although deviations do occur in the results, predictions are accurate enough to predict and evaluate the influence of dynamic wheel loading and spatially varying track stiffness on differential track settlement. A discussion of the assumptions that were made and why the given results are adequate for the prediction of track deterioration is given at the end of this chapter.
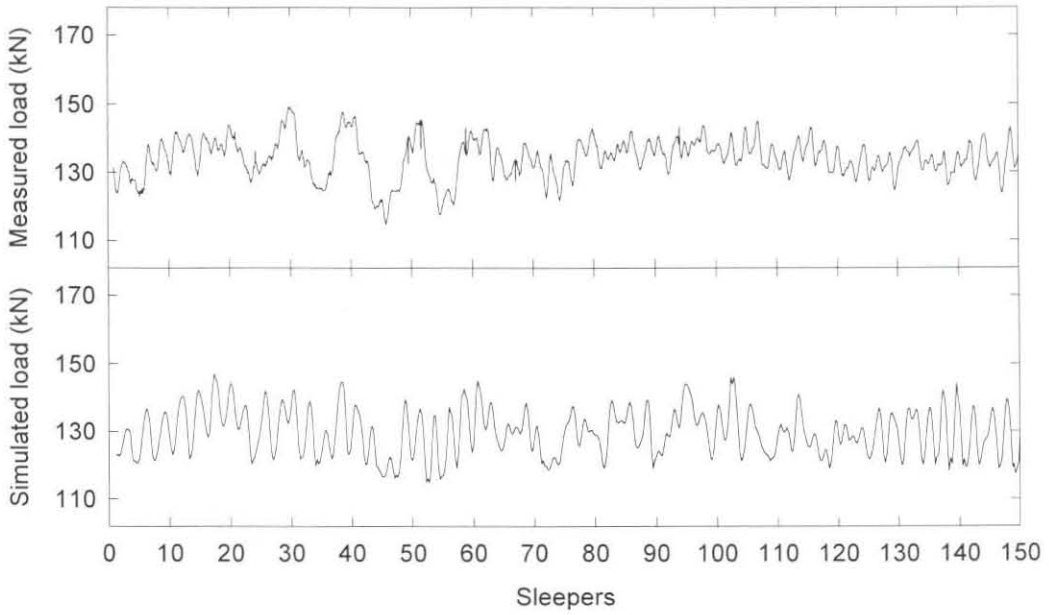
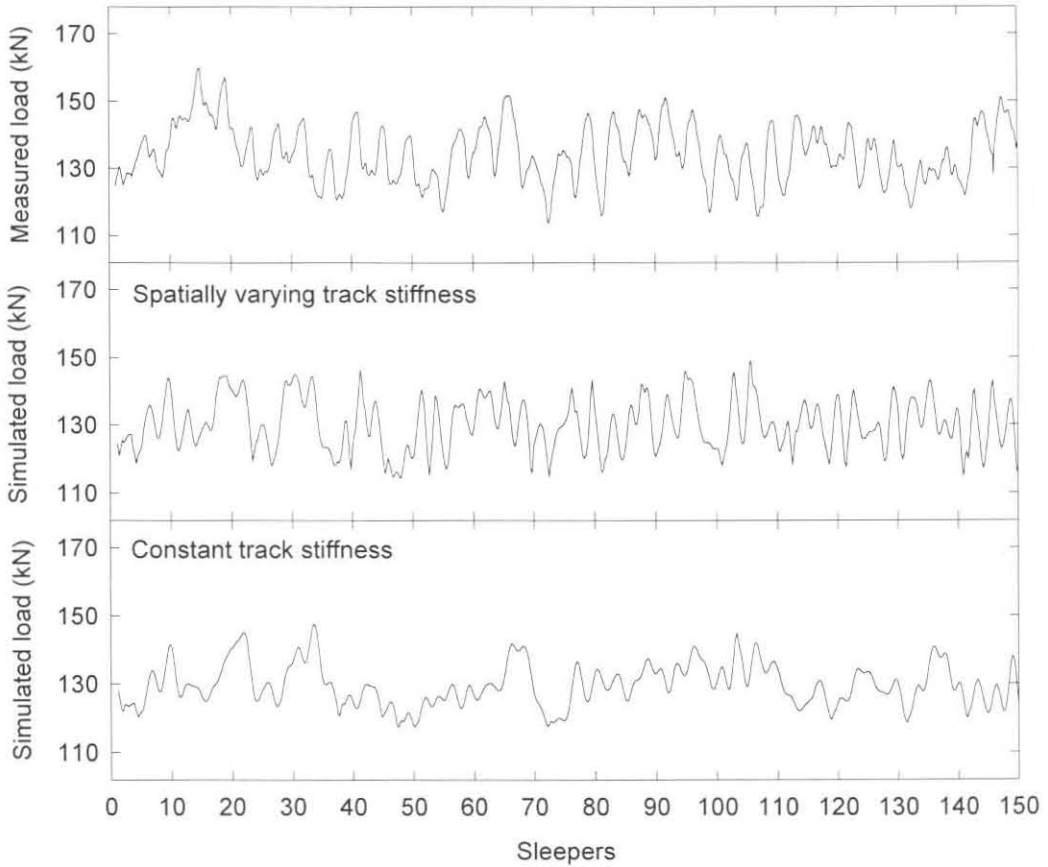Figure 7.1: Wheel load comparison at 30 km/h.
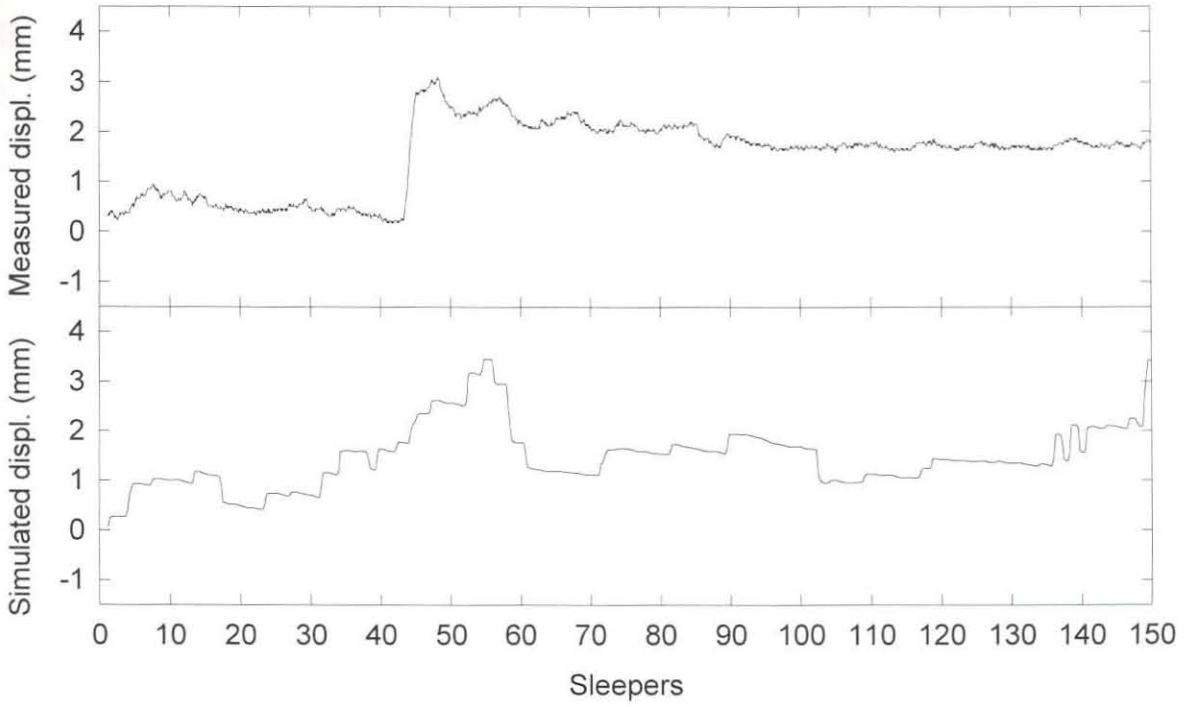

Figure 7.2: Wheel load comparison at 70 km/h.

Figure 7.3: Displacement across secondary suspension at 30 km/h.
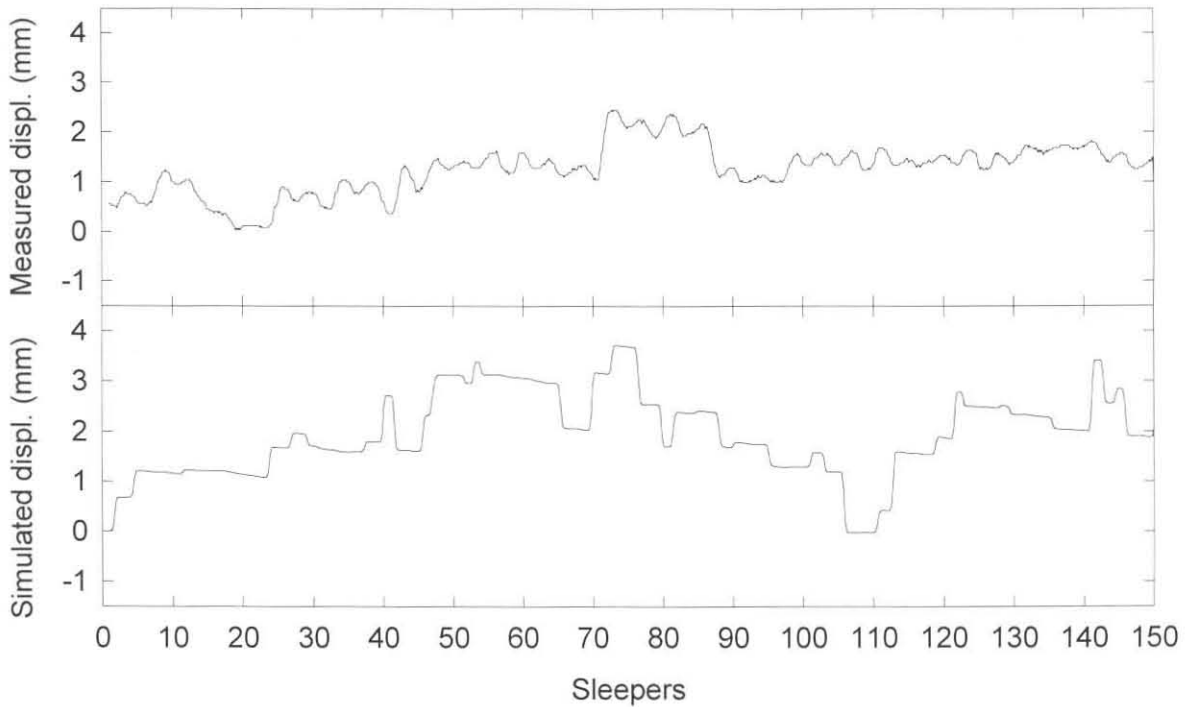
Figure 7.4: Displacement across secondary suspension at 70 km/h.

7.2   TRACK SETTLEMENT

In Figure 7.5, the measured and predicted average track settlement is shown as a function of accumulating traffic. Very little difference is observed between the two graphs, indicating a good prediction of the overall track settlement. The measured as well as predicted differential track settlement is shown in Figure 7.6. From the measured and predicted track settlement on both the left and the right hand rail it can be seen that the patterns of the differential track settlement in the latter half of both graphs is similar. The only difference is that the simulation predicted a higher overall track settlement. This difference is mainly due to the fact that only 26 ton axle loads were assumed for this prediction while in practice an axle load distribution as shown in Figure B1 in Appendix B occurred. If the lower axle load cycles would have been included in this particular simulation, the overall settlement of the track would have been predicted to be lower and thus closer to the measured settlement. The difference between the measured and predicted track settlement in the first part of both graphs can be due to a combination of the dynamic behaviour of the vehicle at the end of the transition curve, lateral track alignment deviations, and track stiffness measurements.

During the numerous simulation runs that were done to predict track settlement it was seen that the predicted results were sensitive to the spatial variation in track stiffness. As an example, the same geometric track input was used but the track stiffness was kept linear and constant at the average liniarised track stiffness throughout the section. Figure 7.7 compares the resulting track settlement with the settlement predicted when using the spatially varying track stiffness. The simulation which included spatial track stiffness variations agrees better with the measured settlement. This emphasises the important relationship between spatially varying track stiffness and track deterioration.
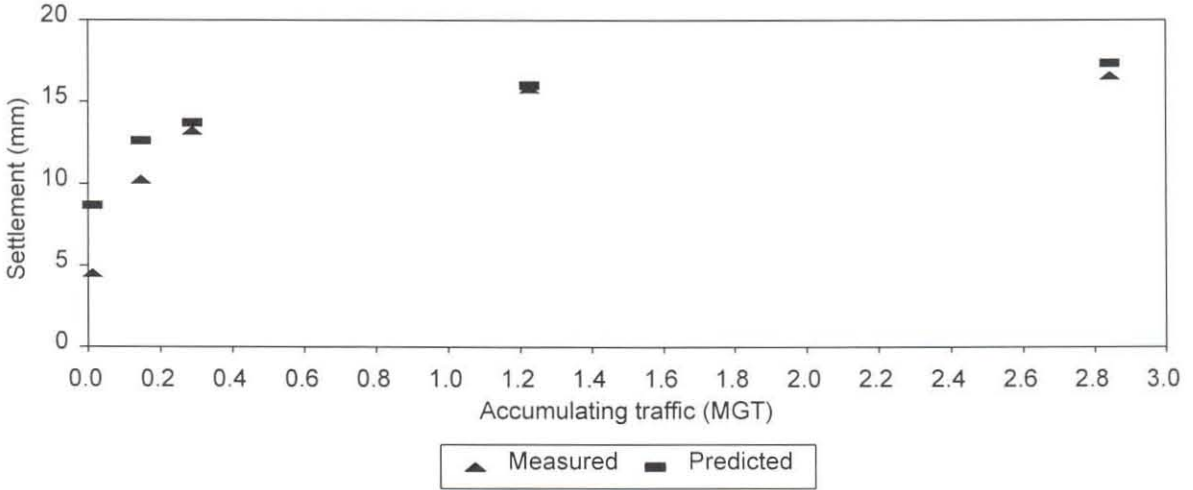
Figure 7.5: Average track settlement versus accumulating traffic.

UNDER THE LEFT RAIL

UNDER THE RIGHT RAIL
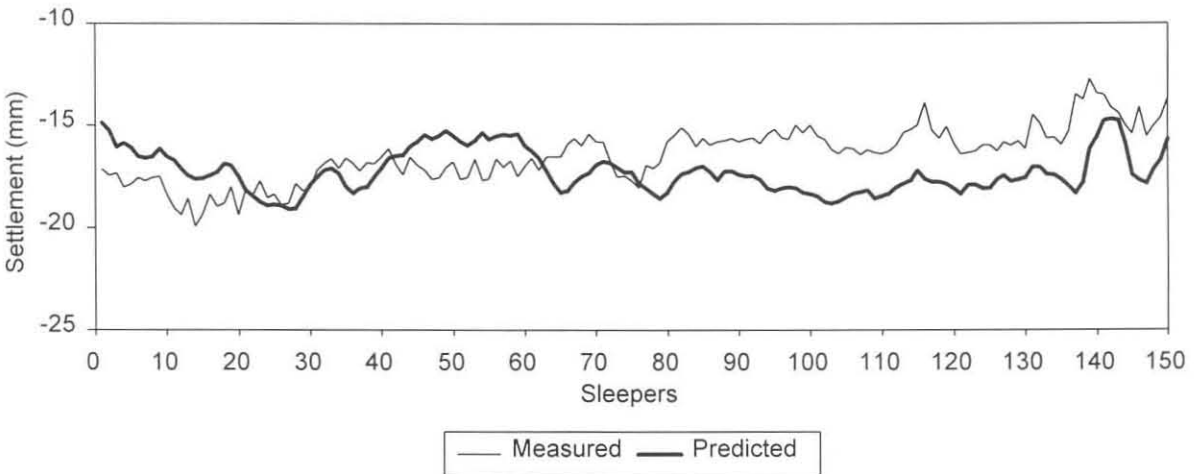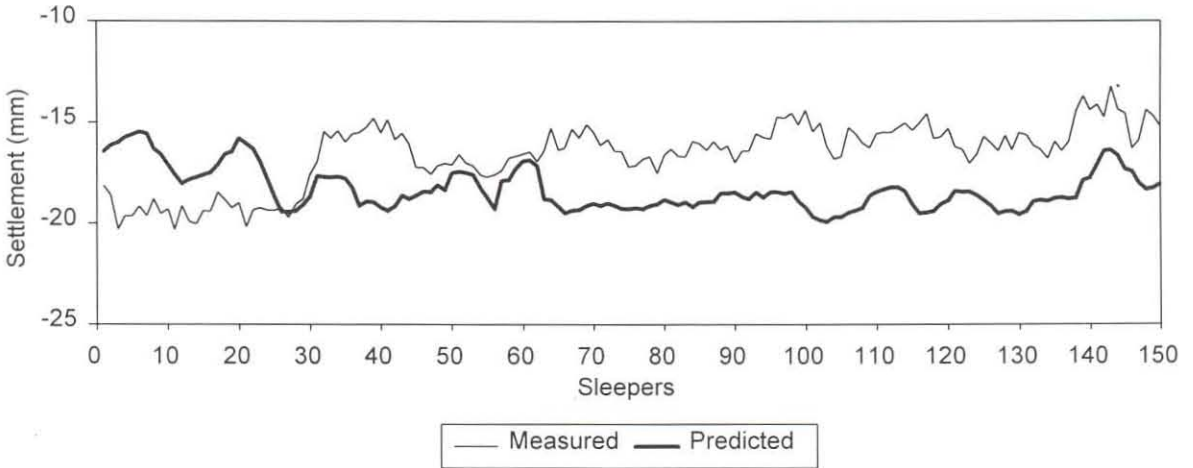
Figure 7.6: Measured and predicted track settlement.
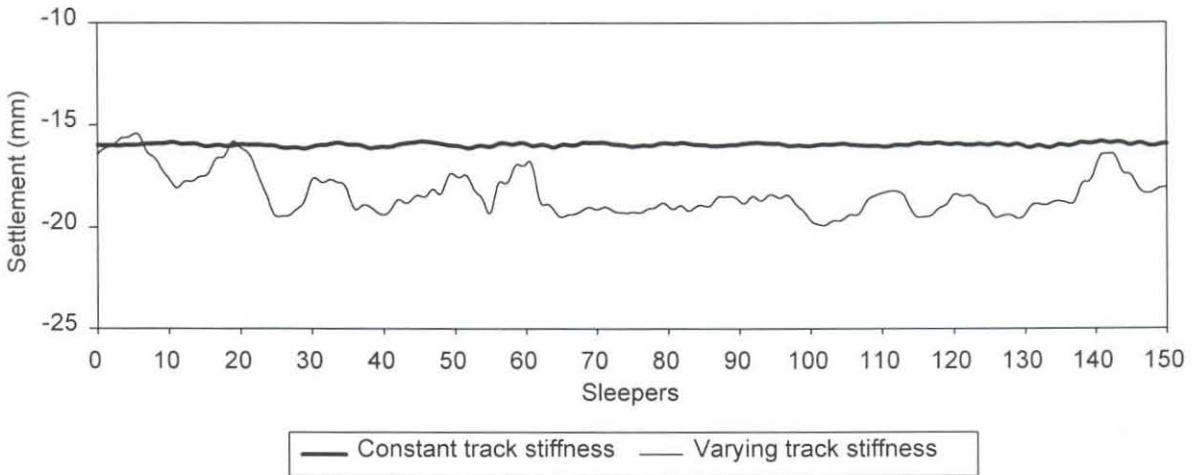
Figure 7.7: The influence of spatially varying track stiffness on track settlement.

The fact that differential track settlement is mainly a function of the spatial variation of the track stiffness can further be illustrated by looking at the wave length of spatial track stiffness variations and subsequent differential track settlement. Referring to Table 7.3, it can be seen that both the spatial track stiffness variation and the differential track settlement show dominant wave lengths of 8.1m and 32.5m. These two wavelengths also occur in the unloaded track geometry. When analysing the dynamic wheel loads, it was noticed that at the average speed of 40km/h these two wave lengths also occur but together with other shorter wave lengths which do not show up in the differential track settlement wave lengths.

In the remainder of this section the differential track settlement as predicted by the Static Track Deterioration Prediction Model is compared with that predicted by the Dynamic Track Deterioration Prediction Model. With all other conditions the same as used in the Dynamic Track Deterioration Prediction Model, the resulting differential track settlement is plotted in Figure 7.8. Comparing the track settlement that excluded the dynamic load component with that which included the dynamic behaviour of the vehicle, it can be seen that there is very little difference in the results. The reason for this small difference is the fact that the dynamic

wheel load is only about 20% of the static wheel load. If the dynamic component would be higher, the influence of the dynamic wheel loading would contribute more towards the differential settlement of the track and the Dynamic Track Deterioration Prediction Model would have to be used.

Table 7.3: Wavelength analysis after 2.84 MGT.

	Wave length [m]	Frequency at 40 km/h [Hz]
Track stiffness	32.5	0.34
	4.64 to 8.1	1.37 to 2.39
Track settlement	32.5	0.34
	8.1	1.37
Vertical surface profile	32.5	0.34
	14.4	0.77
	8.1	1.37
Dynamic wheel load	32.5	0.34
	8.1	1.37
	4.64	2.39
	1.48	7.66
	1.14	9.75
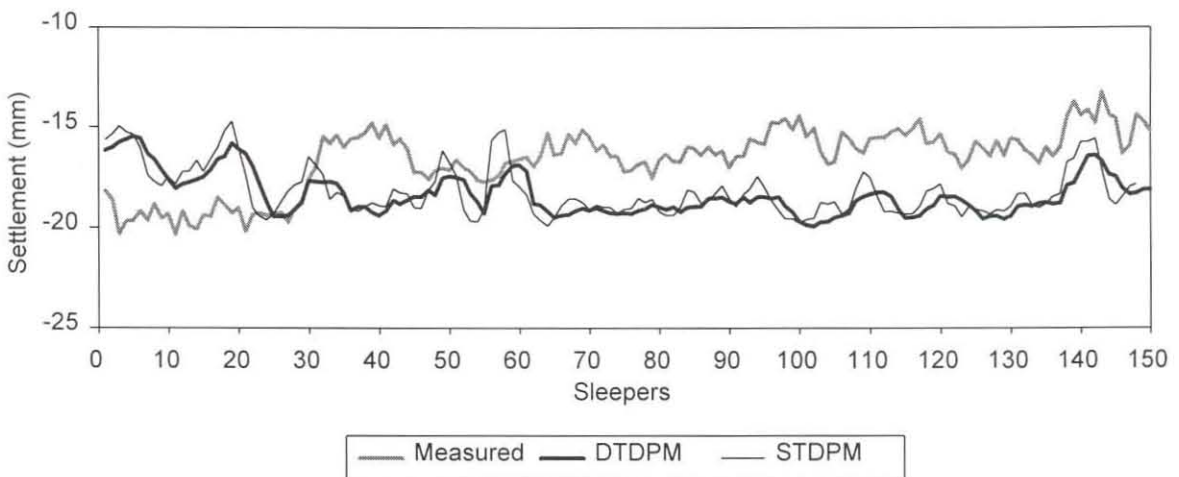
Figure 7.8: Measured and predicted track settlement including the STDPM.

Summary

As indicated, a good comparison is found between the overall envelope of predicted and measured dynamic wheel loading as well as differential track settlement. The models can thus be used to study the relationship between track stiffness, dynamic wheel load and track deterioration and to predict trends in track degradation. Specific applications are presented in Chapter 8.

7.3   ASSUMPTIONS AND SIMPLIFICATIONS

Deviations between measured and predicted results can be due to a number of issues not included in the prediction model. The most important assumptions and simplifications are listed and discussed below in terms of their overall influence on the calculated prediction.

- *No lateral track input* is included although the test section was on the end of a transition curve where deviations in the lateral alignment of the track occurred. The influence of this type of track input was not included as it would have required additional degrees of freedom and the modelling of wheel/rail contact geometry and creep. The system is thus only excited by the vertical space curve of the track and spatial variations in the vertical track support stiffness.

- *No lateral dynamics* is included in the vehicle/track model.

- *Static track stiffness* as measured by the track loading vehicle was used and assumed to be correct and similar to the actual dynamic track stiffness.

- *Constant and linear track damping* was assumed as track dynamics is not investigated as such.

- The correct *traffic mix* was not used in the analysis.

- The *condition of the ballast* was assumed to stay constant.

- *Weather conditions* like rainy spells were not included.

- *Settlement induced by vibration* through the track superstructure to the ballast was not included.

- A constant *vehicle speed* was assumed.

- It was assumed that there are no changes in *track stiffness* with accumulating traffic.

The question is now: "How can the Track Deterioration Prediction Models still be applied to predict track deterioration?" The answer is found by considering the purpose of the prediction models, which is firstly to evaluate the relationship between spatial track stiffness variations and differential track settlement, and secondly to predict the envelope of the prevailing dynamic wheel load. For both these purposes it is not essential to have an absolute match between measured and predicted values, but to be able to predict trends in terms of the dynamic wheel loads and changes in the track roughness. With this information available, improved fatigue assessment of the track superstructure is possible, and the increase in track roughness can be predicted as a function of vehicle type, axle load, vehicle speed, and the geometric as well as structural condition of the track.

The relative influence of the predicted dynamic wheel load and the measured spatial variation of the track stiffness on differential track settlement can be seen by considering Equation (4.7) and investigating the relative influence of the given parameters. The influence of these parameters is summarised in Table 7.4.

The contents of the table can be explained as follows. A 20% increase in the dynamic wheel load, which corresponds with the upper limit of the measured dynamic wheel load, causes the differential track settlement to increase by 5.6%. A lowering of the dynamic wheel load by 20% reduces the differential track settlement by 6.5%. The total variation in the dynamic wheel load of 40% thus corresponds with a 12.1% variation in the differential track settlement.

Considering all the results given in Table 7.4, it can be seen that the predicted differential track settlement is more sensitive to variations in the spatial track stiffness than to prevailing dynamic wheel loads. Furthermore, the actual measured

spatial variation in the track stiffness on the particular test section is higher than the measured variation of the dynamic wheel load. This further enhances the significant influence of spatial track stiffness variations on differential track settlement as against that of the dynamic wheel load.

Table 7.4: Influence of dynamic wheel load and track stiffness variations on differential track settlement.

Parameter variation	Differential track settlement	
	Variation	Range
Dynamic wheel load variations		
Actually measured variation: + 20% - 20%	+ 5.6% - 6.5%	12.1%
Maximum expected variation: + 50% - 50%	+ 13% - 19%	32.0%
Track stiffness variations		
Variation similar to dynamic + 20% wheel load variation: - 20%	+ 9.1% - 11.5%	20.6%
Actually measured variation: + 50% - 30%	+ 55% - 30%	68.0%

Summary

The purpose of the Track Deterioration Prediction Models is to predict the dynamic loading between the vehicle and the track, the differential settlement of the track, and to evaluate the importance of including spatial track stiffness variations in the analysis and prediction of track deterioration. Furthermore, the predicted dynamic wheel loads can now be compared to those assumed by amongst others Eisenmann (1972) for defining the design limits of various track components. In this respect a more realistic dynamic wheel load is now available to establish the rate of track component deterioration. On the other hand the predicted differential track settlement can be used to predict tamping cycles as a function of the prevailing dynamic loading as well as the spatially varying track stiffness.

CHAPTER 8

PREDICTION OF TRACK DETERIORATION

In this chapter two applications of the Dynamic Track Deterioration Prediction Model and the Static Track Deterioration Prediction Model are given. The first application is the prediction of void forming and the second one is the prediction of tamping cycles. Before doing these analysis, the track design and maintenance criteria as used by Spoornet are defined. The criteria are given to illustrate the value of predicting the dynamic loading and differential settlement of the track.

8.1 EVALUATION CRITERIA

In this section a list of track design and maintenance criteria as presently used by Spoornet is given. The limits as used by Spoornet are largely based on a dynamic wheel load as proposed by Eisenmann (1972) and are described in more detail in a paper by Lombard (1978).

- *Track roughness:* Track roughness is a direct indication of track quality and can be described in terms of the standard deviation as well as the Power Spectral Density (PSD) of the vertical track profile. Both criteria have not yet been finalized within Spoornet, but research work done up to now gives a good indication of possible limits. The track roughness, which is the standard deviation of the vertical track profile over 200m, is presently limited to 1.6mm on the coal export line. As can be seen from Figure B39 in Appendix B, the measured track roughness after 2.84 MGT is still well below the proposed limit. With respect to PSD value limits, an international envelop of PSD values as a

function of track geometry wave lengths is recommended (Fröhling, 1995). The advantage of PSD values is that they can be used to analyse the dynamic behaviour of the rail vehicle in the frequency domain.

- *Track geometry standards:* Track geometry standards are clearly defined in the Permanent Way Instructions (1984) of Spoornet. These standards are used to ensure that the track is maintained above a certain specified serviceability level and that the dynamic loading of the track due to passing traffic does not cause track design stresses in excess to those assumed in the design of the track. Predicted track settlement values can directly be related to these standards.

- *Stresses in rails:* The permissible stress in rails with an ultimate tensile strength of 700 to 800 MPa is given as 235 MPa. This allows sufficient reserve for the influence of temperature. Indications are that a 17% increase in the permissible stress (235 MPa to 275 Mpa) could reduce rail life by a factor of ten.

- *Wheel/Rail contact stresses:* The maximum contact stress between a wheel and a rail is proportional to the dynamic wheel load. The exact relationship depends on whether conical or profiled wheel profiles are used. A qualitative indication of the performance which could be expected from the rail is given in terms of the ratio of the dynamic contact stress to the yield strength. In general satisfactory performance can be expected with a ratio less than 2.8.

- *Rail seat load and sleeper bending strength:* Limits of the rail seat load are set at 153 kN or 172 kN depending on the type of track structure. Spoornet requires that the tensile stress in prestressed concrete sleepers is kept below 2.75 MPa.

- *Stresses below the sleeper:* The stresses in the ballast and the formation of the track are not evaluated in terms of limiting values but rather in terms of an expected change in track quality relative to a known condition. This approach makes the absolute stress values of secondary importance.

8.2   VOID FORMING

The influence of spatial track stiffness variations on differential track settlement is now investigated in terms of void forming. Using both the dynamic as well as the

static prediction models, void forming is simulated. Only one set of vehicle parameters, as close as possible to the test vehicle, is used to place the focus on track stiffness variations. To be able to determine and analyse the properties of the ballast and sub-ballast, a trench was excavated 2.84MGT after tamping. After taking the required samples the ballast was replaced without any form of tamping, thus creating a low track stiffness at Sleeper 77. Measurements of the vertical space curve and the spatial variation of the track stiffness were taken at this stage and used as input to the Track Deterioration Prediction Model to simulate void forming. For this analysis it is assumed that the void was created at the same time when the track was tamped. The analysis is thus done as if 13 MGT has passed over the entire test section. Simulated and measured results are shown in Figure 8.1 and Figure 8.2.
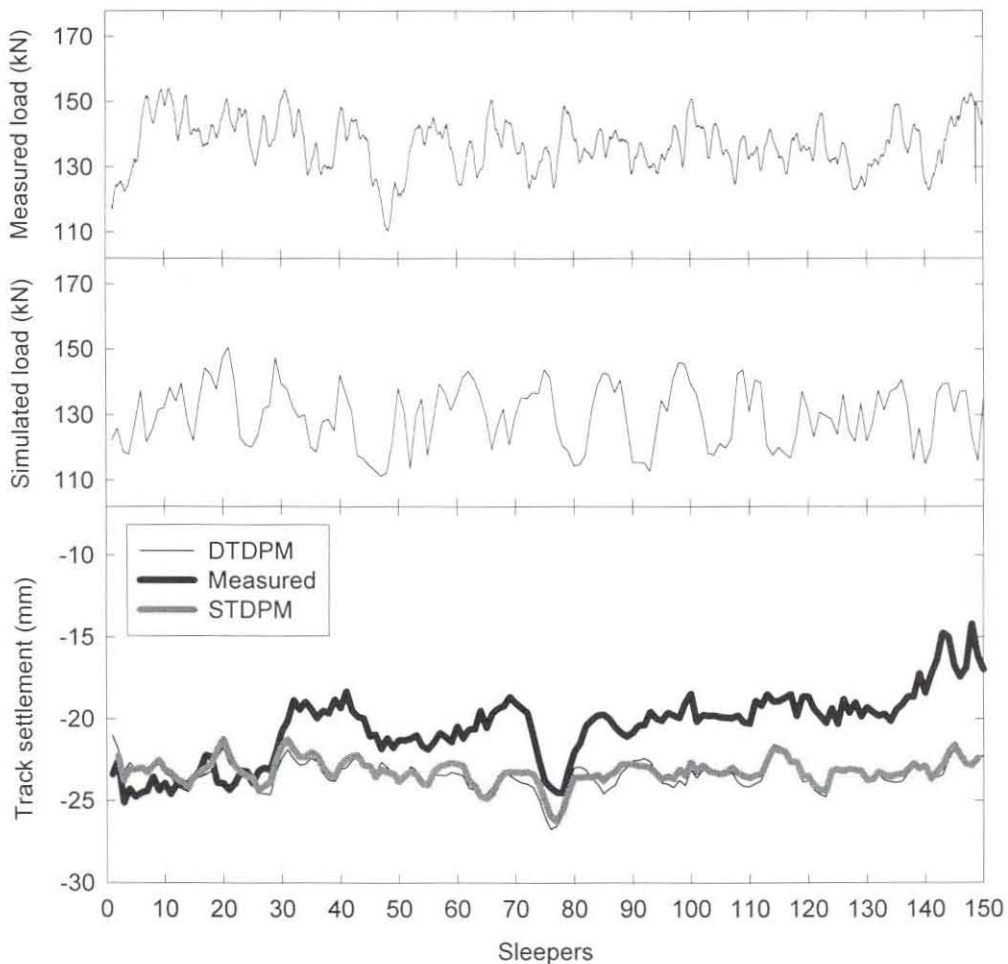
Figure 8.1: Simulated and measured void forming on the left side of the track.
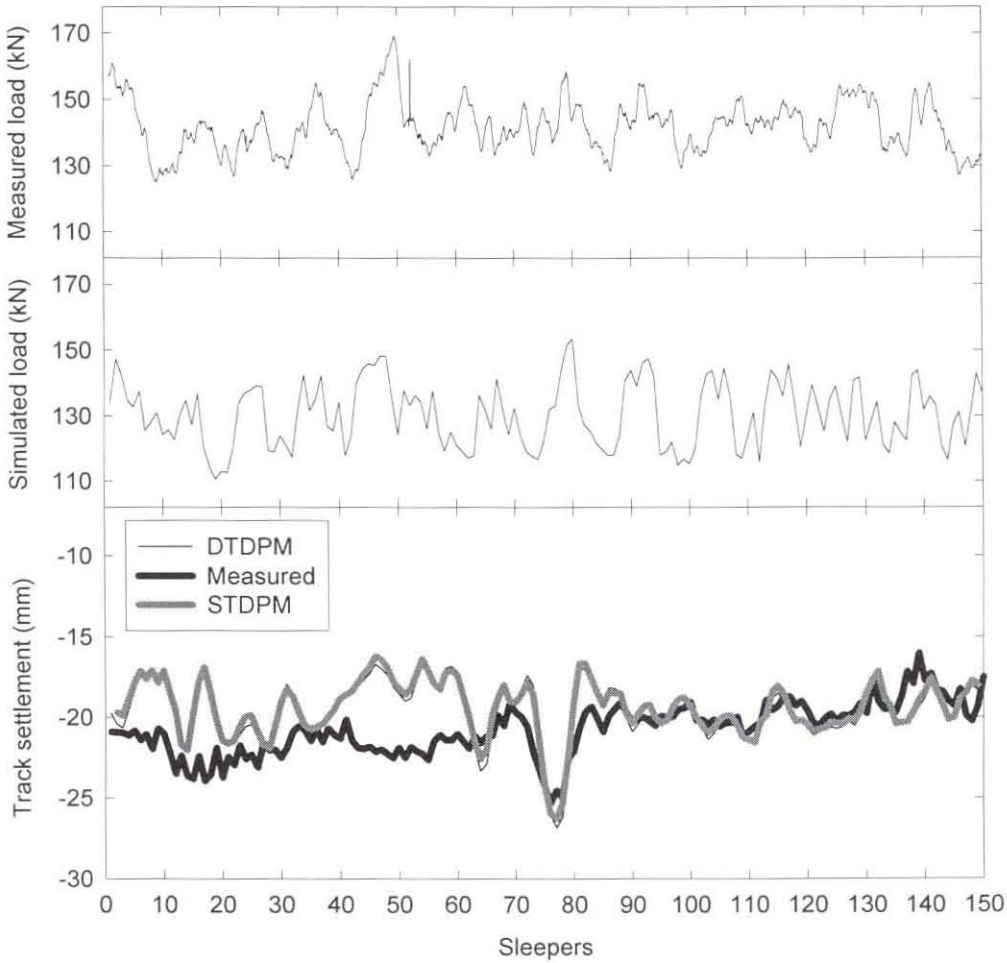
Figure 8.2: Simulated and measured void forming on the right side of the track.

As can be seen from Figure 8.1 and Figure 8.2, the increased settlement in the area around Sleeper 77 where the track was disturbed is predicted successfully. From the traces of both the measured and the simulated dynamic wheel loads it can be noted that the track had not yet deteriorated to such an extend as to significantly influence the dynamic wheel load even after 13 MGT of traffic.

8.3   TAMPING CYCLE

Another item of interest is that of predicted versus actual maintenance cycles. Maintenance history of the test site is given in Table 8.1. At present a standard

deviation of the vertical space curve of 1.6 mm over 200 m is used as the track roughness limit on this particular line. To predict the track roughness nine months after tamping (January to October 1996), 60 MGT of 26 ton axle load traffic was assumed. Using the Static Track Deterioration Prediction Model, the differential track settlement after the nine month period was calculated and converted into a roughness value over the length of the test site. The result was a track roughness of 1.57mm which agrees very well with the track roughness limit.

Table 8.1: Maintenance history at Km 7.

Tamping date	Condition measurement date	Standard deviation of top profile
January 1996		
	June 1996	1.0 mm
	August 1996	1.2 mm
	September 1996	1.4 mm
October 1996		

CHAPTER 9

CONCLUSION

The objective of this thesis was to develop a validated mathematical model to predict track deterioration due to dynamic vehicle loading, and nonlinear and spatially varying track stiffness, and to contribute to a better understanding of the relationship between spatial track stiffness variations and track deterioration. This was achieved by developing the Dynamic Track Deterioration Prediction Model and the Static Track Deterioration Prediction Model, and investigating the influence of track condition, vehicle speed and axle load on the vertical dynamic response of the vehicle/track system and the subsequent deterioration of the vertical space curve of the track. Both on-track measurements and mathematical simulations were used to analyse the current and to predict the future performance of the vehicle/track system.

Having realised the possible consequences of spatial track stiffness variations on track deterioration, the research work done to date and that presented in this thesis contribute towards a better understanding of the qualitative influence of various vehicle and track parameters. Research presented in this document clearly shows that spatial track stiffness variations contribute significantly towards track deterioration, both in terms of differential track settlement and increased dynamic wheel loading. Restoring the vertical space curve of the track by tamping is seen as only a temporary solution. More effective track maintenance would have to include procedures to reduce spatial track stiffness variations.

In Chapter 4 a methodology to predict track settlement was presented. The most important contribution is the development of the modified settlement equation. The constants of this equation are dependent on the basic properties of a certain section of track and can be determined by the procedure outlined in this document.

After considering a number of alternative vehicle/track models an eleven degree-of-freedom model was developed. This model was implemented in the Dynamic Track Deterioration Prediction Model which is able to predict both the dynamic loading of the track and differential track settlement. Results in Chapter 7 and 8 show that a good agreement is found between the overall envelope of predicted and measured dynamic wheel loading as well as differential track settlement.

The predicted dynamic wheel loads can now be related to the design limits of various track components. A reduction in the support resistance can for example be a major cause of over stress in the track and can lead to premature failure. Through the procedure developed in this thesis a more realistic dynamic wheel load is thus available to establish the rate of track component deterioration. On the other hand the predicted differential track settlement can be used to predict tamping cycles as a function of the prevailing dynamic loading as well as the spatially varying track stiffness.

The Track Deterioration Prediction Models developed in this thesis are a first step towards developing mathematical models that can predict vehicle/track system deterioration. In this thesis a simplified vehicle/track system model is used to analyse important relationships in the vehicle/track system. More complex models can be applied to the procedure developed in this research work.

Based on the results of the research done, the following further research and development work are recommended:

- The Track Deterioration Prediction Model developed in this thesis can be used as a basis for the development of a track maintenance planning tool. As the

vehicle/track model developed in this research is simplified and vehicle specific, other vehicle models or a general multi-body modelling package like Medyna, Nucars and Vampire (Schielen, 1990) could be used to model a variety of different rail vehicles while still applying the findings of this research. An essential input is however the spatial variation of the track stiffness. Finally the mathematical model could be expanded to include an economic model which can determine the life cycle costs of maintenance alternatives.

- A method has to be developed to measure the spatial variation of the track stiffness and the vertical space curve of the track over long distances and at a reasonable vehicle speed. Such information is essential for predicting track deterioration. An attempt in this respect has already been made by the China Academy of Railway Sciences (Wangqing *et al.*, 1997).

- Another important contribution of this research work is the measurement of dynamic track stiffness. This technique and the results obtained by it can open a new area of research in terms of geomechanical analysis.

There is no doubt that the findings of this research and the settlement model that was developed can be used to provide valuable information to the design and maintenance engineer of railway track. This thesis has addressed a more comprehensive and quantitative approach to track structure design and track performance evaluation and is seen to contribute to a new approach to track structure design and maintenance procedures in the near future.

APPENDIX A

LITERATURE REVIEW

In the literature review given in this appendix, problems due to the interaction between the vehicle and the track, various approaches to vehicle/track system modelling, and research with respect to track settlement is presented.

A.1 PROBLEMS DUE TO VEHICLE/TRACK INTERACTION

Most of the recent research on the dynamic behaviour of rail vehicles and the track has been stimulated by the need to understand the cause of practical problems arising from the interaction between the vehicle and the track and to develop solutions or treatments for those problems. Problems of vehicle/track interaction can be grouped into various areas of concern and are listed in Table A1 (Knothe and Grassie, 1993). The frequency range of particular interest for the different problems is also given.

Areas of primary concern to the present investigation are vehicle dynamics, bogies and unsprung mass, track ballast and track geometry. These issues are reviewed below.

Vehicle dynamics. The dynamic interaction between the vehicle and the track can cause problems with respect to the ride quality and the structural fatigue of the rail vehicle. In general, literature on the dynamic behaviour of rail vehicles is concerned with determining and evaluating ride quality (ORE Q C116 (Report 8), 1977; Parsons and Whitham, 1979). Hence, there are various ride quality standards

available (Anon., 1961; ORE Q C116 (Report 8), 1977; Becker, 1978; Uetake, 1980; Yamazaki and Hara, 1980; Garg and Dukkipati, 1984; ISO 2631/1, 1985). In recent years the ISO 2631 standard (ISO 2631/1, 1985) is applied in most cases.

Table A1: Problems concerning vehicle/track interaction.

PROBLEMS OF VEHICLE/TRACK INTERACTION		
	Areas of concern	Frequency range (Hz)
1	Vehicles	0-20
2	Bogie and unsprung mass including wheel bearings, fatigue of axles, brake gear etc.	0-500
3	Irregular running surfaces of wheel and rail, due to wheel flats, out-of-round wheels, wheel corrugations, rail corrugations, dipped welds and joints, pitting and shelling	0-1500
4	Track components, that is fatigue of rail in bending, rail pads, concrete sleepers, ballast and track geometry	0-1500
5	Wheel/rail noise in terms of rolling noise, impact noise and squeal	0-5000
6	Structure borne noise and vibration	0-500

With respect to structural fatigue, a great deal of research has been done. Of interest are the more recent techniques that make use of an integrated design methodology to evaluate structural fatigue (Luo *et al.*,1994). These procedures make use of multibody simulation packages (Schielen, 1990; Kortüm and Sharp, 1993) to determine the dynamic loads acting through the suspension onto the vehicle structure. Measured track data is generally used as excitation input. Using a finite element model of the structural component on which the dynamic forces are acting, stress concentrations are identified and analysed. Stress histories are determined under simulated loading and the fatigue life is determined using an appropriate fatigue theory.

Bogie and unsprung mass. Vehicle suspensions are commonly designed to ensure that the rigid body modes of the bogie and the vehicle body occur below 10Hz. This is done to ensure adequate isolation of passengers or sensitive cargo from the vibrations coming from the track and to reduce the effective unsprung mass. Reducing the unsprung mass reduces the dynamic loads at the wheel/rail interface. At frequencies above 20Hz the suspension of the vehicle isolates all but the unsprung mass from the track input. According to Cox and Grassie (1986), the greater the unsprung mass, the greater is the peak contact force at low frequencies, but at high frequencies changing the unsprung mass has a negligible effect. Thus, in the frequency range between 10Hz and 50Hz, the wheelset becomes increasingly well isolated dynamically from the bogie. Problems which may be aggravated if not caused by the dynamic loading of the unsprung mass are for example fatigue of wheel bearings, brake gear, axle-hung traction motors and other bogie components. To control the effects of the unsprung mass it is thus important to prevent suspension devices, which rely on frictional damping, to "freeze up" (Frederick and Round, 1984).

Track ballast and geometry. Deterioration of ballast and the consequential loss of track geometry is an enduring concern of every railway system. According to literature, this problem occurs as a result of low frequency, high amplitude loading, as well as due to high frequency dynamic loading. In a paper by Frederick and Round (1984) it is suggested that if the damping in the suspension of a vehicle is insufficient to curtail the natural frequency response of the vehicle to the forced input from the track, significant deterioration of the track geometry would occur in wavelengths of approximately 9m. At these low frequencies the effects of the vehicle body and bogie frame dynamics need to be examined.

Research work with respect to issues of secondary importance to this investigation is summarised and listed below.

Wheel flats:

- Dong *et al.* (1994): Impact loads due to wheel flats are studied using a finite element model. The effects of varying system parameters on impact loads due to a wheel flat are investigated and presented.

Out-of-round wheels:

- Ahlbeck and Hadden (1985): The development and validation of a computer model for predicting impact loads due to wheel running-surface geometry errors is described.

Rail corrugations:

- Grassie (1980): The influence of vertical forces on the development of both long and short wavelength corrugations is investigated using mathematical models of the wheelset and the track in the frequency range from 100Hz to 1500Hz.

- Grassie *et al.* (1982): Two dynamic models of railway track are presented. These models include the effect of the rail pads and are used to calculate both the response of the track and the contact force between a moving wheel and the rail in the frequency range from 50Hz to 1500Hz. It is shown that the rail pad is of fundamental importance in the attenuation of dynamic loads in this frequency range.

- Clark (1984): Three corrugation theories are described to predict vibrations which reproduce observed wear patterns. Proposals for corrugation avoidance are put forward.

- Knothe and Ripke (1989): A model is used to investigate why surface irregularities of a certain wavelength grow in the corrugation initiation phase. The basic concept assumes a feed-back process between high frequency, transient vibrations and long-term wear processes.

- Ilias and Müller (1994): A semi-analytical method for the analysis of high frequency vibrations of the wheelset and railway track is presented and evaluated with respect to its applicability to technical problems such as the

calculation of corrugation growth rates.

- Hempelmann (1994): In this thesis a linear model for the prediction of short pitch rail corrugations is developed. It represents the formation of corrugation by a feedback between structural dynamics and a damage process.

Dipped welds and joints:

- Jenkins *et al.* (1974): This paper describes research work to understand the mechanisms and characteristics of vehicle/track forces. Particular attention is given to peak forces generated by dipped rail joints.

- Radford (1977): Radford investigated the vertical forces between a wheel and the rail at a dipped rail joint. A computer program is presented which uses continuously supported rail on a flexible foundation. A symmetric dipped rail joint is used, and some results are given. It was found that the first force peak occurs at a very high frequency (500-1000 Hz), corresponding to interactions in the wheel/rail contact zone. This force is believed to fatigue the rail but is not transmitted into the ballast. The second force peak is of greater duration and lower frequency (20-100 Hz). This force is transmitted to the ballast, causing track deflection and is believed to cause ballast compaction and deterioration in track geometry at the joint.

- Botwright (1979): This paper discusses measures taken to reduce impact forces and to minimise rail defects. Specific attention is given to joints in welded track.

Rail pads:

- Grassie (1989): Loading under traffic of concrete sleepers with a variety of resilient rail pads is examined using data from several field experiments. In all cases dynamic loads on sleepers were significantly reduced using the pads.

Concrete sleepers:

- Grassie and Cox (1985): The dynamic response of railway track with a section of unsupported sleepers is examined experimentally and a mathematical model of such track is presented. It is shown that in the absence of support, concrete sleepers are likely to crack if there are modest wheel or railhead irregularities.

- Ahlbeck and Hadden (1985): In this paper impact loads on concrete sleepers are measured and predicted. The sleeper model takes the first four bending

moments of the sleeper into consideration.

- Grassie (1993): The technique proposed in this paper for calculating the dynamic response of railway track to non-sinusoidal irregularities on the running surfaces of wheel and rail is used to emphasise that adequate attention has to be given to moments caused by dynamic loads during the design of a new sleeper.

- Maree (1993): Laboratory and field tests on resilient rail pads for the use on concrete sleepers are discussed. A theoretical model for determining pad and ballast stiffness and damping with receptance curves is discussed.

A.2   MODELLING OF THE VEHICLE/TRACK SYSTEM

Mathematical models of the dynamic behaviour of the vehicle/track system are particularly valuable to the railway engineer because they enable phenomena to be explored which cannot easily be measured, and effects of changes to the vehicle/track system to be examined without making costly and perhaps damaging modifications to the system. Despite the fact that modelling of the behaviour of track has been done for more than 100 years, its behaviour, particularly due to dynamic loading was not as clear as the dynamic behaviour of rail vehicles. This relative ignorance simply reflects the greater importance that was traditionally attached to problems of vehicle dynamics as against problems dealing with track dynamics and vehicle/track interaction.

Traditionally, railway operation authorities, as well as vehicle dynamicists for that matter, have considered the wheel-rail contact patch as the limit of their interests (Ahlbeck, 1995). The structure below the contact patch was only of concern to the track maintenance department, civil engineering and the so-called "dirt and rock" modellers. Contrary to this tradition, the vehicle and track form a single, complex dynamic system in which the dynamic response of the track forms a significant part of the vehicle "suspension system". The success of a railway system design depends on the prediction and understanding of the effects of both vehicle and track

parameter variations due to ageing, wear, and degradation under service loads. The vehicle and the track thus form part of a complex feedback loop in which the dynamic loads generate changes in wheel and rail geometry and track response, which, in turn, result in higher loads. These load induced changes can affect vehicle ride quality, high speed stability, curving performance, vehicle and track maintenance, and operating safety.

The general objective in modelling the dynamic behaviour of the vehicle and the track is thus to reduce or contain the dynamic forces in the system. In 1959 Koffmann stated that a reduction in dynamic forces merits serious consideration. Spring and damper characteristics are matched to improve ride quality and reduce rail stresses. According to Koffmann, the dynamic wheel load depends on a number of factors such as track irregularity, sprung and unsprung mass, inertias and mass of the track, its stiffness, vehicle speed, as well as wheel diameter.

In the rest of this section a survey is given with respect to literature concerned with modelling the vehicle, rail, rail pad, sleeper, track foundation and finally the total vehicle/track system.

Vehicle model. The dynamic behaviour of the vehicle with respect to stability, steering and ride quality is most significant at low frequencies. This behaviour is understood adequately for most practical purposes, as is apparent from the fact that several software packages are commercially available to calculate the dynamic response of the vehicle. A comprehensive overview of these packages and some benchmarking results are given by Schielen (1990) and by Kortüm and Sharp (1993).

When using theoretical investigations to study the dynamic behaviour of a vehicle, criteria which affect the performance and the design of the railway vehicle have to be addressed. A review of some of the vehicle performance and design criteria is given by Newland and Cassidy (1975) and by Bhatti and Garg (1984).

Rail model. For static and stability analyses which were undertaken before 1960, the rail was considered to be a Bernoulli-beam (Winkler, 1867; Winkler, 1875; Timoshenko, 1926; Hetényi, 1946). Even now, it does indeed appear that this model is adequate for representing the response of the rail to vertical dynamic excitation for frequencies of less than 500 Hz (Grassie, 1993). However, such a model is no longer adequate for the response to vertical forces at higher frequencies as the shear deformation of the rail becomes increasingly important.

Rail pad model. In general, linearisation of the rail pads stiffness is justified. For vertical vibrations the pad is usually modelled as a spring and viscous dashpot in parallel. A model of the structural damping of the pad with a constant loss factor has also been used and is seen to be more consistent with the known behaviour of materials such as rubber (Knothe and Grassie, 1993).

Sleeper model. With respect to sleeper modelling two modelling theories are used; the Euler-Bernoulli theory and the Rayleigh-Timoshenko theory. The Rayleigh-Timoshenko theory is more accurate than the classic Euler-Bernoulli theory as it takes rotational inertia and shear deformation of the beam (sleeper) into account (Dahlberg *et al.*, 1993). The most complete sleeper model is a Timoshenko beam of variable thickness, which can be analysed using finite elements. Considerable success in correlating the calculated response of rail and sleepers in track to that measured at frequencies below about 700 Hz has been obtained by representing the sleeper as a uniform beam. In fact, it is known that the dynamic response to forces at the railhead is well represented up to 1kHz by modelling the sleeper simply as a rigid body.

To be able to predict crack development in sleepers under impact loads, Ahlbeck and Hadden (1985) have expanded existing vehicle/track interaction models. They developed and applied a validated seven degree-of-freedom nonlinear time-domain model. The response of track to high frequency excitation (50-1500 Hz) has also been analysed by Grassie *et al* (1982) to investigate short-pitch corrugations of rail.

In their paper Grassie *et al* present two new dynamic models, one continuous and the other incorporating the discrete mass of the sleepers. Rail pads were included in these models as they are of fundamental importance in the attenuation of dynamic loads in this frequency range.

Track foundation model. Through measurements it was found that the ballast generally deflects in a highly non-linear manner under load. In particular, there may be voids between sleepers and ballast, and the ballast itself may deflect nonlinearily (Esveld, 1989). Energy dissipation in the foundation occurs due to dry friction and wave radiation through the substrate. Despite this, most analyses use a simple two-parameter model in the vertical direction (Knothe and Grassie, 1993). A discrete sleeper support is used with the ballast being represented by a linear track stiffness and track damping. This model is justified if only the high-frequency dynamic behaviour is of interest and when the axle is close to the sleeper of interest. Loading and unloading when a bogie passes over a particular sleeper can be analysed approximately by such a linear model.

Other sleeper support models are discussed in a 'State-of-the-Art' paper by Knothe and Grassie (1993). There are in principle two different track support models, that is models with a completely continues support of the rail and those with a discrete support. Although a discrete support appears more representative of track laid on discrete sleepers, the corresponding continuous support is obtained by "smearing out" the discrete support along the track to get a continuous visco-elastic foundation and a continuous layer representing the sleepers. This continuous layer can model the sleepers as rigid bodies or as beams with distributed mass and stiffness. Continuous support models are valid for the calculation of the dynamic response of the track at frequencies below about 500 Hz for vertical excitation. A hierarchy of track models is also presented by Knothe and Grassie. The simplest representation of a continuous elastic foundation has been provided by Winkler in 1867. Winkler assumed the base to consist of closely spaced, independent linear springs. The only foundation constant is the foundation modulus. The most natural extension of the

Winkler model for homogeneous foundations is the Pasternak model where a second foundation constant, the "shear modulus", is also taken into consideration (Kerr, 1964; Dahlberg *et al.*, 1993).

The track structure can also be modelled as being of either finite or infinite in length. The type of structure is closely linked to the solution technique. Track structures of infinite length are commonly used for frequency-domain solutions whereas finite track structures are more appropriate for time-domain solutions.

Models of vehicle/track interaction. The individual sub-systems that form part of the total vehicle/track system are shown in Figure A1. Many similar models have been developed over the years (Zhai and Sun, 1993).
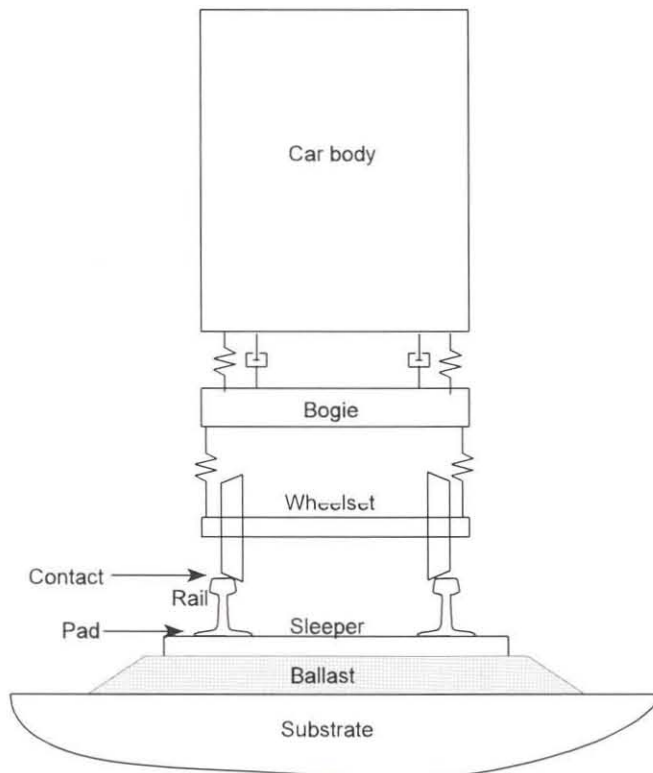

Figure A1: Components of the vehicle/track system.

To evaluate suspension features, Newland and Cassidy (1975) first considered the performance of a very simple single degree-of-freedom analytical model of the suspension system. In this model the mass of the bogie frame was neglected. Although the model yielded interesting data, it did not take account of bogie frame vibrations, which may lead to significant force transmission to the supported vehicle. Using a two-degree-of-freedom model the authors subsequently analysed fundamental design considerations as a function of a variety of track inputs.

The dynamic response of the vehicle/track system to non-sinusoidal irregularities was considered by Grassie (1993). Grassie showed that such calculations underestimate sleeper bending moments while overestimating the contact forces due to stiff and resilient rail pads. The model is used to assist in track design. Grassie's work also includes experimental measurements of the dynamic loads on the track. Irregular wheels are also used in the investigation. According to Grassie the dynamic load can be assumed to be 1.5 times the static load.

Another paper which is dedicated to the dynamic behaviour of the track and its foundation, is the paper by Girardi and Recchia (1991). They study the whole vehicle/track system as a unique mechanical system. The track foundation is modelled as a three-dimensional dissipation medium. Track and vehicle movements are modelled and solved using a classical finite element method.

In a paper by Nielsen (1994), the dynamic interaction between a perfectly round moving rigid wheel mass and an initially straight and non-corrugated continuous railway track is modelled. A parametric study to optimize the dynamic response of the track is done. The emphasis was to determine the maximum bending stress of the rail.

Basic theoretical models for the analysis of railway vehicles and tracks, and principle methods of their solution are also shown in a paper by Frýba (1987). The dynamic interactions between vehicle and track are emphasized and several basic

equations are given to show the behaviour of their elements. Possibilities are described of how to simplify the theoretical models in order to obtain a simple solution.

A.3   TRACK SETTLEMENT

The repetitive dynamic loading and unloading of the track structures from train traffic causes inelastic deformations in the ballast and the underlying foundation. As the traffic accumulates these deformations develop to a point where maintenance is required to restore the required vertical space curve of the track. Subsequently the deformation process starts again. A chronological overview of some of the papers that discuss this issue is given in this section.

A report released by the International Union of Railways' Office for Research and Experiments (ORE Q D71 (Report 10), 1970) describes laboratory and field studies aimed at discovering the fundamental laws describing the response of the ballast layer to repetitive loads. Studies were made by both British Rail and Nederlandse Spoorwegen research teams. The main conclusions were, that ballast becomes more stable, that is the rate of track settlement decreases as the number of load applications increases. Furthermore it was found that the settlement of the ballast is dependent upon the degree of initial ballast compaction. It was found that the use of on-line tamping machines for re-levelling the track, disturbs the underlying ballast only to be followed by a restart of the ballast deformation cycle.

In another research report (ORE Q D117 (Report 5), 1974), results of a series of triaxial tests on dry limestone ballast under repeated axial loading are described. It was found that the deformation of the ballast is proportional to the logarithm of the number of load cycles and proportional to the superimposed axial stress raised to an exponent between 1 and 3. The axial stress was found to depend mainly on the largest load when two load levels were applied. It was also observed that the axial stress reduced when full load removal did not occur between load cycles.

In 1982, Selig and Alva-Hurtado presented a methodology to calculate track settlement for maintenance cycle prediction. To analyse the stress state in the sub-structure of the track under vertical wheel loading, they used the three-dimensional elastic multi-layer computer model GEOTRACK (Chang *et al.*, 1980). Permanent strain behaviour was determined and integrated to estimate track settlement. The methodology described, provides a tool for predicting the elastic and permanent deformation behaviour of railway track systems and takes a variety of factors influencing the deformation behaviour into account. Factors taken into consideration are axle load, number of load cycles, rail and sleeper characteristics, and the properties and thickness of the ballast and underlying layers. According to Selig and Alva-Hurtado there is no general constitutive law available to account for the effect of cyclic loading in ballast and subgrade materials.

In another paper by Stewart and Selig (1982), the previous methodology is further described and the prediction of stresses and deformations that develop in the track due to residual horizontal stresses in the ballast, and due to the effects of shear stress reversal on the resilient modulus of the ballast is presented. A method to predict the strains in the ballast due to mixed wheel loads is also presented.

The paper by Leshchinsky *et al* (1982) presents a different simplified methodology for evaluating the effect of varying loads on the subgrade while also considering the non-linear properties of the substructure. A definition of a so-called "damage factor" is given. The damage factor is defined as the ratio of permanent settlement under heavier axle load to the permanent settlement under an existing axle load. A two-step technique is proposed. Firstly, the sleeper reaction has to be determined using a beam on elastic foundation model. Then the stress distribution can be calculated to evaluate the subgrade performance. After calculating the sleeper reaction due to an applied force, it is possible to determine the reaction of a sleeper away from the applied load. This makes it possible to use the method of superposition to determine the sleeper load due to several axles in the adjacent area.

The deterioration of the vertical track profile was also investigated by Lane (1982) using a computer model to calculate the deterioration of the track. Static and dynamic sleeper-ballast forces were predicted. Two models were used; one for localised discrete irregularities and the other for extended spatially distributed irregularities. In the extended irregularity model a Gaussian distribution of the ballast properties in terms of ballast stiffness was used. Ballast settlement properties were determined experimentally and calculations showed how the roughness of the track depends on both track and vehicle parameters.

In 1985, Shenton studied the deterioration of the vertical track geometry. Factors influencing the deterioration of the track were examined using a computer model which simulates the deterioration of the track due to various factors. The paper identifies six possible causes of track deterioration. They are, dynamic forces, rail shape, sleeper spacing, sleeper support, ballast settlement, and the substructure. These mechanisms can all take place simultaneously and are often interactive. Shenton described the quality of the track over a 200m section by the standard deviation of the vertical track profile. The deterioration under traffic was found to be a function of track quality. Observations over many kilometres of track lead to the conclusion that in general good track remains good and poor track remains poor throughout a period of many maintenance cycles. The number of tamping operations seem to have very little influence. It is concluded that the track has an inherent quality which is determined during the early part of its life in terms of the quality of track components, track foundation and work done during installation.

In a report released by the Office for Research and Experiments (ORE Q D161 (Report 1), 1987), historical data from work done by previous ORE Specialist Committees is analysed and the main factors influencing the deterioration of the track geometry are discussed. The relationship between the deterioration of the track geometry and the traffic carried is shown, but it was impossible to establishing laws relating to different traffic and track conditions. It was also found impossible to statistically differentiate between the effect of traffic, track

construction and foundation on the rate of track deterioration. Consequently further experimental research was recommended to obtain a better understanding of the discrete causes that lead to the deterioration of track geometry.

In 1989 Schwab and Mauer simulated the track settlement behaviour under dynamic loading conditions using an interactive algorithm comprising of three model components. The components consisted of a dynamic vertical vehicle model, a discrete finite element track model, and a mathematical model for the track settlement based on the settlement algorithm derived by Hettler (1984). Simulations of track settlement under various rail and track geometry errors are described and simulated results are discussed.

Extensive research work on elastic ballast deflection and settlement was also presented by Eisenmann *et al* (1993). By means of a power rule, which is in line with other European research work (ORE Q D71 (Report 10), 1970; ORE Q D117 (Report 5), 1974; ORE Q D161 (Report 1), 1987), the deterioration of the track was established on the basis of the prevailing ballast pressure.

In recent times more emphasis is being placed on efficient track maintenance. Using a variety of old or new track settlement equations and track settlement prediction models a mechanistic method to schedule track maintenance is combined with an economic model to determine the life cycle cost of maintenance alternatives. Chrismer and Selig (1993) for example used information on track and ballast conditions, together with a specific maintenance strategy, to calculate and relate the settlement of ballast, sub-ballast, and subgrade to differential settlement limits. Riessberger and Wenty (1993) state that track quality is the key to improved load bearing capacity and efficient maintenance. In their paper both practical experience and theoretical considerations are used to maintain the required load bearing capacity of the track and maintain excellent track quality under high axle load or high speed operating conditions. Machine systems for economical track maintenance are also considered.

APPENDIX B

EXPERIMENTAL WORK

Full details on the tests that were conducted as part of this research are given in this appendix. This appendix can be seen as a separate document describing the practical tools used to assess the performance of the vehicle/track system. Not only are factors such as the influence of axle load, vehicle speed and accumulating traffic on the performance of the vehicle/track system investigated, but full details are given on the test that was designed to simultaneously measure the performance of the vehicle and the track. An important contribution to track research in particular is the measurement and interpretation of the dynamic track stiffness under a variety of circumstances.

B.1 ROLLING STOCK

In this section the rolling stock that was used in the test train and that of the general traffic passing over the test section is described. Detail with respect to the suspension of the bogie of the test vehicle and vehicle instrumentation is also given.

B.1.1 Test Trains and Passing Traffic

A specially configured test train was used to conduct repeatable and controlled tests as a function of deteriorating track conditions. Initially, a so-called long test train was used to evaluate the effect of axle loading on the dynamic performance of the track. This test train was made up of one Class 6E1 electric locomotive, followed by a test coach, two CCL-5 wagons loaded to 26 ton axle load, two CCL-5 wagons

loaded to 30 ton axle load, two CCL-5 wagons loaded to 20 ton axle load, and two empty CCL-5 wagons . Figure B1 shows the axle load profile of the long test train. After three days only the wagons with 26 ton axle load remained in the test train.
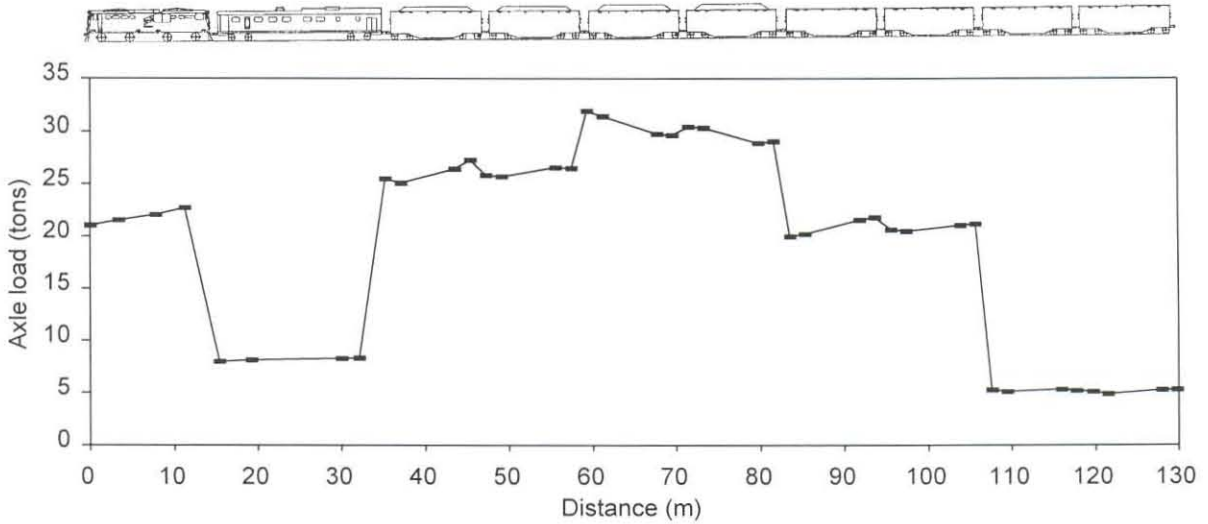

Figure B1: Loading profile of long test train.

Revenue earning traffic that passed over the test section was generally made up out of the following train configurations: 200 CCL-5 coal wagons, 100 CCL-1,2, or 3 coal wagons together with 100 CCL-5 coal wagons, or only 100 CCL-1,2, or 3 coal wagons. The loaded CCL-5 wagons have an axle load of 26 tons and the loaded CCL-1, 2 and 3 wagons have an axle load of 22 tons. These long trains were hauled by Class 7E1 or Class 11E electric locomotives with an axle load of 21 and 28 tons respectively. The distribution of the axle load over the test site after 13 MGT as obtained from traffic statistics from the Central Traffic Control Office in Vryheid is given in Figure B2. Figure B3 shows the distribution of the wheel loads as obtained from on-track measurements for two typical 200 wagon train configurations.
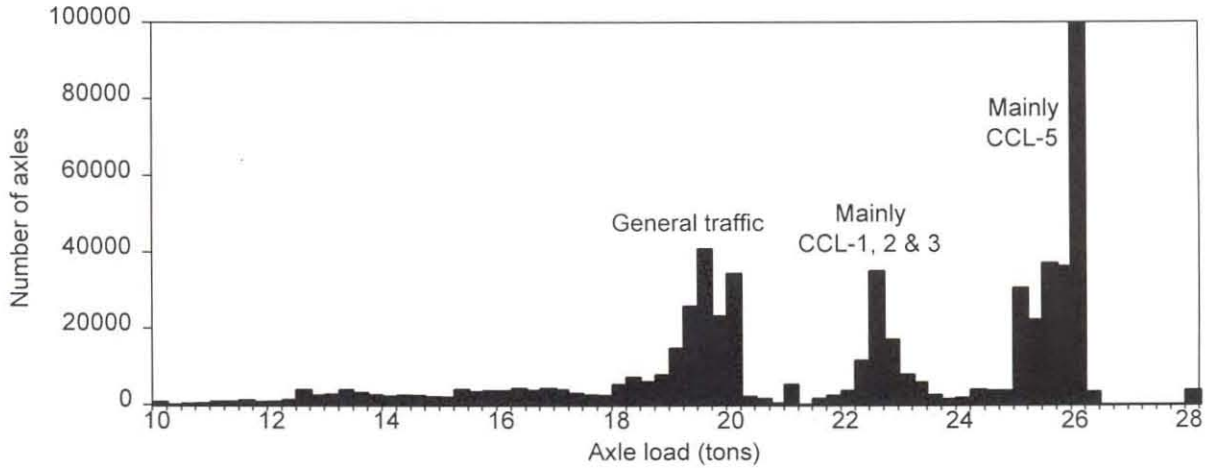
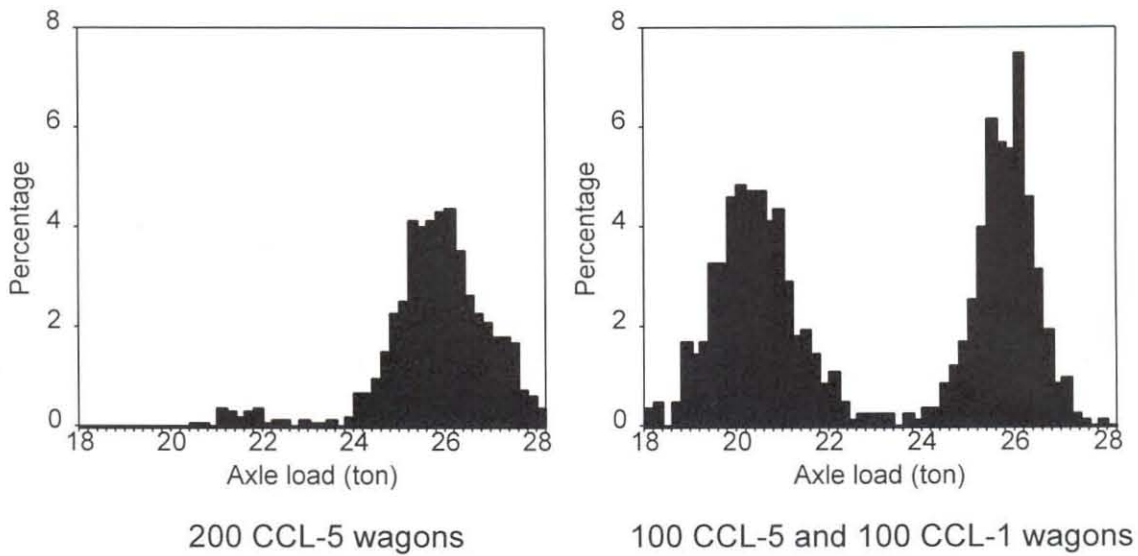Figure B2: Axle load histogram after 13 MGT of traffic.

200 CCL-5 wagons   100 CCL-5 and 100 CCL-1 wagons

Figure B3: Axle load histograms for two typical in-service trains.

B.1.2 CCL-5 Suspension Characteristics

The CCL-5 gondola coal wagon is equipped with two three-piece self-steering bogies of the type HS MkV which have a 26 ton axle load capacity. Pictures of the side and top view of the HS MkV bogie are given in Figure B4. In Figure B5, a drawing of the bogie is given for further clarity. From Figure B5 it can be seen that the bogie has both a primary and a secondary suspension. The primary suspension consists of two

vertically stiff (50 MN/m) rubber sandwiches per axle box. As this element is vertically very stiff, no displacement measurement were made across the element. A schematic of the secondary suspension which sits at the bolster/sideframe interface is also shown in Figure B5. The schematic clearly shows the position of the friction wedges which are resting on the stabilizer springs.
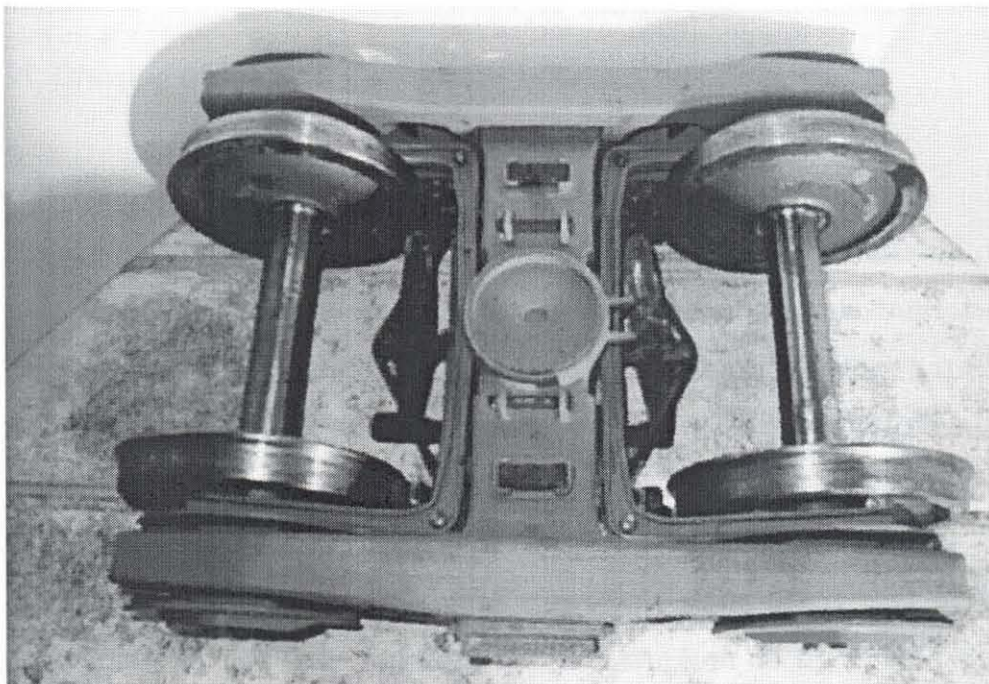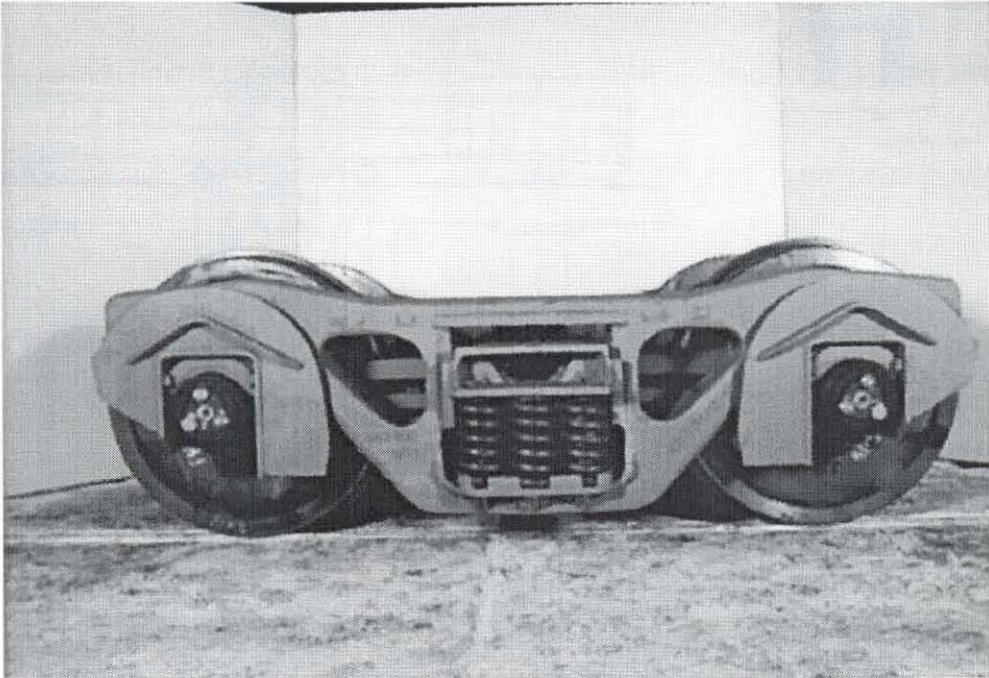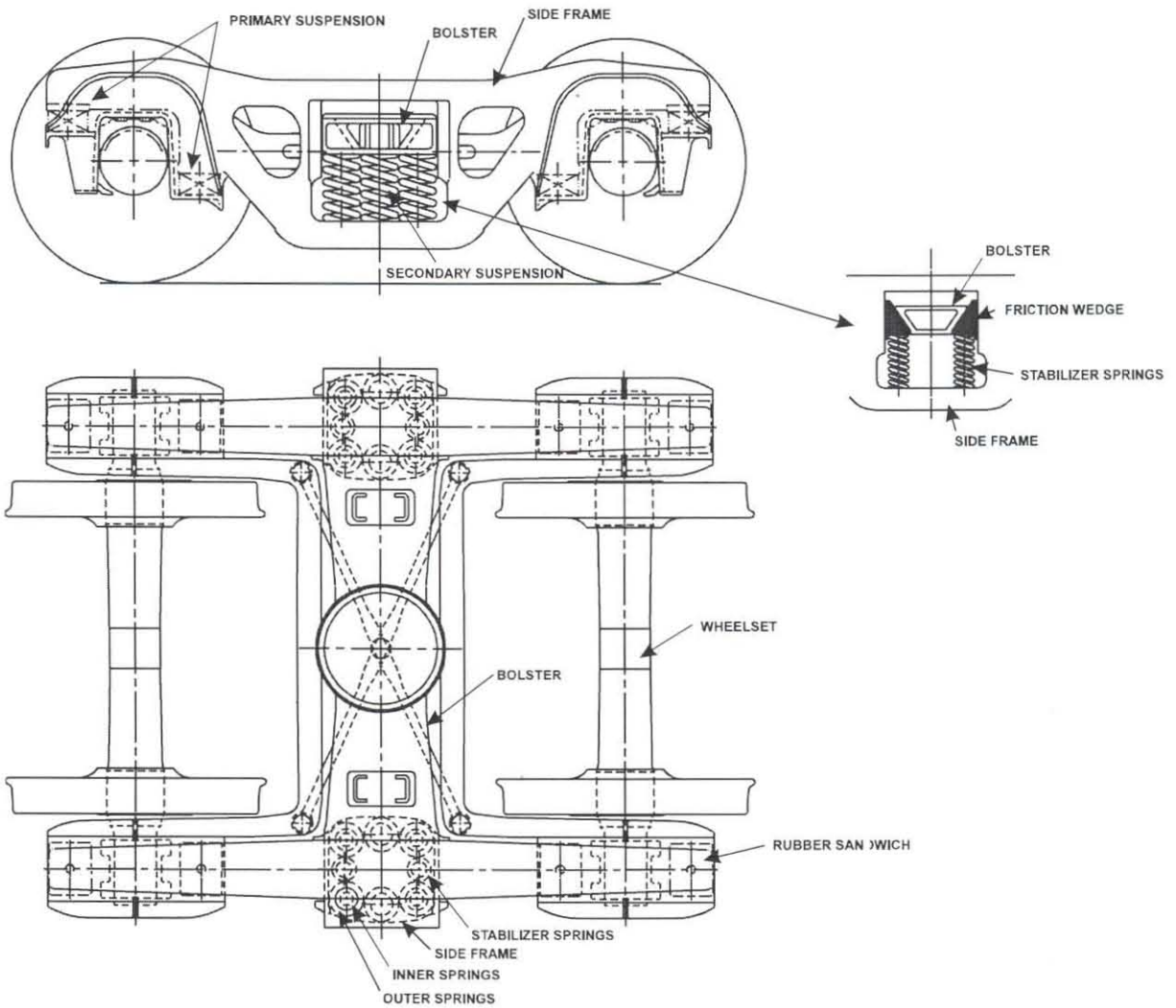

Figure B4: HS Mk V bogie.

Figure B5: Drawing of a typical three-piece self-steering bogie.

The secondary suspension is designed to provide load sensitive frictional damping between the side frame and the bolster, and to keep the side frames and the bolster square relative to each other. This is achieved by the friction wedge arrangement between the bolster and the side frame pocket. The weakness of friction damping is however well recognized (Giuns, 1980; Yabuto et al., 1981; Fröhling et al., 1996b). The problem is that energy absorbed by friction will always be lower than the energy input for the suspension element to work. As the decay rate of frictional damping is constant, the time required for the complete decay of energy is fixed. This means that as the speed of the vehicle increases, the time of travel between

track inputs decreases but the decay of energy remains constant. Thus, when the speed exceeds a certain limit, the following energy input comes before the preceding energy input has completely decayed. Under this condition, energy input exceeds decay and there is a build-up of energy into the vehicle. When this build-up and frequency of input approaches the natural frequency of the spring-mass system, resonance occurs. A reason why the system performs as well as it does in practice, is that track causes a random rather than a harmonic input of energy.

Extensive work has been done locally and internationally on characterising the behaviour of the secondary suspension of the three-piece bogie (Urban, 1991a; Urban 1991b; Fröhling et al., 1996b; Howard et al., 1997). Research conducted by Spoornet has shown that load dependant friction damping can be modelled using the following definitions for the friction force, Fff:

$$\text{Down stroke:} \quad \text{If } (\dot{y}_1 - \dot{y}_2) < 0.0 \text{ then} \quad F_{ff} = \frac{-(x_{ss} + (y_2 - y_1)) k_{ss} \mu}{\tan \alpha_w + \mu} \tag{B1}$$

$$\text{Up stroke:} \quad \text{If } (\dot{y}_1 - \dot{y}_2) > 0.0 \text{ then} \quad F_{ff} = \frac{(x_{ss} + (y_2 - y_1)) k_{ss} \mu}{\tan \alpha_w - \mu} \tag{B2}$$

$$\text{If } |C_{slope}(\dot{y}_1 - \dot{y}_2)| < |F_{ff}| \text{ then} \quad F_{ff} = C_{slope}(\dot{y}_1 - \dot{y}_2) \tag{B3}$$

This model has been validated against test results. A comparison between the measured and the calculated hysteresis loop for a similar bogie to that used during the on-track tests is shown in Figure B6.

In an attempt to linearise the load sensitive frictional damper (Yabuto et al., 1981; Fröhling et al., 1996b; Howard et al., 1997), it was found that this is difficult because the characteristics of any nonlinear system receiving random input is dependent on the level of energy input. The basic problem is that when the track geometry is smooth, the input from the track is small, and therefore the equivalent damping coefficient must be high. Conversely, when the track geometry is rough, the input from the track is large, and consequently the equivalent damping

coefficient must be low. In addition, vehicle speed also has an effect. The lower the vehicle speed, the greater the required equivalent damping coefficient.
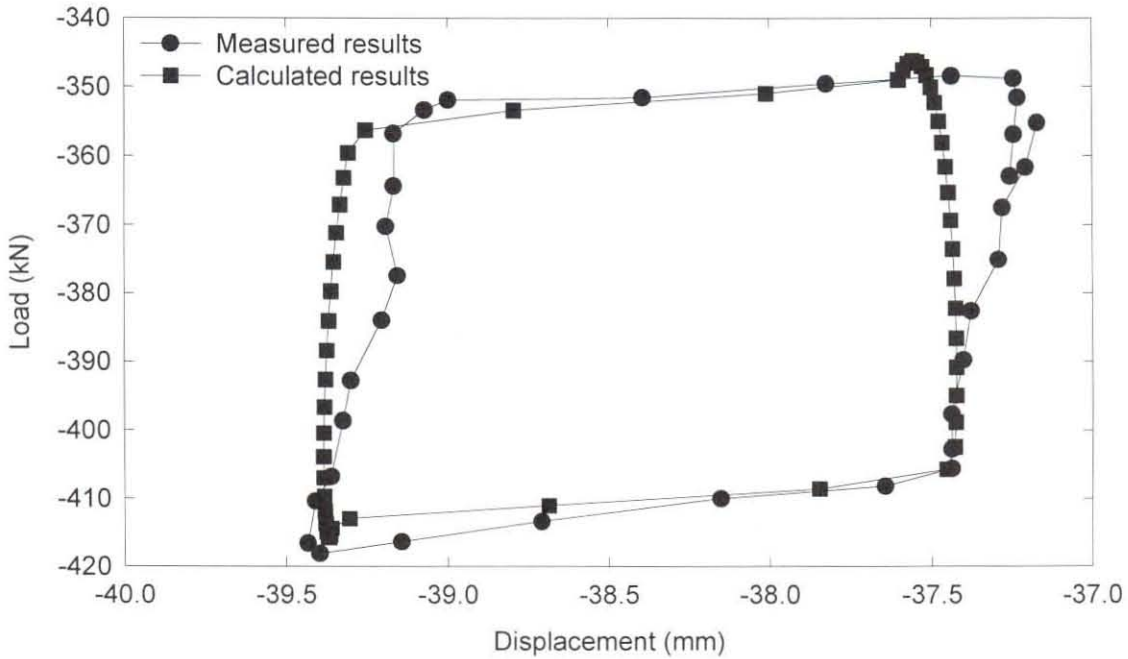

Figure B6: Measured and calculated hysteresis loop for a loaded HS Mk VII bogie.

B.1.3 Vehicle Instrumentation

In this section the purpose of each measuring device mounted to the test vehicle is given together with a full description thereof. Samples of recorded measurements are also included together with a short interpretation of the results. The photo of the test bogie in Figure B7 shows the position of the instrumentation used during the tests.
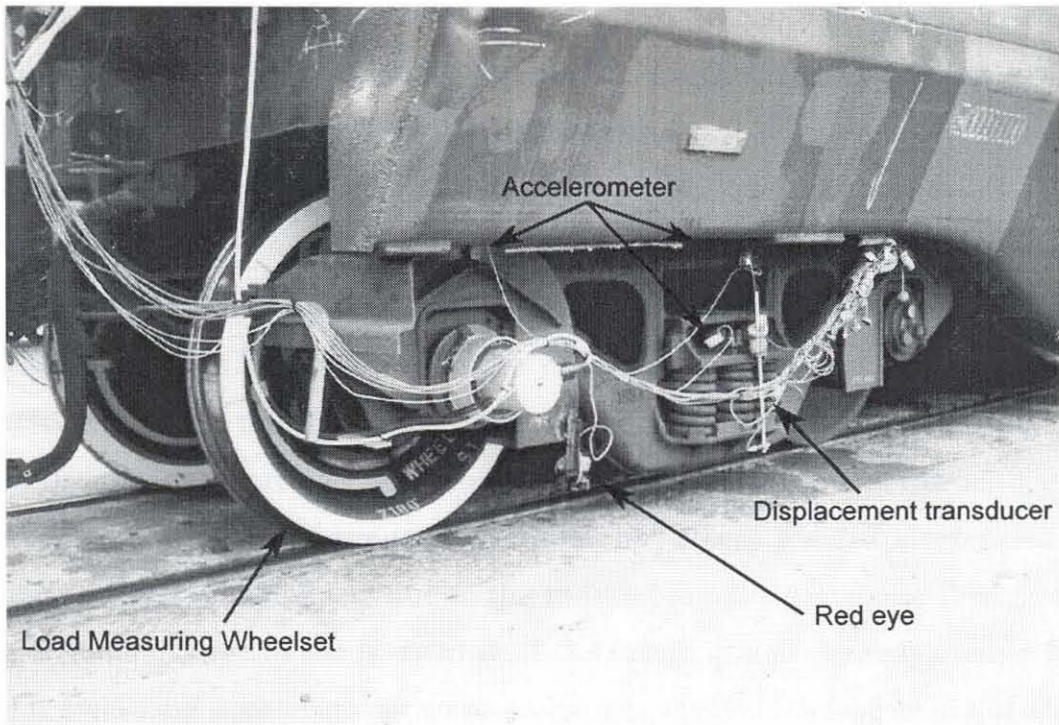
Figure B7: Test bogie and instrumentation.

B.1.3.1 Purpose and Description

The purpose and a brief description of the vehicle instrumentation is given below:

Data acquisition system: The primary elements to collect data are the instrumentation transducers, that is strain gauges, displacement transducers and accelerometers. These transducers translate the physical phenomenon of interest into an analogue signal with a calibrated relationship between the input and output quantities. This calibrated quantity is then converted into digital format and routed to a computer for real time data processing and/or storage. For the tests described in this document the CMS128 Continuous Monitoring System from TLC Software CC was used. The system is capable of sampling 128 channels at a disk spooling speed of 300kHz. During the tests, a sampling rate of 2kHz and 2.5kHz was used for the vehicle and track sensors respectively. The data was stored in a disk file which was subsequently retrieved and analysed using a post processing software module called CMSG128.

Red eye: The red eye was used to send out an infrared signal and pick up a reflection from reflector boards put out along the track to mark specific positions along the test track like the start and end position of the test section. The red eye was positioned 330 mm to the back of the leading wheelset of the test bogie.

Accelerometers: Accelerometers are electromechanical transducers which produce an electrical output proportional to the vibratory acceleration to which they are subjected. During the on-track tests, miniature Kyowa strain gauge type acceleration transducers were used to measure the vertical acceleration of various bogie components. In this type of accelerometer, strain gauges are bonded to an internal spring which deflects due to the induced accelerations and thus produces a proportional change in the resistance of the strain gauge. As indicated in Figure B7, the following accelerations were measured on the leading bogie of the test vehicle:

- Vertical acceleration of both axle boxes of the leading wheelset.
- Vertical acceleration at the centre of both side frames.
- Vertical acceleration at the left and the right outer ends of the bolster.

Linear Variable Differential Transformer (LVDT): LVDTs are used for measuring the displacement between two bodies. An LVDT consists of a movable magnetic core passing through a primary and two secondary coils. An Alternating Current (AC) voltage, called the excitation voltage, is applied to the primary coil, thereby inducing an AC voltage in each secondary coil, with a magnitude that depends on the proximity between the magnetic core and each secondary coil. The secondary voltages are connected in series opposition, so that the net output of the LVDT is the difference between these two voltages. When the core is at its midposition, the net output voltage is zero. When the core moves off centre, the net output voltage increases linearly in magnitude with a polarity depending on the direction of core displacement. For the tests conducted in this research two 100mm HBM LVDTs were used to measure the vertical deflection at both sides of the secondary suspension on the leading bogie.

Load measuring wheelset: The leading wheelset of the leading bogie was replaced by a load measuring wheelset. This wheelset was used to measure the vertical dynamic forces between the wheel and the rail. To determine the forces at the wheel/rail contact point, the load measuring wheelset is equipped with strain gauges on both the axle shaft and the wheel disk (Zeilhofer *et al.*, 1972; Ostermeyer *et al.*, 1980; Berg *et al.*, 1996). This is seen to be the correct combination for measuring the wheel/rail contact forces, because due to the variation of the wheel contact point, the lateral guiding forces as determined by the strain gauges on the axle include a systematic, analytically quantifiable error. Including the wheel disk in the measuring circuit allows an exact determination of the wheel guiding forces as well as a continuous recording of the wheel/rail contact point. Calculations are done in accordance with force and moment equilibrium equations by a digital computer.

B.1.3.2 Sample Measurement and Interpretation

In Figure B8, a set of measured results are given to illustrate the typical behaviour of the test vehicle over the test track. In the example given, the speed of the test vehicle was 40km/h. The two vertical lines at position B and C in the middle of the top graph indicate the position of the middle thirteen sleepers of the test site that were instrumented. The whole section between position A and D includes 150 sleepers at a 0.65 m sleeper spacing.

By comparing the vertical accelerations on the axle box with those on the side frame it can be seen that the high accelerations occurring at the axle box are significantly reduced in the side frame. This is due to primary suspension of the bogie. However, by comparing the vertical acceleration of the side frame with that of the bolster it is noticed that the acceleration of the bolster is more or less equal to the acceleration of the side frame. Hence, the secondary suspension seems to be unable to reduce the magnitude or frequency of the forces due to friction locking.
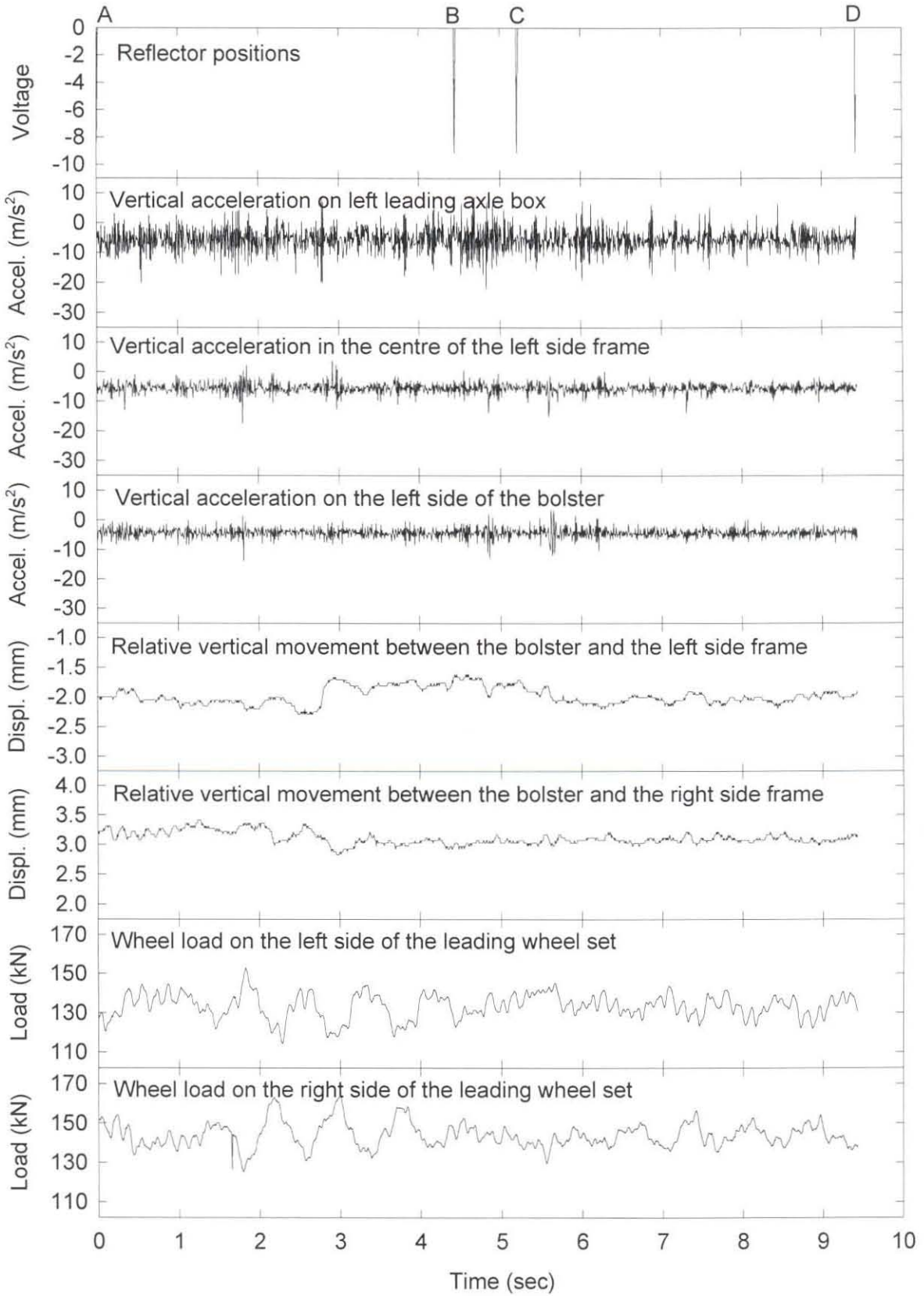
Figure B8: Measurements taken on the instrumented bogie.

Another point of interest is the fact that there is very little movement across the secondary suspension. Only about a 1mm displacement was measured in this instance. This confirms the fact that there is a high resistance to movement in the secondary suspension. A further observation can be made in terms of the measured dynamic wheel load. Here it can be seen that some rolling motion of the vehicle takes place and the dynamic wheel load component is about 20% of the static wheel load.

B.2   INFRASTRUCTURE

In this section a description of the test site is given, followed by detail with respect to track instrumentation and measurements done.

B.2.1 Test Site

The test site was between mast pole 7/2 and mast pole 7/4 on the line between Vryheid and Richards Bay on the Heavy Haul Coal Export Line. The test section was 150 sleepers long and the middle thirteen sleepers were instrumented to measure the dynamic behaviour of the track. Design details of the track are given in Table B1.

Table B1: Track design details.

Parameter	Value
Sleeper length	2200 mm
Sleeper spacing	650 mm
Sleeper width	259 mm
Sleeper area	$5.981E+004$ mm^2
Sleeper weight	285 kg
Sleeper stiffness (EI)	$1.235E+004$ kN.m^2
Rail spacing	1140 mm
Rail area	7703 mm^2
Rail weight	60 kg/m
Rail stiffness (EI)	6558 kN.m^2
Rail fastener stiffness (HDPE rail pads)	$1.2E+006$ kN/m

The photos in Figure B9 give an overview of the track cross section at Sleeper 77 in the middle of the test section. After excavating a trench, the substructure was analysed. In Figure B10 a schematic cross section at Sleeper 77 is given. Relevant properties of the ballast samples are given in Table B2. From this information the following observations were made:

- Clean ballast was found under the sleeper while the shoulder ballast was contaminated with a substantial amount of coal.
- The bitumen layer was solid with a mixture of fowling material, ballast and bitumen.
- The bottom of the sub-ballast was 560mm and the natural soil was 770mm below the sleeper.

Site overview

Clean ballast under sleeper

Layers above and below bitumen layer

Layers down to natural soil

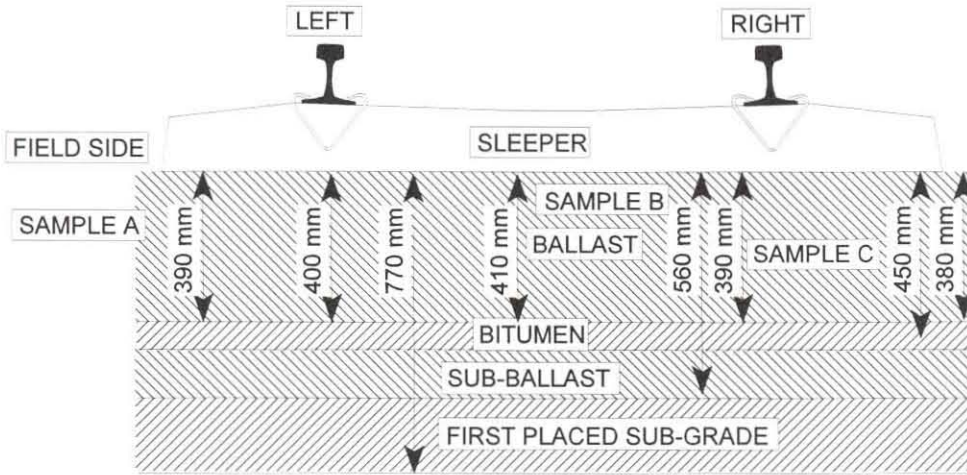Figure B9: Details of the track cross section at Sleeper 77.

Figure B10: Schematic cross section at Sleeper 77.

Table B2: Ballast properties.

Test	Sample A: Shoulder sample above bitumen	Sample B: Ballast under sleeper	Sample C: Ballast below sleeper under right hand rail down to bitumen layer
L.A. Abrasion (Specification < 22%)	10.88%	18.36%	11.24%
Absorption (Specification < 1%)	0.08%	0.18%	0.18%
Sieve analysis			
Sieve size	% Passing	% Passing	% Passing
63.0 mm	100.0	100.0	100.0
53.0 mm	97.5	98.6	100.0
37.5 mm	63.9	69.7	77.7
26.5 mm	20.8	23.6	29.8
19.0 mm	7.5	5.7	10.4
13.2 mm	6.0	2.5	7.3
9.5 mm	5.7	1.9	6.2
Pan	0.0	0.0	0.0

In Figure B11 the layout of the track around the selected test section is given together with the track geometry as measured with the Plasserail EMV80 track recording car. With reference to Table B3, which gives a summary of South African track standards (Permanent Way Instructions, 1984), it can be seen that the cant, the lateral alignment as well as the vertical surface profile of the track are well within the given track maintenance standard. In Figure B12 the resulting root mean square (RMS) values of the measured dynamic wheel load as calculated over 50m while the test vehicle was travelling at 70 km/h is given.

Table B3: Spoornet track standards.

	Construction standard A	Maintenance standard B	Safety standard C
Vertical surface profile (7m chord)	+3mm; -3.5mm	+14mm; -14mm	+19.4mm; -19.4mm
Lateral alignment (10m chord)	2.5mm	10mm	14mm
Cant	±3mm	±12mm	±16mm

In Figure B13 a selection of cross sections along the test track are shown. From the figure it is clear that the whole test section was in a cutting. The depth of the cutting increases from Sleeper 1 to Sleeper 150.

In general, track condition is defined by its functional as well as its structural condition. The functional condition is described by the geometric irregularity of the track, and the structural condition of the track is defined by the structural strength of the track components which is measured in terms of the track stiffness and the variation thereof. More information in this respect is given below.
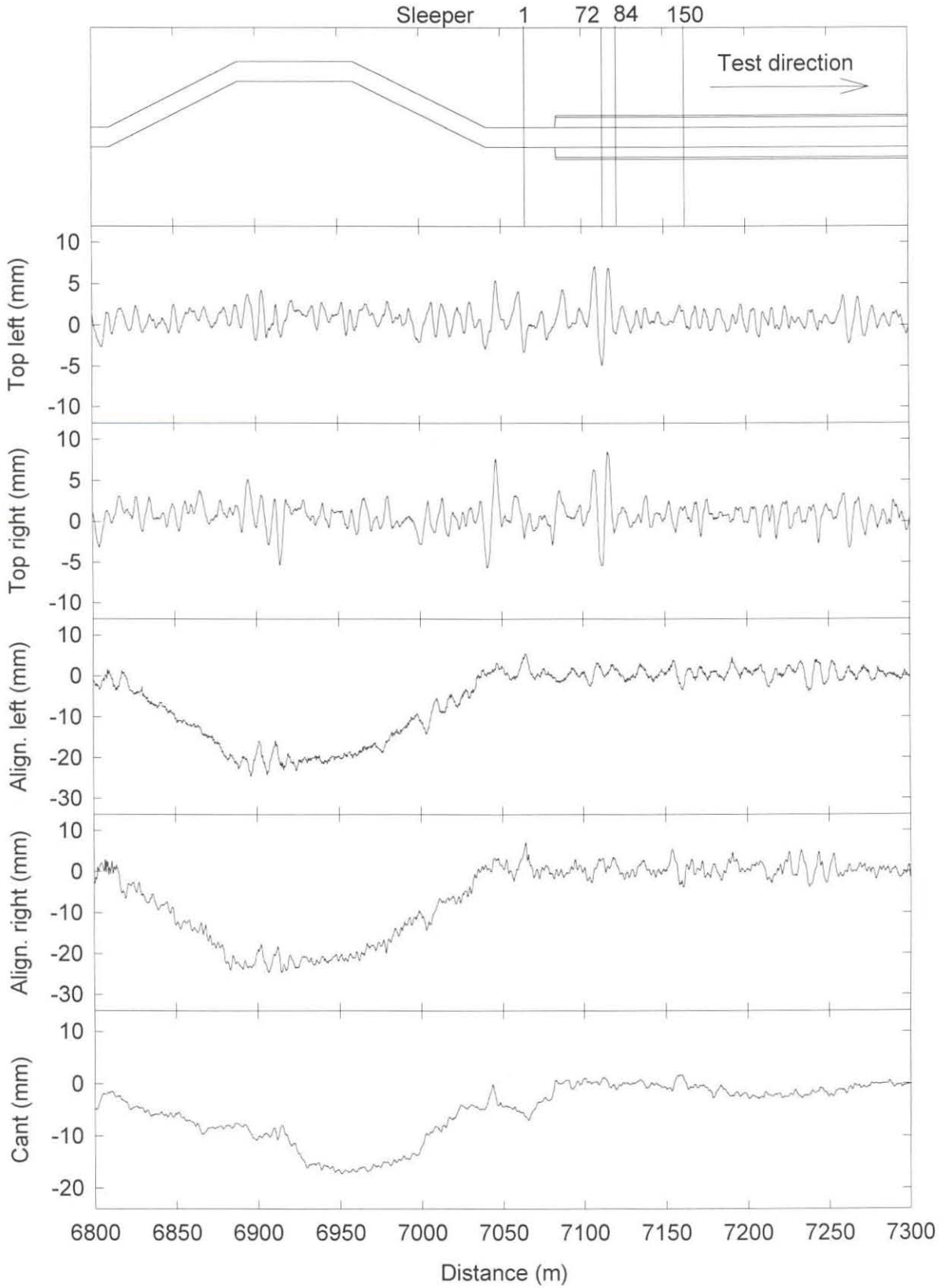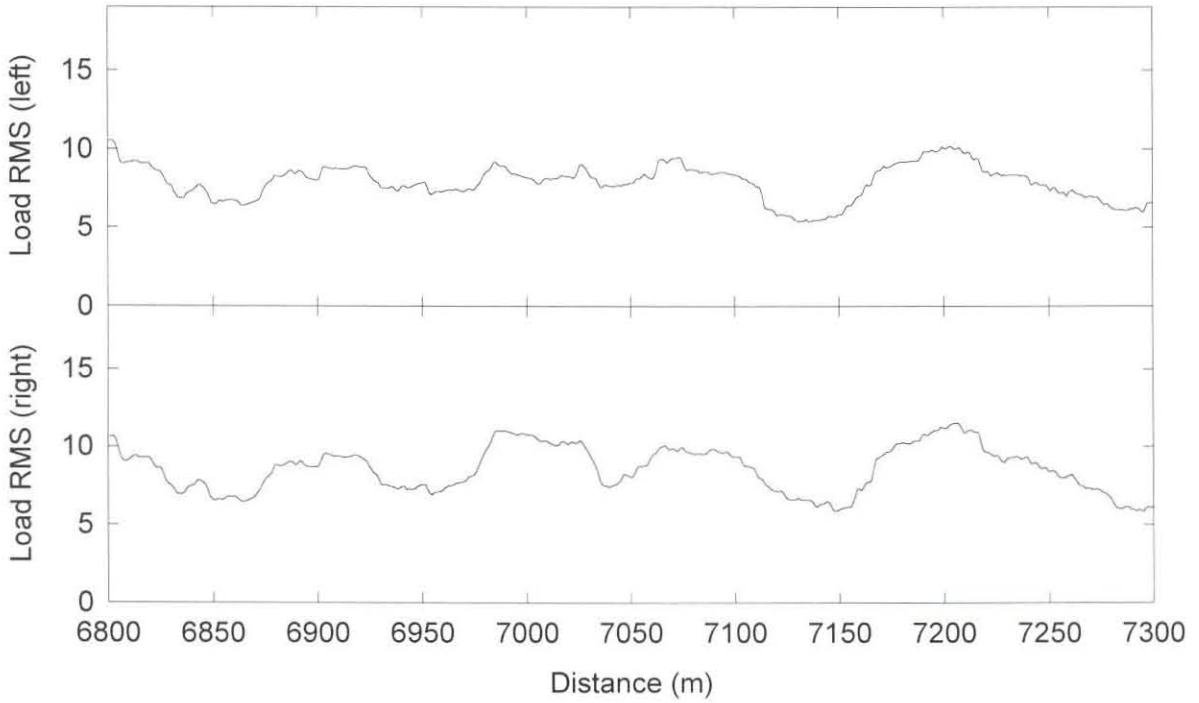
Figure B11: Track layout and geometry.

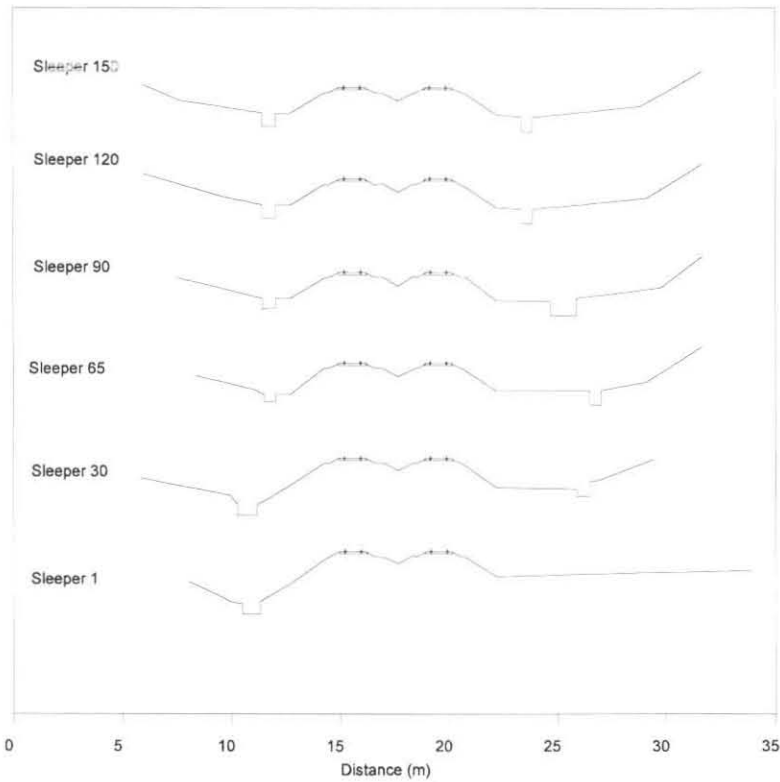Figure B12: Root Mean Square values of the wheel load at 70km/h.

Figure B13: Cross sections at test site.

B.2.2 Level Measurements

One of the elements describing the functional condition of the track is the vertical profile of the track. The most common methods used to measure the vertical alignment of the track are, absolute measurements, mid-chord ordinate measurements, dynamic measurement, and inertial measurements (Frederich and Hecht, 1986; Hecht, 1988). The general method used in South Africa is the mid-chord ordinate measurement method (Fröhling, 1995). Unfortunately the relationship between the fixed measuring chord length used and the variable track wavelengths causes a wavelength dependant response. Methods to obtain the "true" longitudinal track profile from such measurements have been proposed in literature (Cohen and Hutchens, 1970; Fröhling, 1995; Mauer, 1995).

For the purpose of this investigation the track geometry was only required for a short section of track and thus the absolute measuring technique was used. Measurement of the absolute unloaded vertical track profile was done with a digital level Wild NA3003 with a resolution of 0.001mm. To be able to do a settlement analysis, the track geometry measurements at each time interval were referenced to two fixed beacons on either side of the test site. Measurements were done before each test series in order to monitor the settlement of the track as a function of accumulating traffic.

B.2.3 Static Track Stiffness Measurements

As mentioned, the structural condition of the track is primarily defined by the stiffness of the track. It is known that the stiffness of the track is generally nonlinear and varies from point to point along the track (Fröhling *et al*, 1996a). For this research the "BSSM" (Baan Styheids en Stabiliteits Meeting) track loading vehicle as shown in Figure B14 (Ebersöhn, 1995) was used. Track stiffness was measured by applying a single point load to each rail above the sleeper using two independent hydraulic cylinders (Ebersöhn and Selig, 1994) and measuring the

vertical displacement of the sleeper via a tiltmeter. The tiltmeters were mounted on a beam independent of the "BSSM" machine.

Before each measurement, the tiltmeter offset was zeroed and then simultaneous readings were taken at a zero, 29kN (3 tons), 49kN (5 tons), 78kN (8 tons) and 128kN (13 tons) load on each rail. Once the target load had been reached, a waiting period of ten seconds was required before the displacement was recorded. This was necessary to eliminate any vibrations that occurred in the beam due to the load applications by the machine. Before each test series the tiltmeters were checked with a digital level and recalibrated if required. Track stiffness measurements were conducted over the entire 150 sleeper test track and measurements were done at the same time as the track geometry measurements. Hence, a continuous measurement of the varying track support stiffness was obtained.

The unloaded vertical space curve and the loaded profile of the left and right rail as measured directly after tamping is shown in Figure B15. Figure B15 also shows the track deflection due to a 29kN and a 128kN load on the left and the right rail. From Figure B15 it can be seen that the left side is softer and has a higher stiffness variation than the right hand side. This is because the test track is on a double line and the left rail is on the field side.
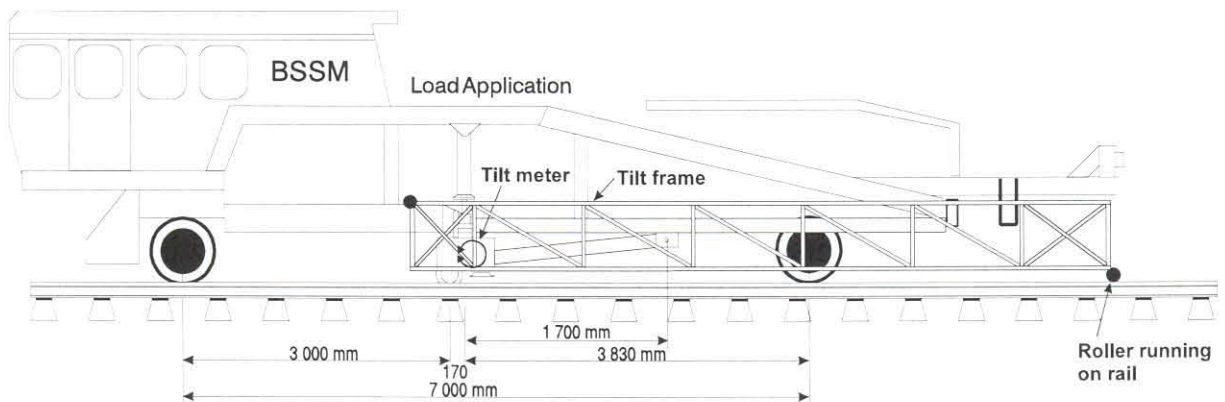

Figure B14: "BSSM" track loading vehicle.
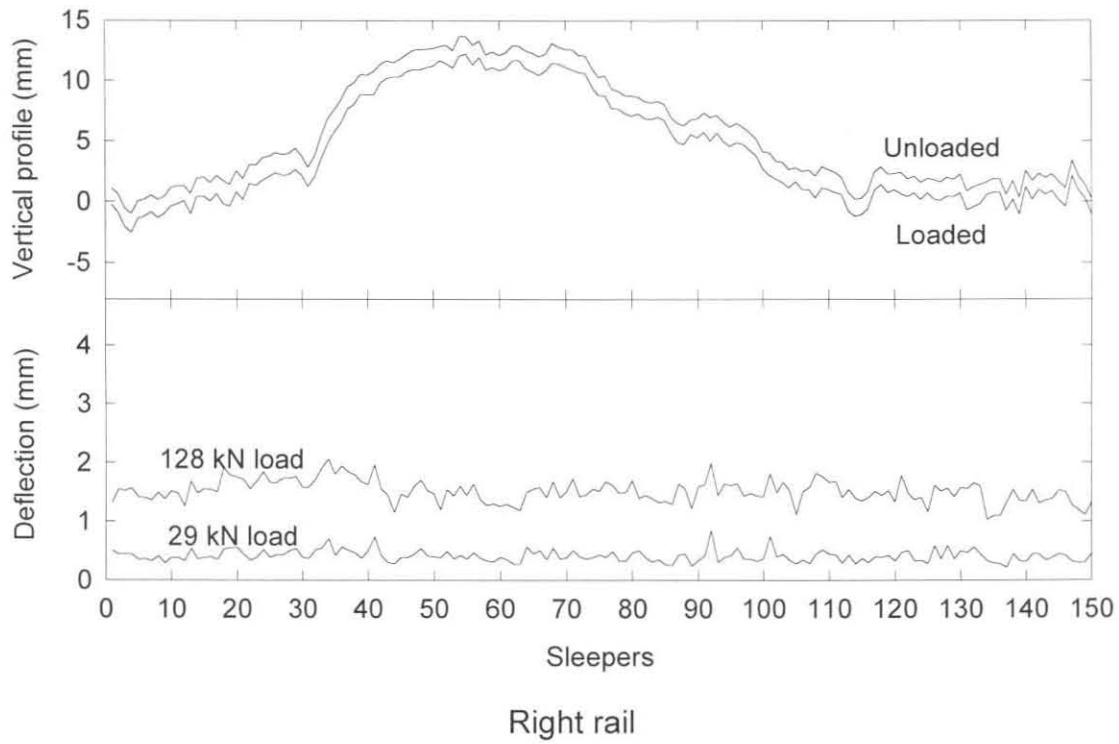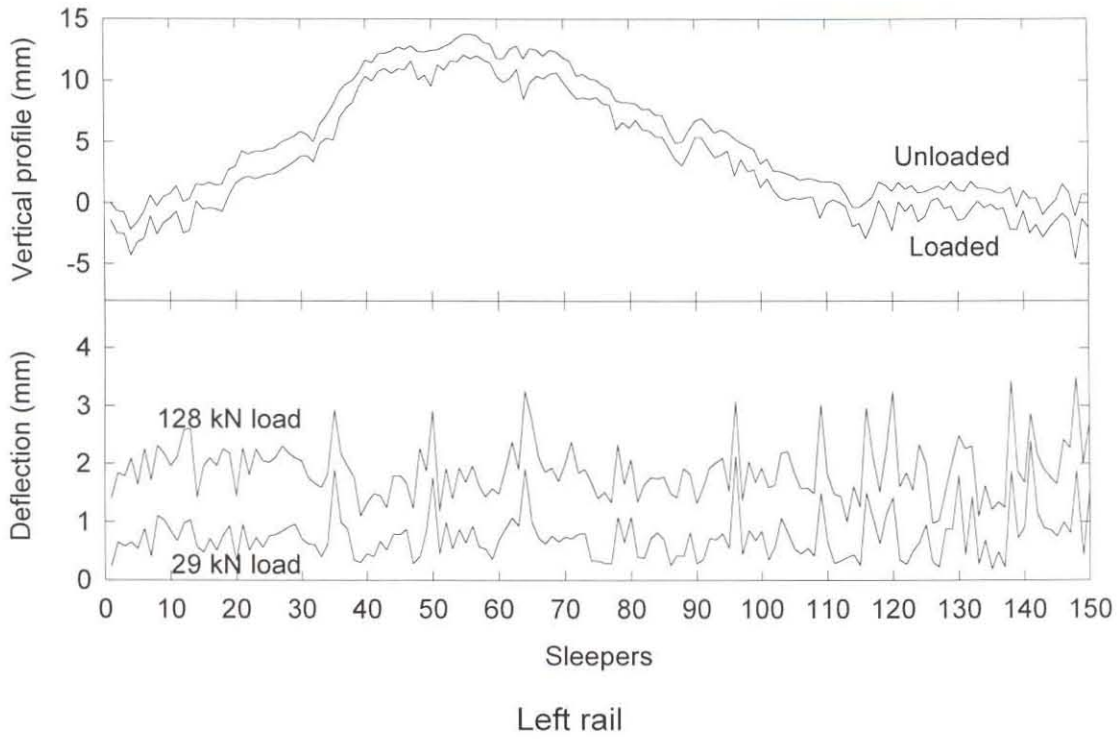
Left rail

Right rail

Figure B15: Unloaded and loaded vertical space curve and track deflection due to a 29kN and a 128kN load on the rail.

In Figure B16 the track deflection due to a vertical load of 29kN, 49kN, 78kN and 128kN load is shown for track with a low spatial variation in the track stiffness and track with a high variation in spatial track stiffness due to a void at Sleeper 77.

Low spatial stiffness variation

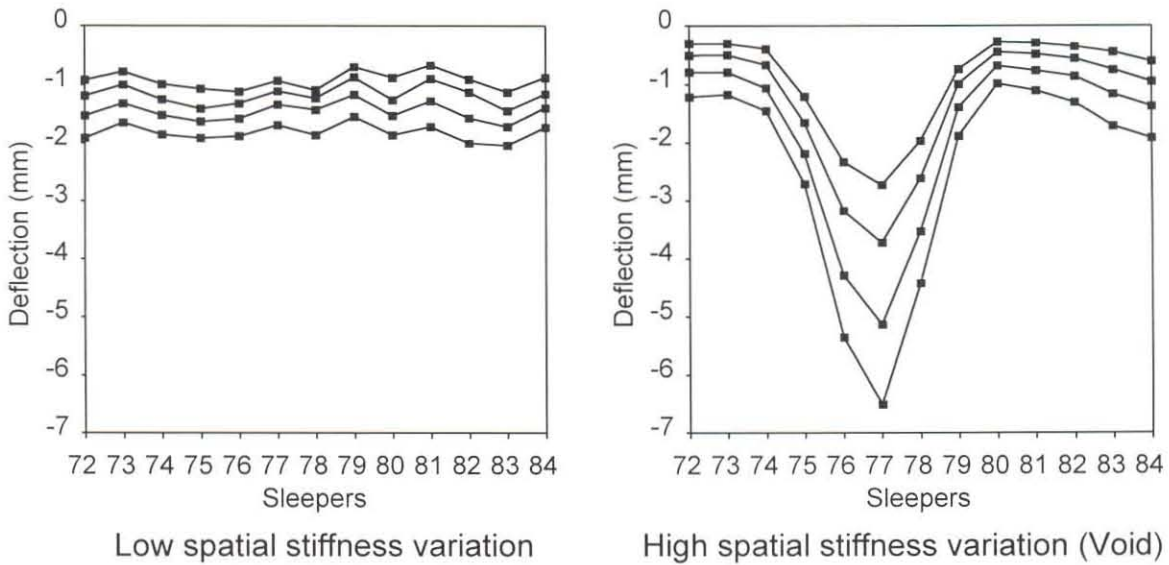High spatial stiffness variation (Void)

Figure B16: Track deflection due to vertical loads of 29kN, 49kN, 78kN and 128kN.

From the track stiffness measurements described in this section, a selection of static load-deflection curves are shown in Figure B17. From these curves it is clear that not only does the stiffness change from sleeper to sleeper along the track but the stiffness characteristic also changes. The initial lower slope of the nonlinear stiffness is due to voids or soft spots between the sleeper and the ballast. This initial stiffness is known as the seating stiffness. The second part of the stiffness, that is approximately between 29kN and 128kN, is called the contact stiffness and is a function of substructure stiffness properties. Here the relationship between load and deflection is found to be more linear, although in some cases stiffening is observed (Ebersöhn et al., 1993).
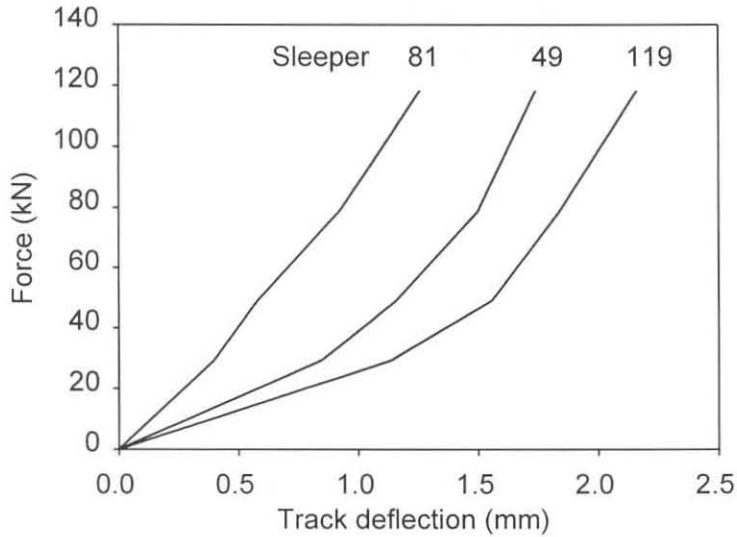
Figure B17: Static force-deflection curves.

B.2.4 Track Instrumentation

To be able to analyse the dynamic behaviour of the track, wheel loads, sleeper reactions, and sleeper displacement measurements were taken at thirteen consecutive sleepers in the middle of the 150 sleeper test section. Using Multi-Depth-Deflection Meters (MDDs) (Maree, 1989), displacements in the various layers of the sub-structure were also measured at Sleeper 76. In Figure B18 a schematic layout of the instrumented test site shows the position of the strain gauges, the displacement transducers, the holes for the MDDs, and the displacement transducer frame with its anchor holes.

Due to the fact that both the sleeper reactions as well as the sleeper deflections were measured simultaneously while the test train, or for that matter any train running on that line, passed over the test site, it was possible to make an extensive study of the dynamic track stiffness at thirteen consecutive sleepers. Details with respect to the specific purpose of the instrumentation, together with a detailed description of the instrumentation and some sample measurements are given in the following sub-sections.
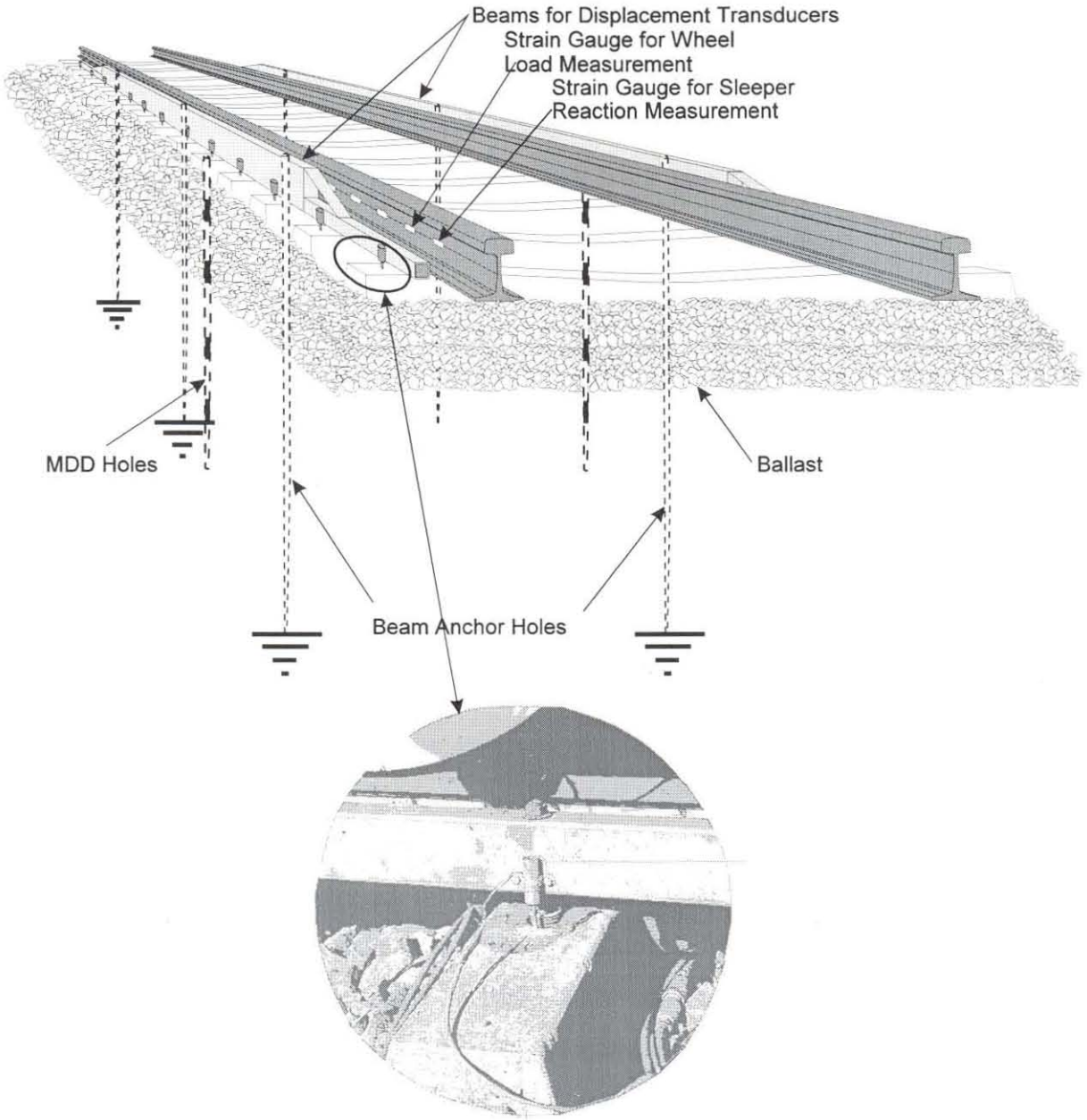
Figure B18: Layout of test track instrumentation.

B.2.4.1 Purpose and Description

Measurement of vertical sleeper displacement and sleeper reaction forces requires ingenuity. In 1994, Jeffs measured the rail seat load by inserting a water filled cell between the rail and the sleeper after having removed the existing rail pad. The

load cell was connected to a pressure transducer which then provided a signal proportional to the load transmitted through the cell. Jeffs measured the displacement of the sleeper using a laser system, with the reflector mounted on the sleeper. The laser system was placed 20m from the track and noise became a problem for an accuracy below 0.1mm.

The method used in this research makes use of a innovative combination of strain gauges on the rail and displacement transducers that measured the displacement between a reference frame and the sleepers. A detailed description of the instrumentation is given below.

Strain gauges: Vertical wheel loads and sleeper reaction forces were measured with shear strain gauges coupled into a full Wheatstone bridge circuit as shown in Figure B19. Reaction forces in the rail were determined by measuring the shear strain in the rail and converting it to the vertical reaction force (ORE Q D71 (Report 1), 1965). The strain gauge bridges were calibrated with a hydraulic ram and load cell to measure to an accuracy of 2%. To measure the dynamic vertical wheel load, these shear strain bridges were mounted on both rails between fourteen consecutive sleepers. To measure the dynamic sleeper reaction, additional shear strain bridges were mounted on both rails inline with the thirteen test sleepers. The measurements of the wheel load by the load measuring wheelset and by strain gauges on the rail were compared and found to deviate only slightly from one another. A comparison can be seen in Figure B20.
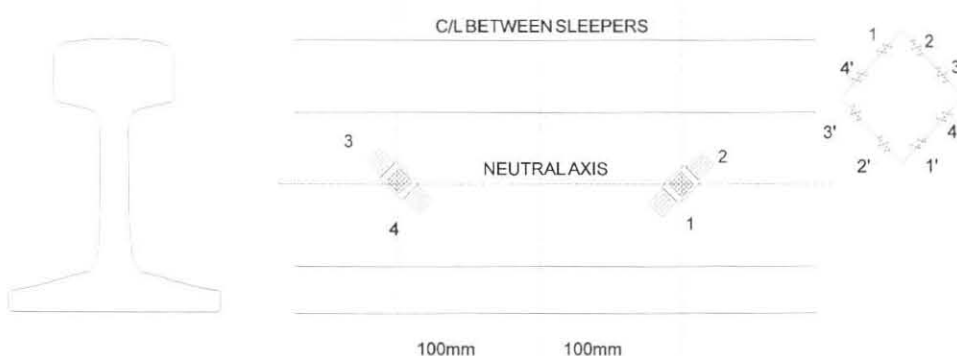

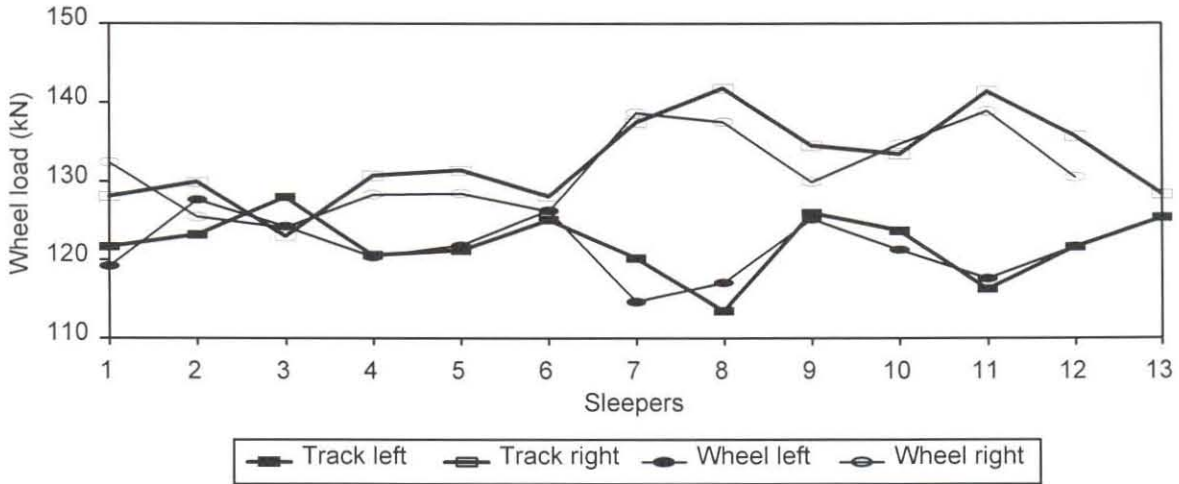Figure B19: Position of shear strain gauges on the rail.

Figure B20: Comparison between wheel load as measured on track and by the load measuring wheelset.

Displacement transducers: Sleeper deflections were measured using displacement transducers mounted on a beam which was anchored at three positions 3.15 meters below the top of the sleepers as shown in Figure B18 and B21. The beam assembly was constructed, to be able to measure the absolute vertical displacement of thirteen sleepers on each side of the track as a train passes over the instrumented test site. Figure B21 shows the beam and displacement transducer mounting. 20mm inductive LVDTs were used to measure the relative displacement between the beam and the sleepers. The construction of the frame was such that the beam could be removed from its anchor rods before tamping the track or before measuring the stiffness of the track with the "BSSM" track loading vehicle.

Multi-Depth-Deflectionmeters: MDDs were installed on the left and right hand side of Sleeper 76 to electronically measure the vertical movement in the track sub-structure layers. Each of the two MDD holes as indicated in Figure B18 contained six measuring modules. These multi-stage sensors were used to measure resilient deflections and permanent deformation at various depths under loading from rolling stock relative to the anchor 3.15m below the rail. The displacement transducers used in the modules were the same as used on the beam and were calibrated to measure to a resolution of 0.01mm. Figure B22 shows the construction of a MDD

module and the instrumentation placed into the hole. MDDs for the use in track structures, were developed by Spoornet and the Council for Scientific and Industrial Research (CSIR) Division for Roads and Transport Technology (Maree, 1989).

20 mm LVDT between
Beam and Sleeper

100*50*2 mm Steel Beam
attached to Anchor Rods
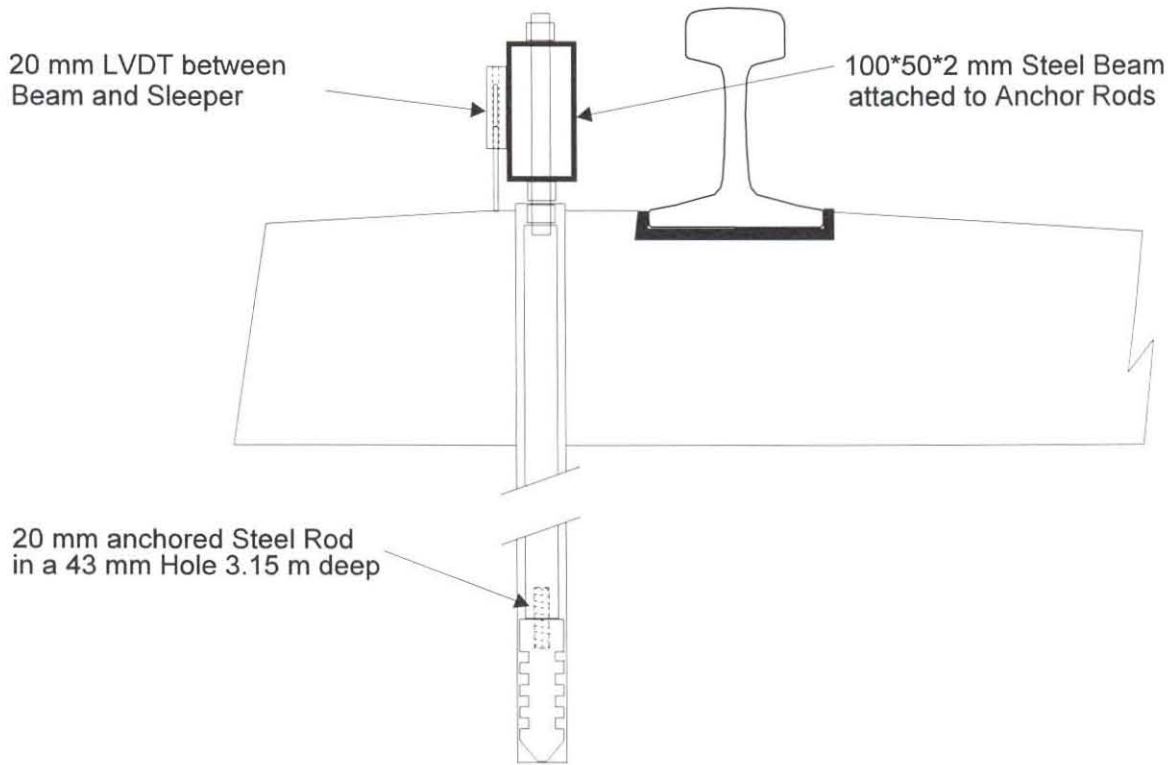
20 mm anchored Steel Rod
in a 43 mm Hole 3.15 m deep

Figure B21: Beam and displacement transducer mounting.

The MDDs were placed into the sub-structure of the track to provide information required to determine the stiffness of the track and the properties of the different sub-structure layers using the program GEOTRACK (Chang *et al*, (1980)). Using the measured wheel loads and given track design parameters as input to GEOTRACK, layer deflections were calculated and compared to the layer deflections measured by the MDDs. Three to five iterations were usually enough to achieve a good convergence. Once a good comparison between the calculated and the measured results had been reached, the stiffness of the different structural layers and the modulus of elasticity was calculated. It was found that the ballast and first soil layer had a random variation in stiffness from test to test, but that the lower

layers provided very consistent results. Multiple wheel loads were used to determine the modulus of elasticity of the track sub-structure layers. A maximum of five layers can be handled with this program. The last layer is assumed to be of infinite depth.
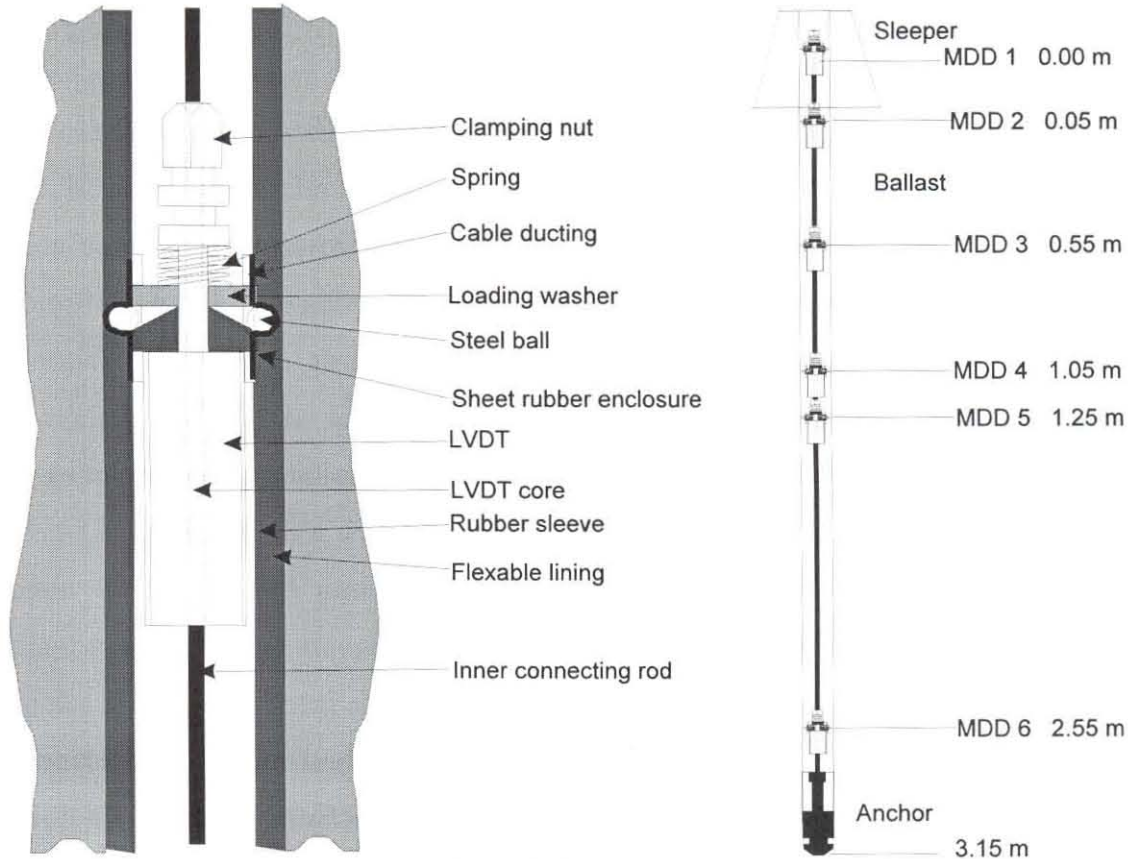
Figure B22: Multi-Depth Deflection Meter Construction.

B.2.4.2 Sample Measurements and Interpretation

In this section a selection of measurements are given. In the first example, the concept of determining the dynamic track stiffness from on-track measurements is shown. In the second part of this section the wheel loads, sleeper reactions and sleeper deflections are shown as the test locomotive passes over a selected sleeper in the test section. Furthermore, the deflections in the various sub-structure layers are also shown.

To obtain the dynamic behaviour of the track, there are basically three parameters to be observed. The parameters are the wheel load, the sleeper reaction, and the sleeper deflection due to a passing wheel. In Figure B23, measurements of these three parameters are shown. It can be seen that the wheel load was measured slightly before the sleeper reaction and sleeper displacement. This is due to the fact that the wheel load can only be measured between two sleepers, while sleeper reaction and sleeper displacement are measured while the wheel passes directly over the sleeper. As the rail between the sleepers only senses the wheel load as the wheel passes over the section measuring the shear strain, the wheel load shows a single and clearly defined spike. The sleeper reaction on the other hand has a more complex shape. The shape can be explained as follows. As the wheel approaches the sleeper where the shear strain is measured, the sleeper progressively starts carrying more of the load. As soon as the wheel is directly above the sleeper and thus in the section where the shear strain is measured, the measured load changes direction and shows a wheel load spike on top of the measured sleeper reaction. As soon as the wheel passes over the top of the sleeper the wheel load portion disappears and the sleeper reaction slowly decreases back to zero. Thus, to be able to determine the total sleeper reaction force, the wheel load measured just before a particular sleeper is mathematically shifted forward by half a sleeper spacing and then the sleeper reaction is subtracted from the wheel load to give the resultant effective sleeper reaction force against time. From Figure B23 it can be seen that the maximum sleeper reaction is about 45% of the actual wheel load. This is due to the fact that the adjacent sleepers carry part of the load.

In Figure B24 a dynamic force-deflection curve, or dynamic track stiffness curve is shown. This curve is obtained by plotting the resultant effective sleeper reaction force against the measured sleeper deflection. From Figure B24 it can be seen that the track stiffness is progressive and has a clearly defined hysteresis loop due to structural damping.
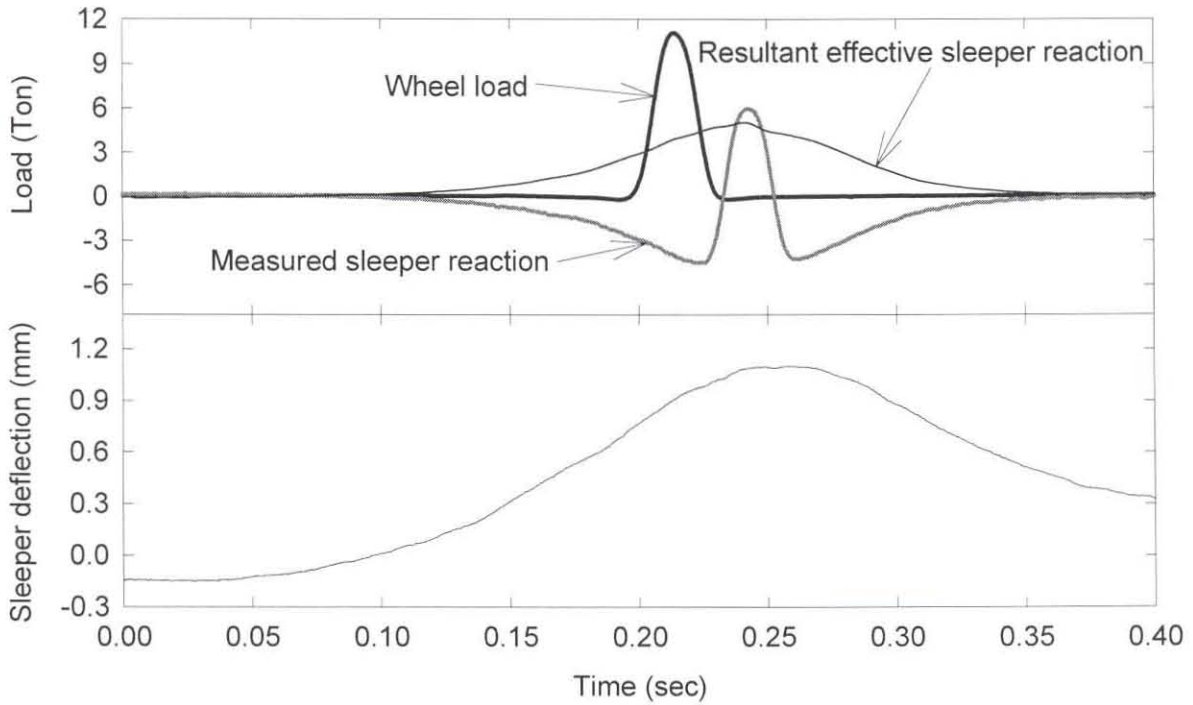
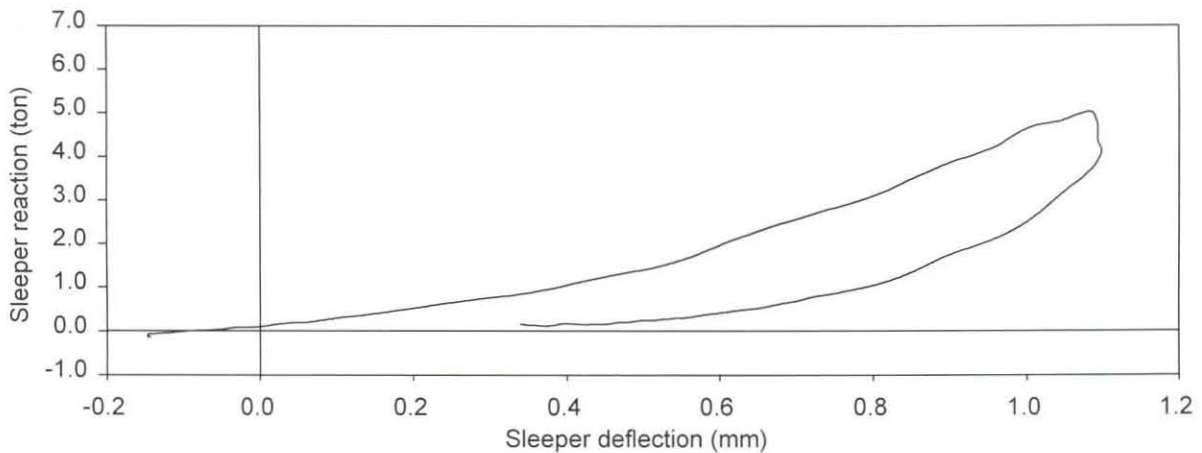Figure B23: Measured dynamic track parameters.

Figure B24: Dynamic track stiffness under one wheel.

To illustrate the behaviour of a selected sleeper in the test section as the test locomotive passes over it, the corresponding wheel loads, sleeper reactions and

sleeper deflections are shown in Figure B25. In Figure B26 the resultant dynamic track stiffness is shown. The deviation in the different dynamic track stiffness loops is due to a slight variation in the wheel loads of the locomotive. This can be due to the static load distribution of the locomotive as well as effects due to dynamic wheel loading.
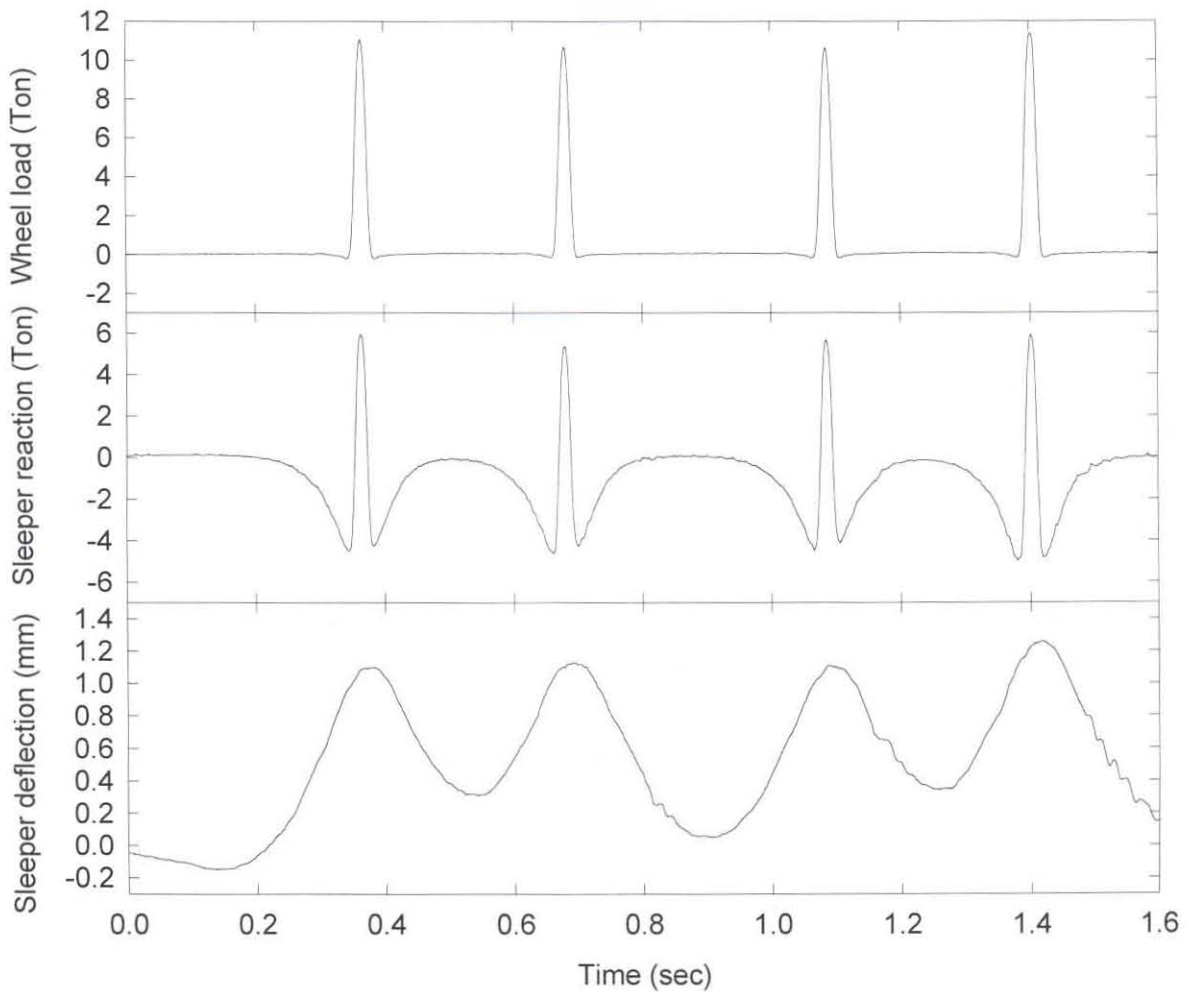

Figure B25: Track reaction due to a passing locomotive.
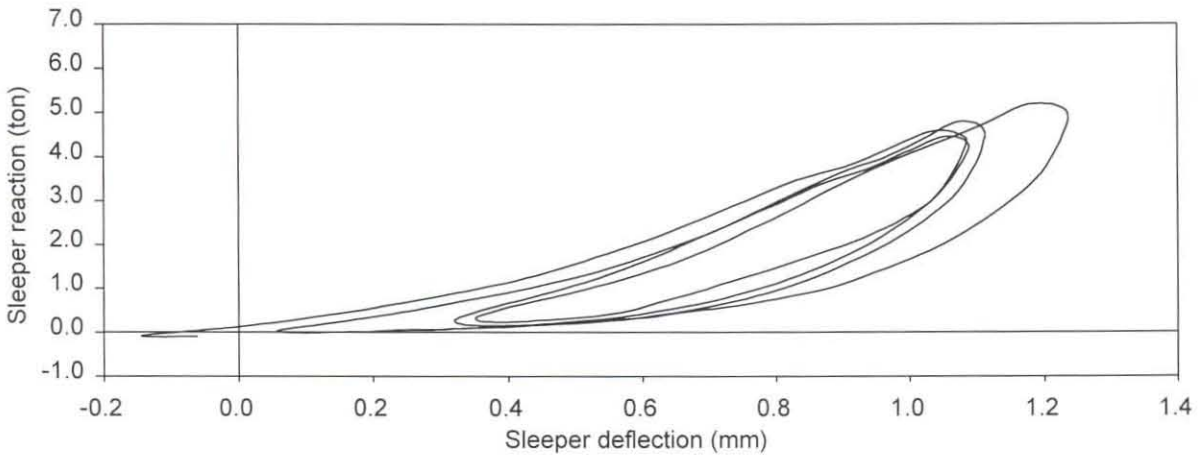
Figure B26: Dynamic track stiffness due to a passing locomotive.

In Figure B27 the cumulative deflections in the various sub-structure layers are shown as the locomotive passes over the MDDs at Sleeper 76. Considering the various layer thicknesses as shown in Figure B22, it is noted that the highest relative track deflection takes place in the ballast layer.

Figure B27: Deflection in sub-structure layers at Sleeper 76 as a function of time.

B.2.5 Dynamic Track Stiffness

In Figure B28 examples of the dynamic track stiffness and the track damping properties as measured at four consecutive sleepers are given. Superimposed on the

dynamic load-deflection curve are the static load-deflection values as measured by the BSSM track loading vehicle. The static values are indicated by the little squares. From t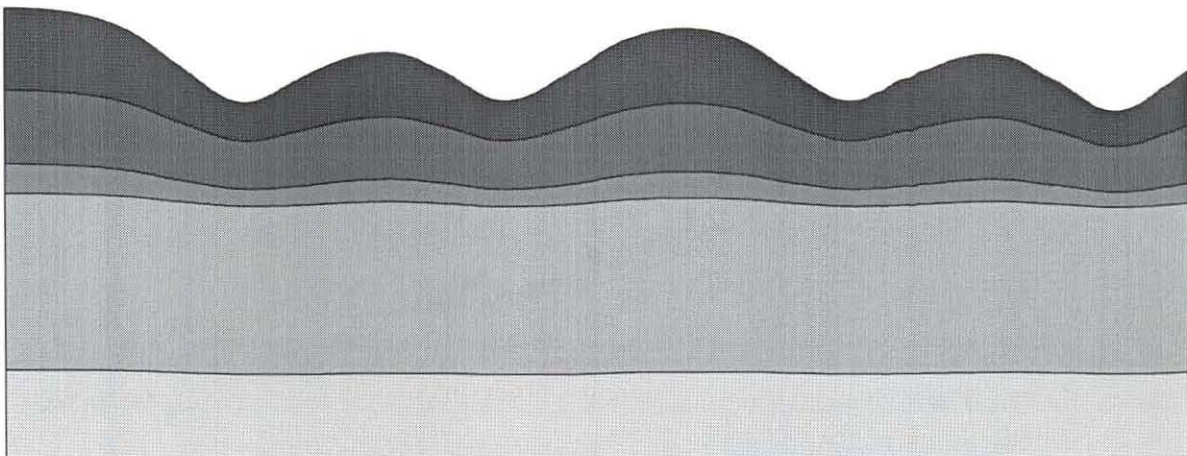he plotted values it can be seen that there is good agreement between these two measuring techniques. Further research to establish whether the static values should be below, on or above the dynamic values is proposed. It should be noted that the sleeper reaction force and not the actual wheel load is plotted against sleeper deflection. The difference between the wheel load and the sleeper reaction force is due to a part of the wheel load being carried by adjacent sleepers.
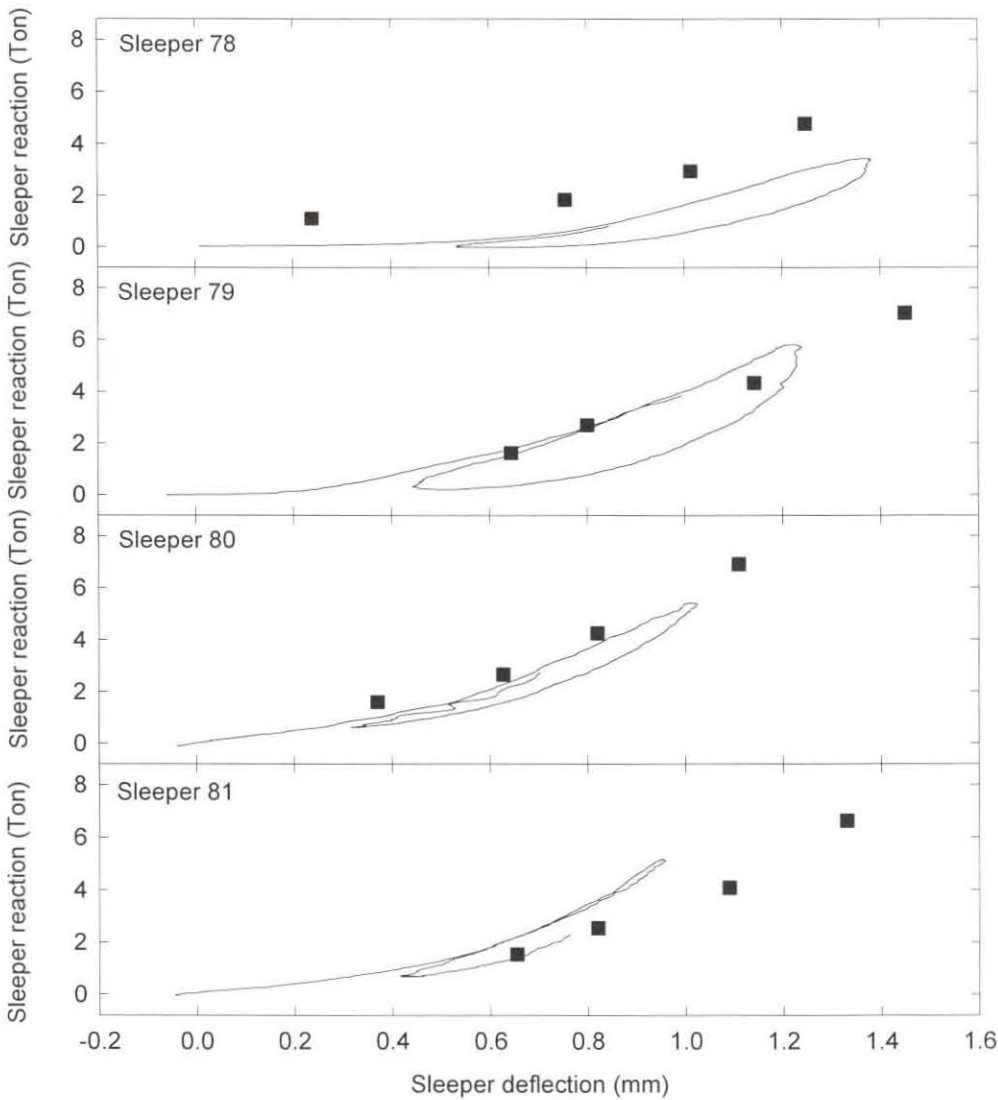

Figure B28: Dynamic and static track stiffness.

B.3   TEST RESULTS

In this section experimental results are presented and discussed. Particular attention is given to the influence of axle load, vehicle speed and accumulating traffic on the behaviour of the vehicle/track system.

B.3.1 Influence of Axle Load on Track Behaviour

The influence of axle load on track behaviour, in particular the effect on the dynamic track stiffness and the ratio between the sleeper reaction and the wheel load was investigated. Figure B29 shows the sleeper deflection, the sleeper reaction, the wheel load, and Figure B30 the resultant dynamic track stiffness as the long test train travelled over a particular sleeper in the test section. It was found that, as the wheel load increased, the ratio of the sleeper reaction force to the applied wheel load increased. This is due to the fact that the length of the deflection basin does not increase significantly with an increase in vertical loading. The increase in the sleeper deflection, and the sleeper reaction to wheel load ratio, as a function of increasing wheel load is shown in Figure B31.

A closer examination of Figure B30 shows that there is no significant difference in the path of the dynamic downward stroke due to changes in the wheel load. The only difference is that the amount of track deflection increases with increasing wheel load. Also seen in Figure B30 is the increase in structural damping due to increased wheel loading.

Another observation in the graph of the dynamic track stiffness can be seen in the grey shaded area. This area represents the dynamic track behaviour due to the wheels in the trailing bogie of one CCL-5 wagon and the wheels of the leading bogie of the next CCL-5 wagon. Due to the short axle spacing the track is not able to return to zero deflection and thus a significant change in sleeper reaction occurs with only a small change in sleeper deflection. Very little damping is observed

under these conditions. When long wheel base rail vehicles like locomotives move over the track the situation is different and the track is able to return to zero deflection between the wheelsets. This can be seen in Figure B26.
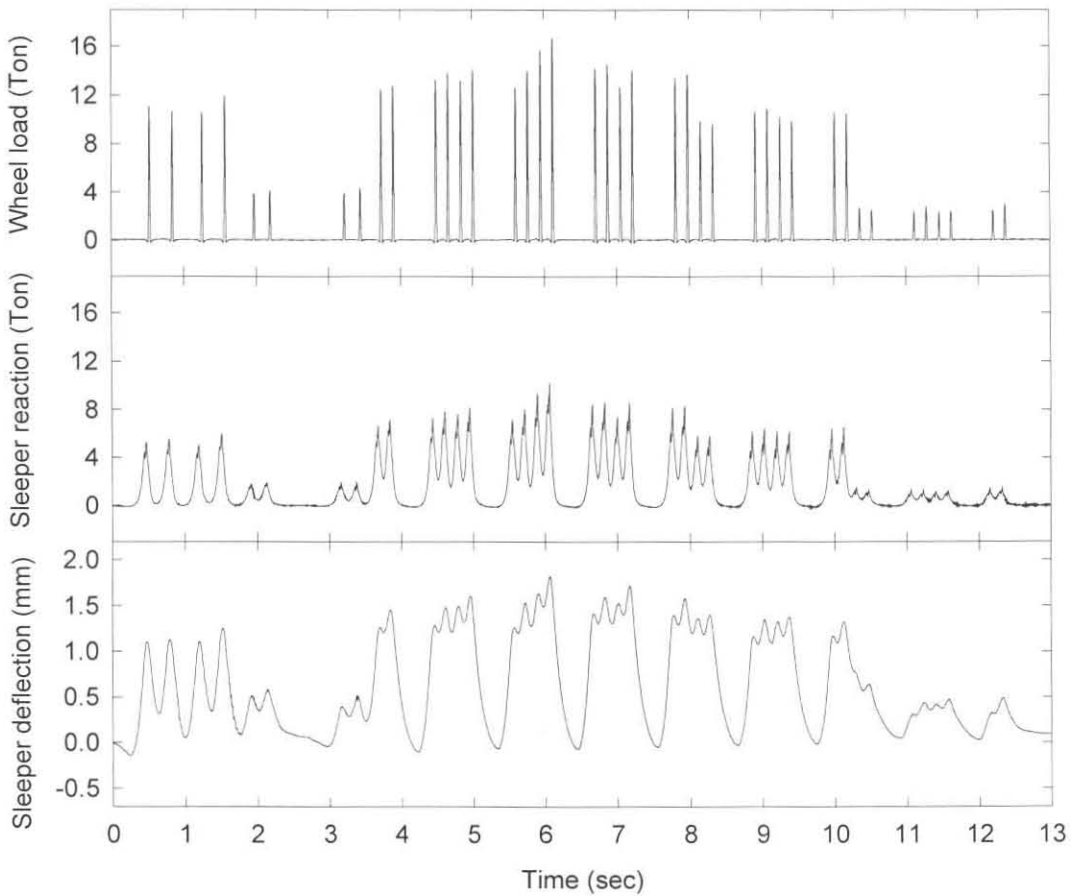

Figure B29: Dynamic track behaviour under varying wheel loads.

B.3.2 Vehicle and Track Performance as a Function of Vehicle Speed

In this section the influence of vehicle speed on the dynamic wheel load, the dynamic performance of the secondary suspension of the vehicle and the dynamic behaviour of the track is presented.
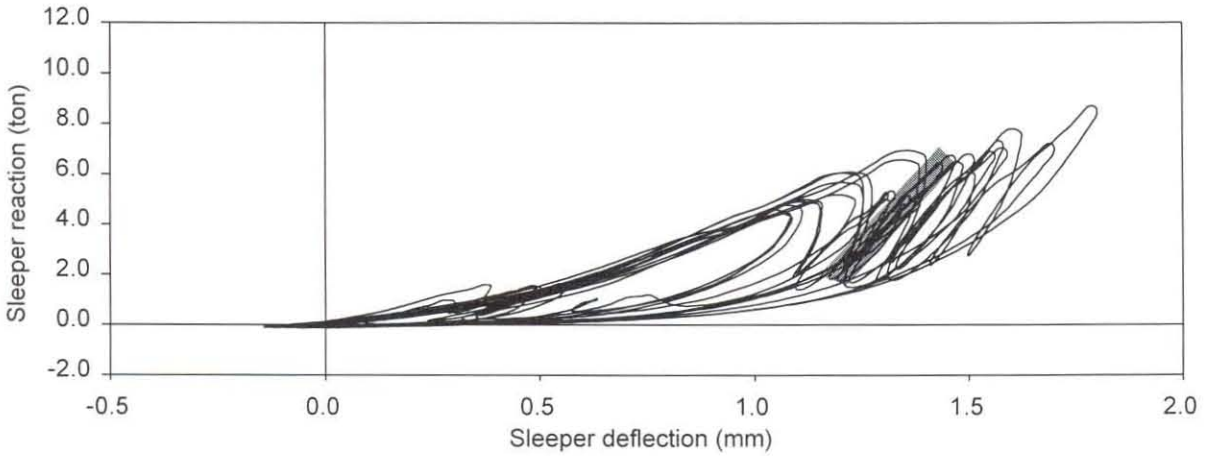
Figure B30: Dynamic track stiffness under varying wheel loads.
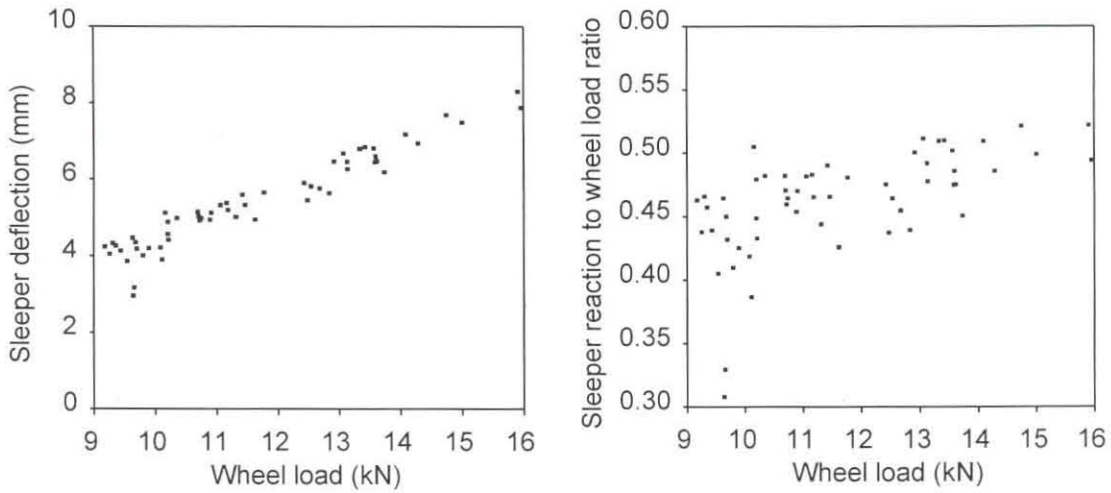
Figure B31: Influence of vehicle load on track behaviour.

B.3.2.1 Dynamic Wheel Load

In Figure B32 the dynamic wheel load as measured by the left wheel of the load measuring wheelset is shown for various vehicle speeds and in Figure B33 the Root Mean Square (RMS) values of the dynamic wheel load are plotted against vehicle speed at various stages of accumulating traffic. From these graphs it can be seen that by reducing the speed of trains passing over a deteriorated track, the dynamic wheel load can be reduced. The increase in the dynamic wheel load with accumulating traffic is due to the increase in track roughness with accumulating traffic.
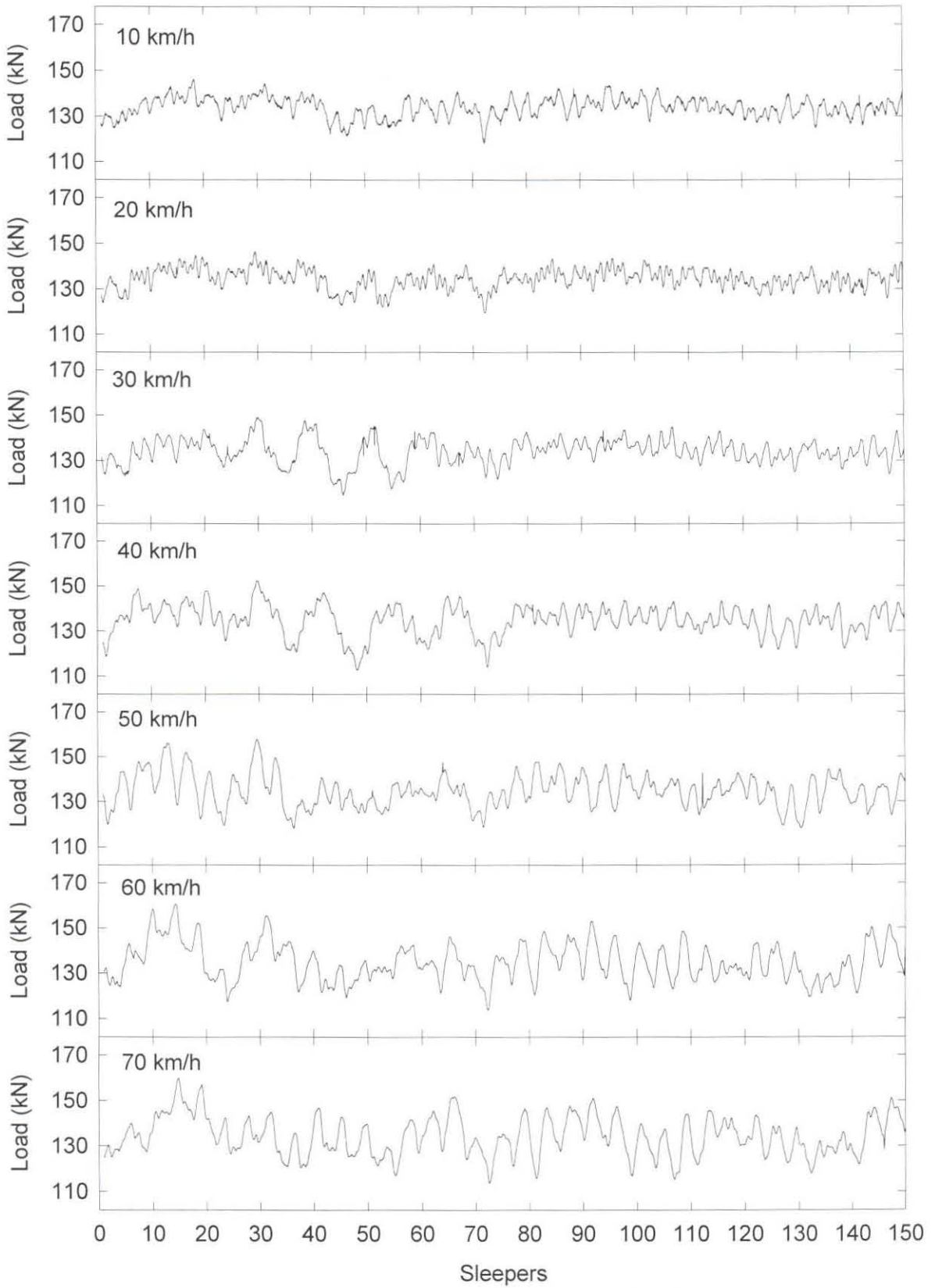
Figure B32: Dynamic wheel loads under the left wheel at various speeds.
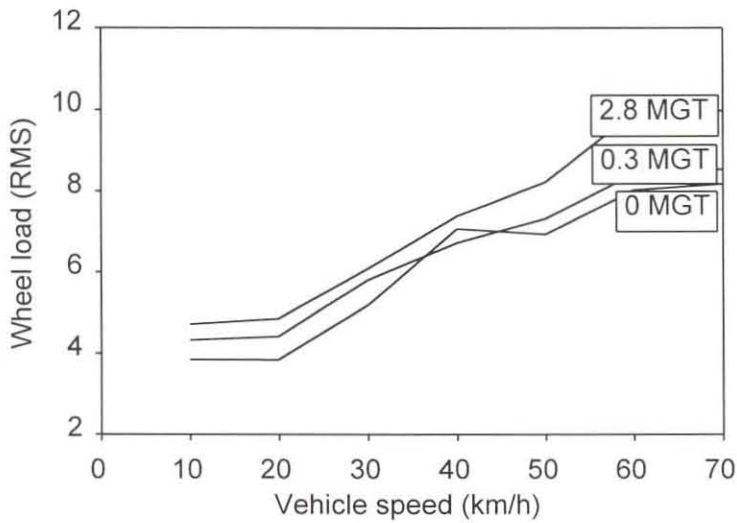
Figure B33: Dynamic wheel load as a function of vehicle speed.

In Figure B34 the Power Spectral Density (PSD) values for the body roll and bounce frequencies as measured in terms of the wheel load are shown for vehicle speeds ranging from 10km/h to 70km/h. The PSD provides information about the statistical properties of the signal in the frequency domain by showing how the energy of the signal is distributed over the frequency range.

The PSD values were calculated using the Fast Fourier Transform (FFT) algorithm (Bendat and Piersol, 1971). When calculating the PSD, frequency smoothing was applied. This means that the average value of the PSD was calculated at a certain frequency in a narrow bandwidth. For the PSD graphs shown in Figure B34 a normalized standard error of 0.5 was used. The definition of the normalized standard error is given by:

$$\epsilon_r = \sqrt{1/l_{fc}} \tag{B4}$$

where l_{fc} is the number of neighbouring frequency components. The effective resolution bandwidth is defined as:

$$B_e' = l_{fc}/T = \frac{1}{\epsilon_r^2 \, T} \tag{B5}$$

where T is the total measuring time. For example if T is 33.31 seconds and the normalized standard error is 0.5, the effective resolution bandwidth is 0.1201 Hz. Calculations of the PSD values were done using the program RDAP (Fröhling, 1994). From the graphs in Figure B34 it is clear that the frequency pattern changes with increasing vehicle speed. These changes are due to the occurrence of resonance in the suspension system at certain vehicle speeds, out-of-round wheels, and track geometry input excitations.

B.3.2.2 Vehicle Performance

The performance of the test vehicle is given in terms of the vertical displacement across the secondary suspension of the bogie. Time traces of the vertical displacement across the secondary suspension for vehicle speeds from 10km/h to 70km/h are shown in Figure B35. As can be seen, the displacement shows a tendency to increase with increasing vehicle speed. However, due to the non-linearity in the secondary suspension system, the displacement is often abrupt and unpredictable. Due to the relatively good condition of the track, the displacement in the secondary suspension is also very small, reaching a maximum displacement of only approximately 3mm.

B.3.2.3 Dynamic Track Behaviour

The dynamic behaviour of the track as a function of vehicle speed is discussed in terms of sleeper deflection, sleeper reaction, wheel load, and the ratio between the sleeper reaction and the wheel load. Figure B36 shows a 8% decrease in the sleeper deflection with increasing vehicle speed. In absolute terms the decrease is only 0.1mm. Figure B36 also shows a small increase in the sleeper reaction, the dynamic wheel load and the sleeper reaction to wheel load ratio with increasing vehicle speed. At around 30km/h there are a few stray points due to nonlinearities in the vehicle suspension system and the natural frequencies of the vehicle components as well as wave lengths of track input.
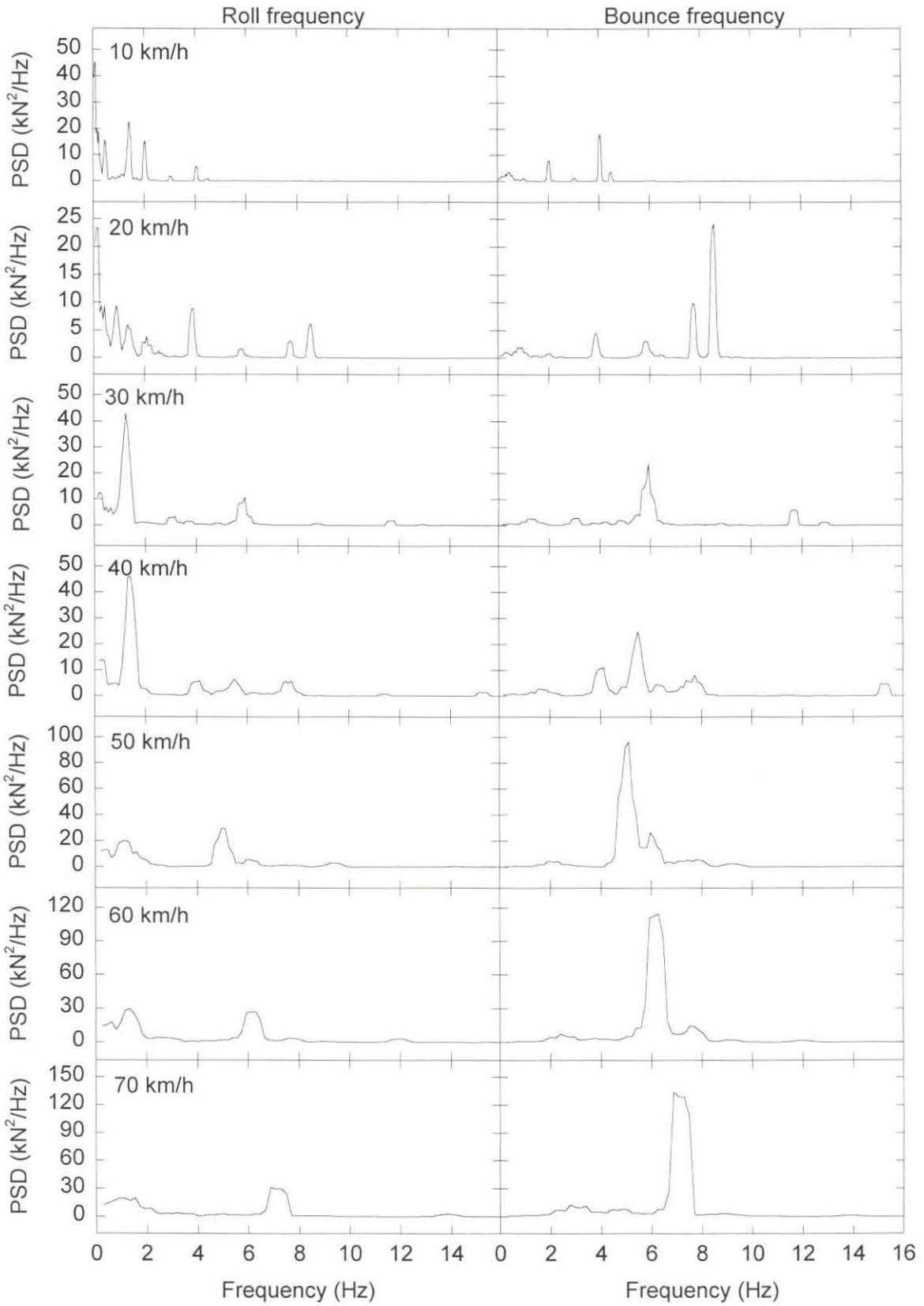
Figure B34: Frequency response as a function of vehicle speed.
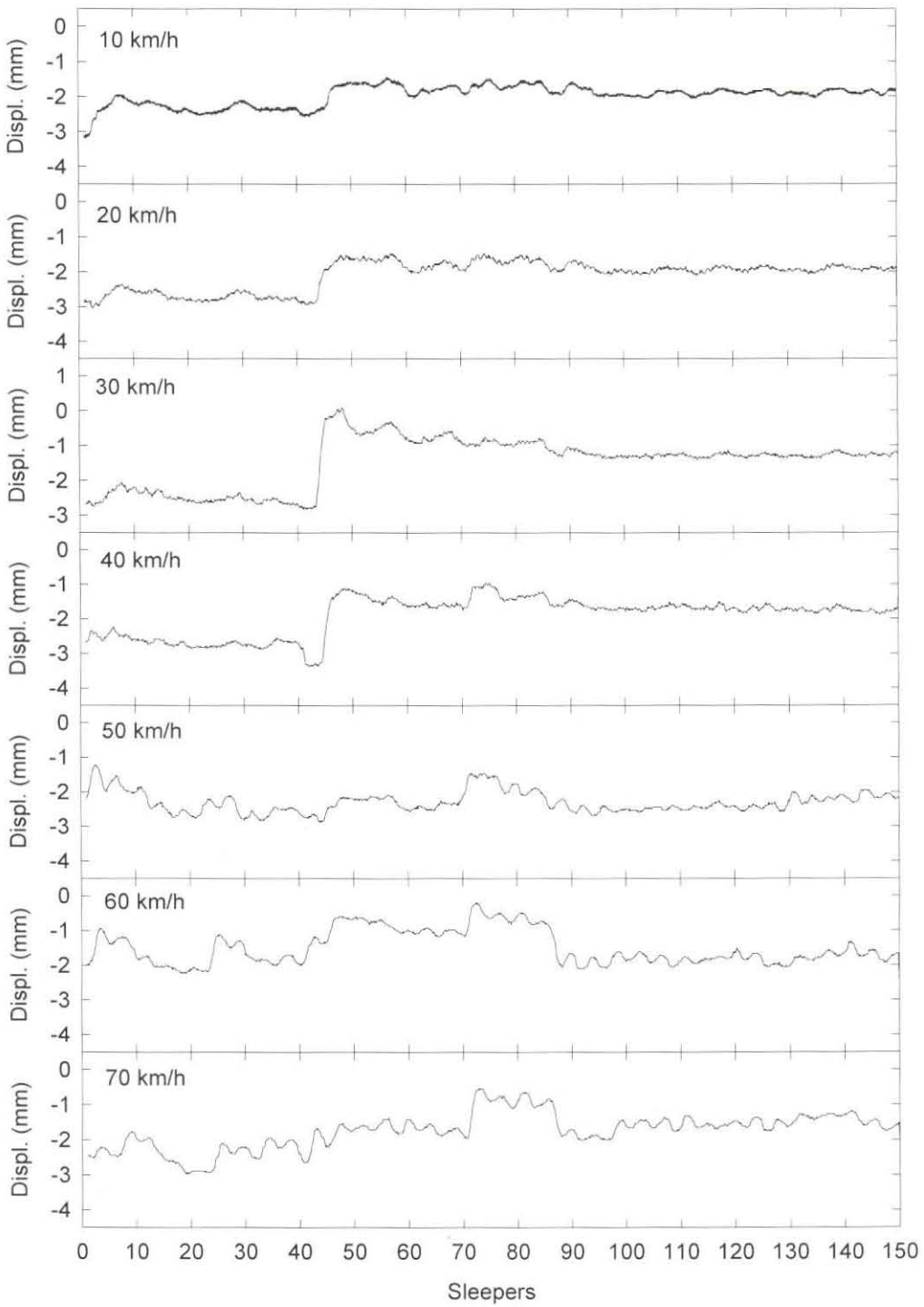
Figure B35: Vertical displacement across secondary suspension as a function of vehicle speed.
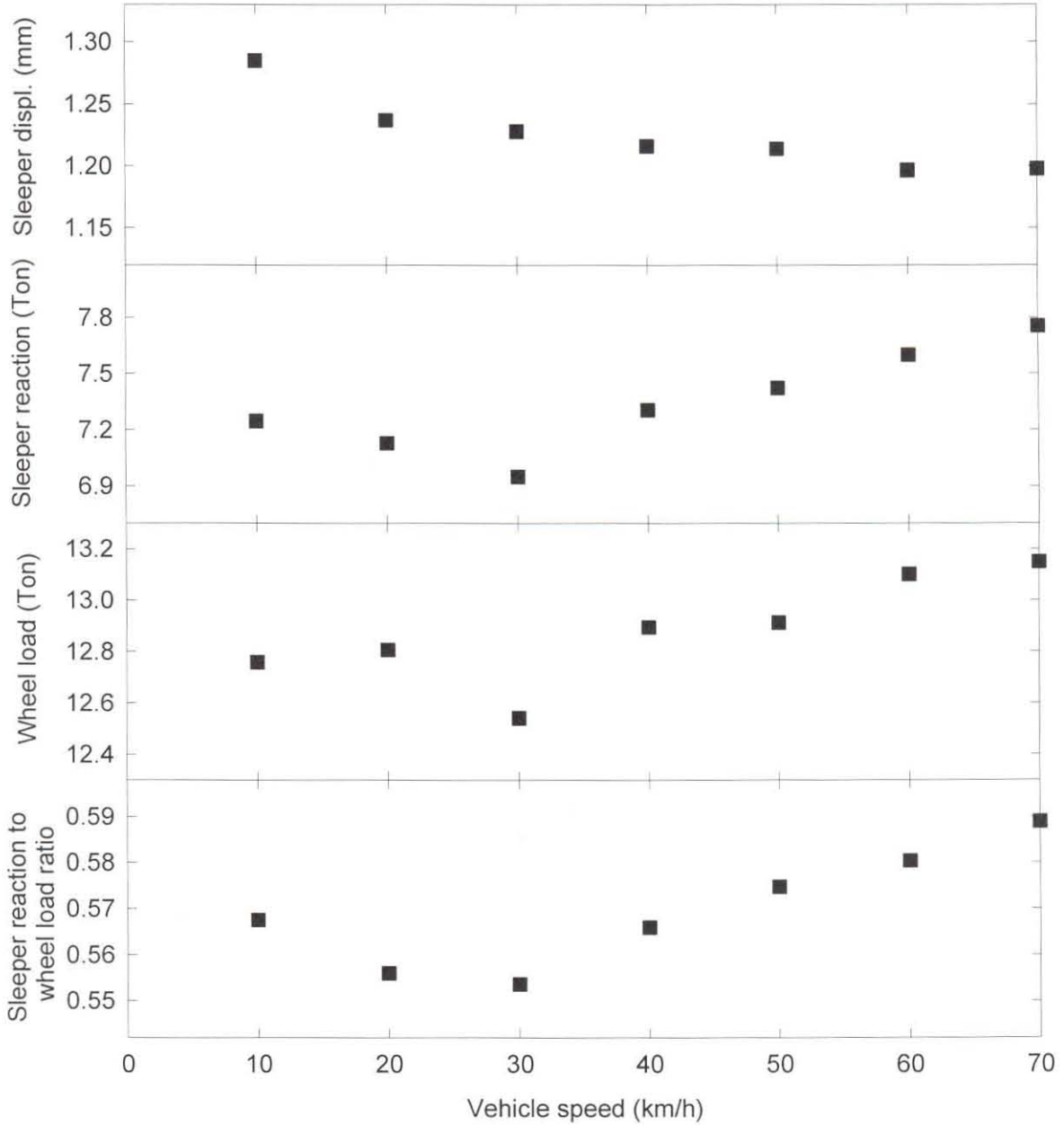
Figure B36: Dynamic track behaviour as a function of vehicle speed.

B.3.3 Vehicle and Track Performance Versus Accumulating Traffic

In this section the performance of the vehicle and the track is analysed as a function of accumulating traffic. Attention is given to the overall track settlement, the

development of track roughness, the changes in the dynamic wheel load, the behaviour of the vehicle suspension, the dynamic performance of the track, and changes in the sub-structure properties.

B.3.3.1 Track Settlement

Using digital levels, the absolute unloaded vertical space curve of the left and the right rail was measured over the 150 sleeper long test section. This was done directly after tamping and at regular intervals as the gross tonnage accumulated over the test site. As time went by, the time between measurements increased to adjust to the lower rate of track settlement. A curve of track settlement against million gross tons (MGT) of accumulating traffic is shown in Figure B37. From the figure it is clear that the rate of track settlement decreases as a function of accumulating cyclic track loading.
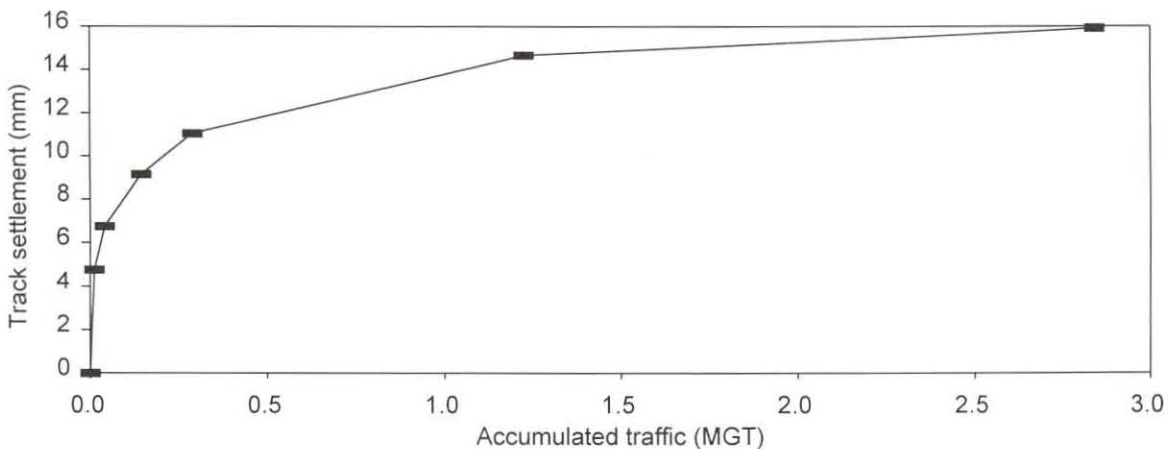
Figure B37: Average overall track settlement.

In Figure B38 the absolute vertical space curve as measured directly after tamping and after 2.84 MGT is shown together with a curve showing the relative differential track settlement.
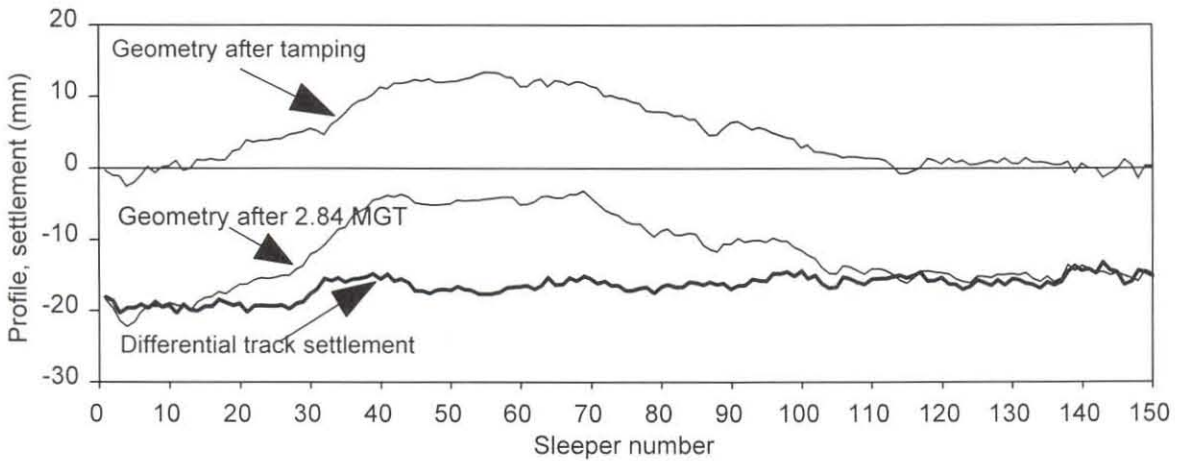
Figure B38: Track settlement profiles.

B.3.3.2 Track Roughness

Track roughness or track quality is directly related to differential track settlement and is defined as

$$
R = \sqrt{\frac{\sum\limits_{i=1}^{n} d_i^2}{n}} \tag{B6}
$$

where d_i = difference between the elevation of the point measured and the mean filtered elevation, and

n = number of measurements in the length of track under consideration.

The track roughness values that are plotted in Figure B39 represent a single roughness value calculated over the entire 150 sleeper section. As with the average track settlement, the increase in track roughness also decreases with accumulating traffic.

Track quality is the key to track load bearing capacity and efficient track maintenance. Generally track tamping is done to eliminate voids under the sleepers and to improve track quality before it becomes irreparable. This ensures safe

operation and good ride quality of passing vehicles. Although the concept of tamping is good something has to be done to make tamping effective over a longer time period. This can be achieved by for example spatial consolidation of the ballast layer after every tamping cycle. In contrast to natural settlement under train loading, the application of dynamic track stabilisation anticipates part of the initial settlement in a controlled way, without causing any change in the vertical track geometry. The subsequent further settlements are therefore smaller, the maintenance intervals become longer and the overall maintenance cost drops.
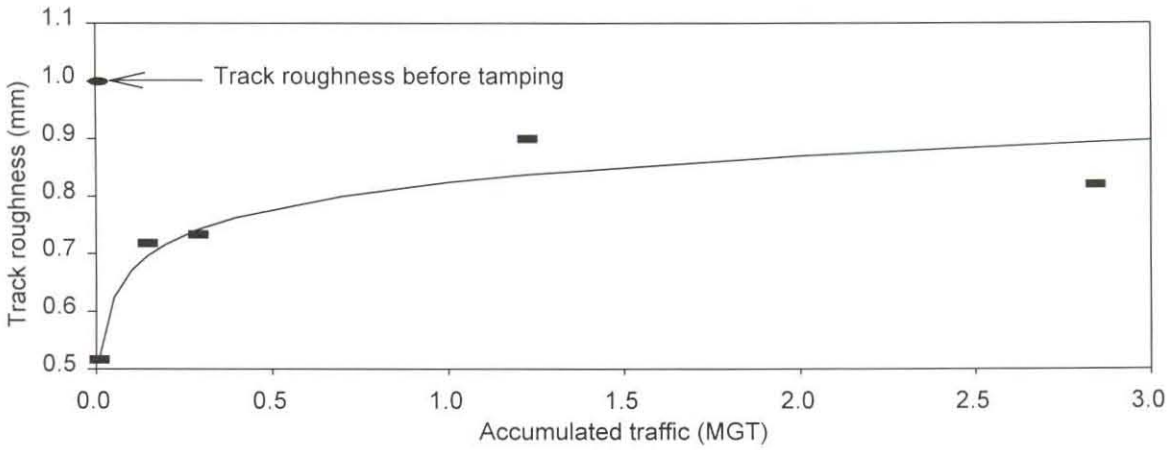
Figure B39: Changes in average track roughness.

B.3.3.3 Dynamic Wheel Load

As seen before, the dynamic wheel load changes with changing vehicle speed. Some changes are also observed as a function of changing track roughness. The variation of the RMS of the dynamic wheel load as measured by the load measuring wheelset increases with accumulating traffic due to an increasing track roughness. This is shown in Figure B40 for a vehicle speed of 40 km/h.

A time trace showing the dynamic wheel load as measured on the leading left wheel of the test bogie directly after tamping and after 2.84 MGT is presented in Figure

B41. From the traces it can be seen that the dynamic wheel load changed its pattern due to changes in the effective loaded track geometry.
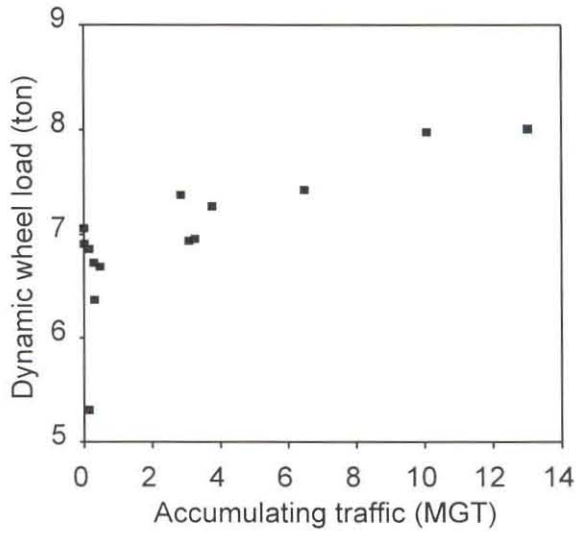
Figure B40: Variation of dynamic wheel load with accumulating traffic.
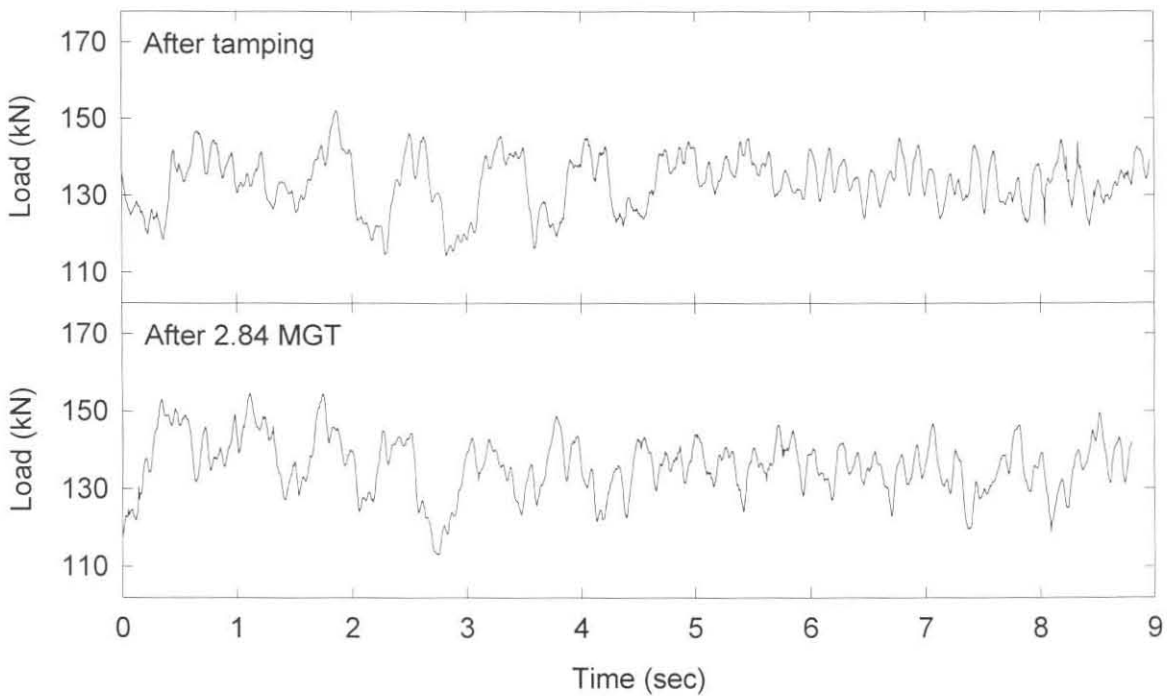
Figure B41: Wheel load as a function of accumulating traffic.

B.3.3.4 Vehicle Suspension Behaviour

A time trace showing the vertical displacement across the left side of the secondary suspension as measured directly after tamping and after 2.84 MGT is presented in Figure B42. From the traces it can be seen that the maximum displacement increased slightly, and that the overall displacement is still very small.
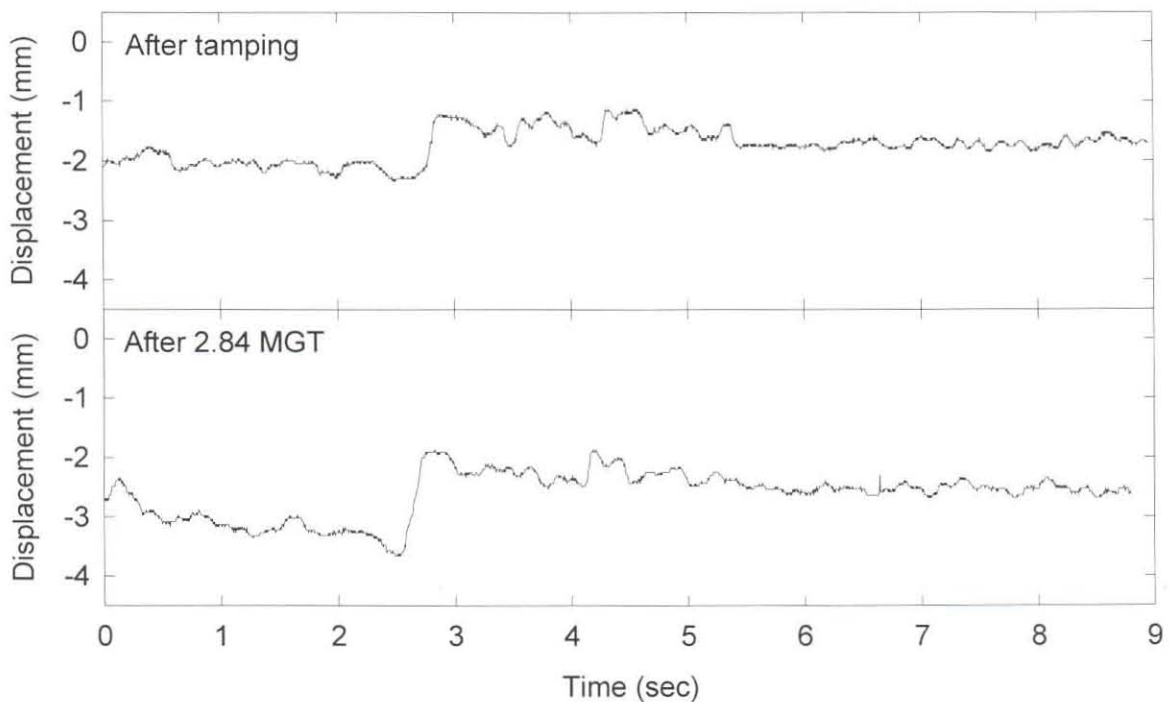
Figure B42: Displacement across secondary suspension as a function of accumulating traffic.

B.3.3.5 Dynamic Track Behaviour

The dynamic behaviour of the track as a function of accumulating traffic is discussed in terms of wheel load, sleeper reaction and sleeper deflection. In Figure B43, the behaviour as measured at Sleeper 73 and Sleeper 77 is given. Of particular importance in the interpretation of these two graphs is the fact that after 2.84 MGT a void was created at Sleeper 77. The resulting change in the dynamic behaviour

with respect to the sleeper reaction and the sleeper deflection of the track can clearly be seen.
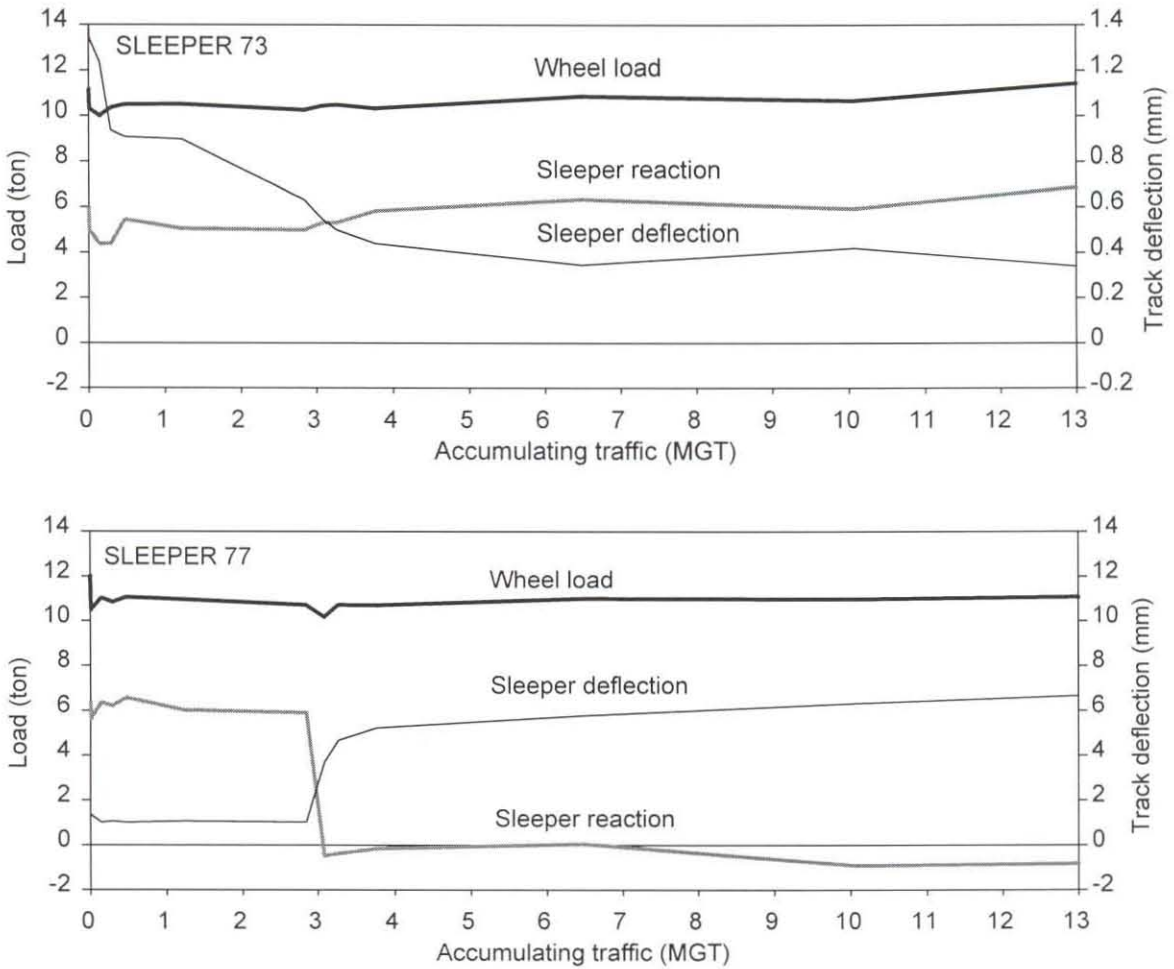
Figure B43: Wheel load, sleeper reaction and sleeper deflection at two different sleepers.

Every sleeper tends to have its own characteristic dynamic force deflection curve. There are variations with accumulating traffic, but in general a stiffer sleeper support stays stiffer, a softer sleeper support stays softer, a more nonlinear stiffness stays more nonlinear, and the hysteresis damping also does not change significantly. Variations in the dynamic track stiffness with accumulating tonnage are shown in Figure B44. Changes in the continuous plot of the static track deflection under a given load have already been shown in Figure B15.
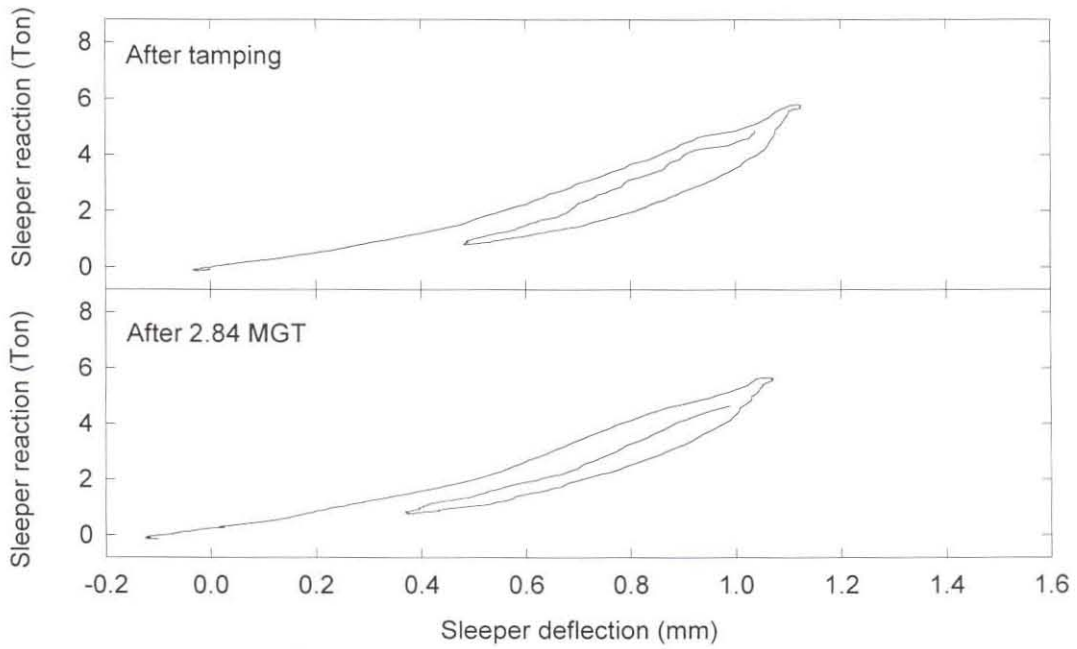
Sleeper 77
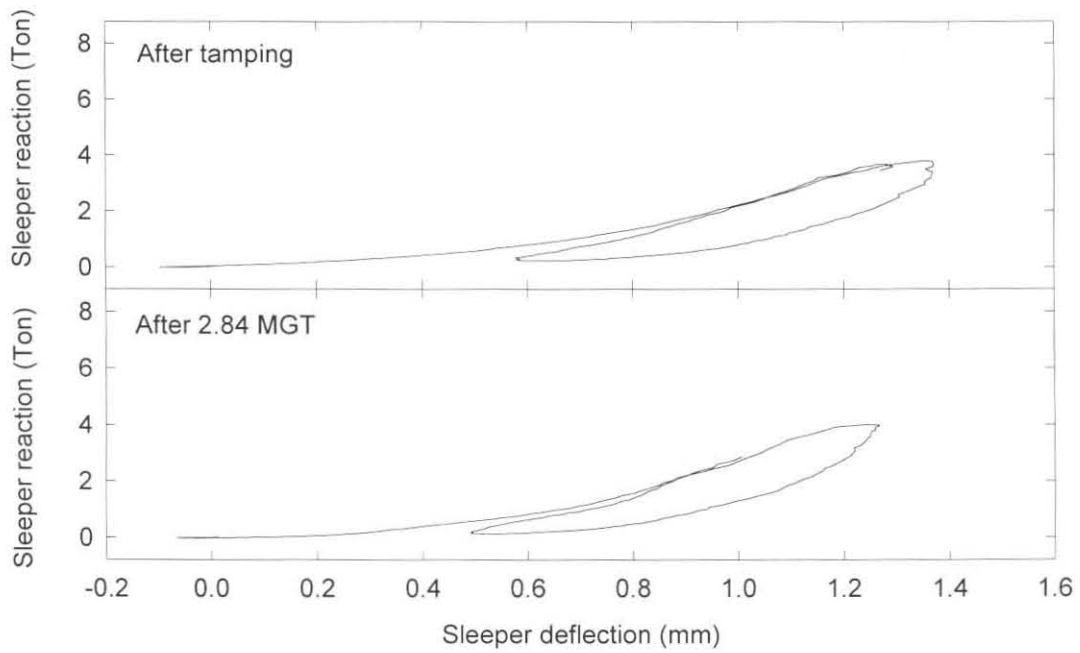
Sleeper 78

Figure B44: Changes in the dynamic track stiffness due to accumulating traffic.

B.3.3.6 Track Substructure Property

The property of the various substructure layers is best described in terms of their relevant modulus of elasticity, and the changes thereof as a function of accumulating traffic. The values of the various modulus of elasticity as given in Table B4 were derived from the MDD measurements using the technique described in Section B.2.4.1. The values were obtained for a 26 ton axle load. The modulus of elasticity as measured after 2.84 MGT shows a significant softening due to the excavation of a trench at the adjacent sleeper. The area of the trench was not tamped after being filled up to observe void forming.

Table B4: Modulus of elasticity of substructure layers.

Layer type	Ballast/ class	Sandy/ clay	Clay	Clay	Ballast/ class	Sandy/ clay	Clay	Clay
Layer depth	50- 550mm	550- 1050mm	1050- 1250mm	1250- 2550mm	50- 550mm	550- 1050mm	1050- 1250mm	1250- 2550mm
Tonnage MGT	Modulus of elasticity [Mpa] Left hand side				Modulus of elasticity [Mpa] Right hand side			
0.000	128	33	33	63	121	26	53	100
0.012	168	33	32	59	186	24	47	93
0.146	185	34	35	69	131	25	49	101
0.291	259	28	33	67	145	23	61	103
0.470	252	28	33	78	154	20	61	116
1.227	203	26	33	78	167	19	69	118
2.842	331	21	34	65	194	16	72	86
3.085	66	38	35	87	72	25	71	123
3.263	60	48	38	94	81	26	86	129

B.3.4 Void Forming

In Figure B43, it can be seen that the wheel load did not change significantly after the void was created. The sleeper reaction and sleeper displacement however showed a significant change because Sleeper 77 had lost its structural support and adjacent sleepers had to help carry the load. The result was an increased

differential ballast settlement in this area as can be seen in Figure B45. The resulting vertical displacement across the secondary suspension after 13 MGT is shown in Figure B46 together with the resulting wheel load. At this point in time there was still very little change in the dynamic behaviour of the test vehicle.
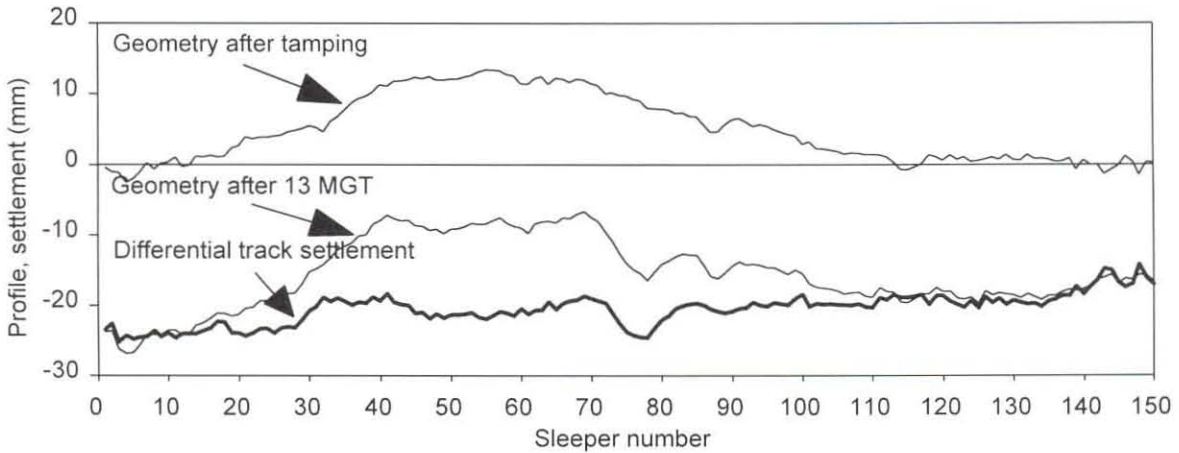
Figure B45: Differential ballast settlement after 13 MGT.
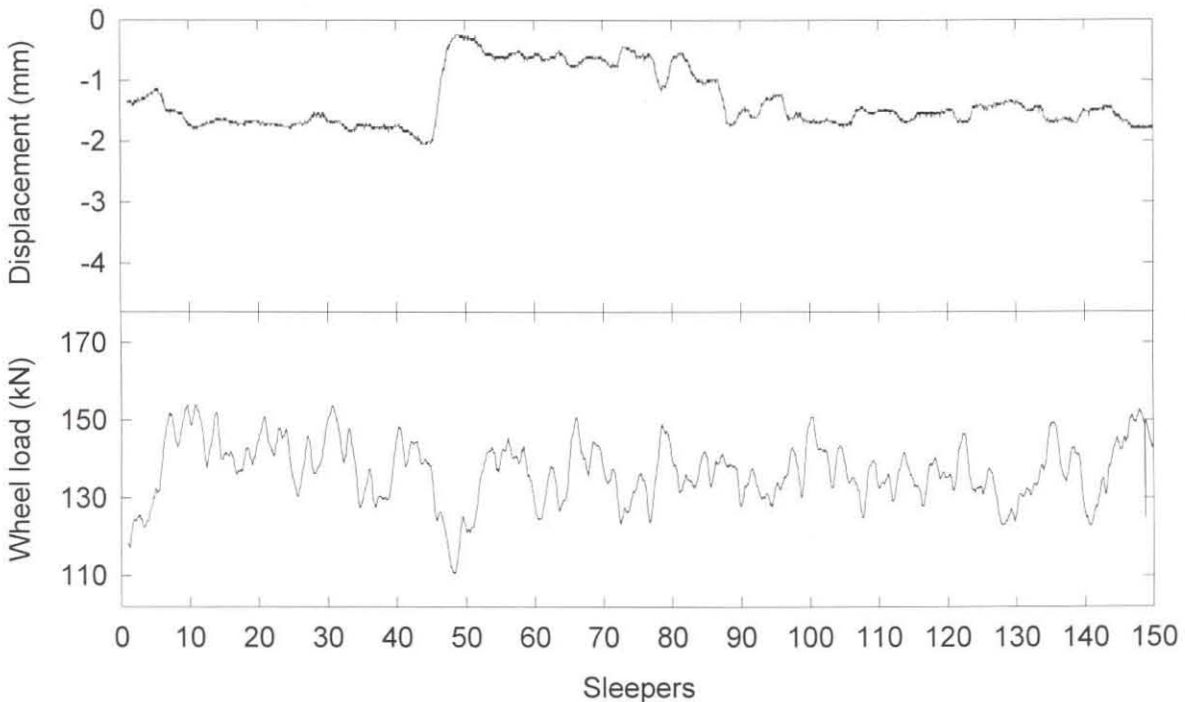
Figure B46: Dynamic vehicle behaviour including displacement across secondary suspension and dynamic wheel load.

APPENDIX C

GEOTRACK INPUT AND OUTPUT

Tie length .... 2200 mm
Number of segments per tie 10
Number of segments between rails ... 6
Tie spacing .... 650.2 mm
Tie width .... 259.1 mm
Tie area .... 5.981e+004 mm^2
Tie weight .... 285 kg
Tie EI .... 1.235e+004 kN.m^2
Rail spacing .... 1140 mm
Rail area .... 7703 mm^2
Rail weight .... 60.02 kg/m
Rail EI .... 6558 kN.m^2
Rail fastener stiffness .... 1.2e+006 kN/m

Number of axle loads 1
Axle loads are on tie number(s) 1   0   0   0
Wheel load per axle (Tonnes. 17   0   0   0
Number of soil layers 5

Layer	Modulus (Mpa)	Vrat	Depth (mm)	Gamma (kN/m^3)	Knot	Ktype
1	344.83	0.30	549.91	19.49	3.00	0
2	36.00	0.40	500.13	20.50	0.70	0
3	34.65	0.40	199.90	20.50	0.70	0
4	62.68	0.40	1300.0	20.50	0.70	0
5	62.68	0.40	0.00	20.50	0.70	0

Different Depths at Which Moduli are Computed

$$Z(1) = 50.04 \text{ mm}$$
$$Z(2) = 554.99 \text{ mm}$$
$$Z(3) = 1055.12 \text{ mm}$$
$$Z(4) = 1255.02 \text{ mm}$$
$$Z(5) = 2555.25 \text{ mm}$$

CALC. STEP NO. 1

DEFLECTIONS AND REACTIONS
NEGATIVE DEFLECTION IS DOWNWARD
NEGATIVE REACTION IS TENSION

---- SINGLE AXLE ----

TIE NO.	DEFLECTION RAIL mm	REACTION RAIL SEAT kN	DEFLECTION TIE mm
1	-2.367996	88.1	-2.294615
2	-1.860706	35.9	-1.830836
3	-1.205842	5.4	-1.201321
4	-0.771222	0.9	-0.770511
5	-0.508306	-1.3	-0.509423
6	-0.315113	-1.4	-0.316256

PEAK RAIL BENDING MOMENT= 2.40e+001 kN.m

TRACK MODULUS U = 5.673 KIPS/IN./IN. = 39.106 MN/M/M

SOIL VERTICAL DISPLACEMENTS AND INCREMENTAL STRESSES

        T = TIE NUMBER (1=CENTER TIE)
    SEG = SEGMENT NUMBER
        Z = DEPTH POINT NUMBER
    XX = DIRECTION PARALLEL TO TIES
    YY = DIRECTION PARALLEL TO RAILS
    ZZ = VERTICAL DIRECTION
Units are mm and kPa
COMPRESSION IS NEGATIVE FOR STRESSES
DOWNWARD IS POSITIVE FOR DEFLECTIONS

            Z(1) = 50.04 mm
            Z(2) = 554.99 mm
            Z(3) = 1055.12 mm
            Z(4) = 1255.02 mm
            Z(5) = 2555.25 mm

T	SEG	Z	W	THETA	S-XX	S-YY	S-ZZ	S-XY	S-XZ	S-YZ
1	1	1	2.0447	-1009.66	-251.72	-262.76	-495.17	0.00	-28.28	0.00
1	1	2	1.7942	-77.93	-17.24	-13.10	-47.59	0.00	-10.34	0.00
1	1	3	1.3799	-57.93	-13.10	-10.34	-34.48	0.00	-8.28	0.00
1	1	4	1.2509	-43.45	-8.28	-4.83	-30.34	0.00	-8.97	0.00
1	1	5	0.8521	-17.93	-2.07	-0.69	-15.17	0.00	-4.14	0.00
1	2	1	2.1864	-825.52	-258.62	-239.31	-326.90	0.00	6.90	0.00
1	2	2	1.9667	-89.66	-19.31	-14.48	-55.86	0.00	-6.21	0.00
				*						
				*						
				*						
1	5	4	1.4480	-55.17	-8.97	-6.21	-40.69	0.00	-0.69	0.00
1	5	5	0.9238	-20.00	-1.38	-0.69	-18.62	0.00	-0.69	0.00

T	SEG	Z	W	THETA	S-XX	S-YY	S-ZZ	S-XY	S-XZ	S-YZ
2	1	1	1.6759	-546.90	-144.83	-134.48	-266.90	-21.38	-13.79	4.83
2	1	2	1.5415	-61.38	-13.79	-14.48	-33.79	2.76	-6.90	6.90
2	1	3	1.2545	-48.28	-11.03	-10.34	-26.90	2.07	-6.90	6.21
2	1	4	1.1554	-37.93	-6.90	-6.21	-24.83	2.07	-6.90	6.21
2	1	5	0.8194	-16.55	-1.38	-0.69	-13.79	0.69	-3.45	2.76
2	2	1	1.7673	-375.17	-135.86	-104.83	-134.48	-17.24	6.90	6.21
2	2	2	1.6675	-68.97	-15.17	-15.86	-37.93	2.07	-3.45	7.59
2	2	3	1.3347	-54.48	-11.72	-11.72	-31.03	1.38	-5.52	6.90
				*						
				*						
				*						
5	5	4	0.5565	-7.59	-0.69	-4.83	-1.38	0.00	0.00	4.14
5	5	5	0.5303	-7.59	0.00	-3.45	-4.14	0.00	0.00	4.14

T	SEG	Z	W	THETA	S-XX	S-YY	S-ZZ	S-XY	S-XZ	S-YZ
6	1	1	0.3154	7.59	0.00	8.97	-1.38	-2.07	0.69	-0.69
6	1	2	0.3180	0.00	0.00	-0.69	0.69	0.00	0.00	0.69
6	1	3	0.3340	-1.38	0.00	-1.38	0.00	0.00	0.00	1.38
6	1	4	0.3385	-2.76	0.00	-2.07	0.00	0.69	0.00	1.38
6	1	5	0.3426	-4.14	0.00	-2.07	-1.38	0.69	-0.69	2.07
6	2	1	0.3157	14.48	1.38	11.03	1.38	-1.38	0.69	-0.69
6	2	2	0.3200	0.00	0.00	-0.69	1.38	0.00	0.00	0.69
6	2	3	0.3383	-1.38	0.00	-1.38	0.69	0.00	0.00	1.38
				*						
				*						
				*						
6	5	4	0.3512	-2.76	0.00	-2.76	0.00	0.00	0.00	1.38
6	5	5	0.3561	-4.14	0.00	-2.07	-2.07	0.00	0.00	2.76

| | | | GEOSTAT. (mm) | INIT. KNOT | INIT. VERT.STR. (kPa) -> | P | Q | EQUIVALENT TRIAXIAL STATES | | | | | |
| | | | DEPTH | | | | | SOCT | TOCT | SIG 1 | SIG 3 | MAX P | MAX Q |
TIE	SEG	POINT											
1	1	1	50.80	3.00	6.14	12.34	-6.14	350.97	108.76	504.76	274.07	389.38	115.38
1	1	2	556.26	0.70	16.00	13.59	2.41	38.83	18.69	65.24	25.66	45.45	19.79
1	1	3	1054.10	0.70	26.28	22.34	3.93	40.34	14.90	61.38	29.79	45.59	15.79
1	1	4	1254.76	0.70	30.34	25.79	4.55	38.90	16.90	62.76	26.97	44.83	17.93
1	1	5	2555.25	0.70	57.03	48.48	8.55	51.52	14.90	72.62	41.03	56.83	15.79
1	2	1	50.80	3.00	6.41	12.83	-6.41	290.07	31.86	335.10	267.52	301.31	33.79
1	2	2	556.26	0.70	16.28	13.86	2.41	42.83	21.10	72.62	27.93	50.28	22.34
1	2	3	1054.10	0.70	26.55	22.55	4.00	42.90	16.90	66.76	30.90	48.83	17.93
1	2	4	1254.76	0.70	30.62	26.00	4.62	40.55	17.79	65.79	28.00	46.90	18.90
1	2	5	2555.25	0.70	57.31	48.69	8.62	52.00	14.90	73.10	41.52	57.31	15.79
1	3	1	50.80	3.00	10.83	21.66	-10.83	289.66	21.10	319.45	274.76	297.10	22.34
1	3	2	556.26	0.70	20.69	17.59	3.10	48.69	21.79	79.52	33.24	56.34	23.10
				*									
				*									
				*									
6	5	3	1054.10	0.70	26.34	22.34	3.93	21.45	0.00	21.45	21.45	21.45	0.00
6	5	4	1254.76	0.70	30.41	25.86	4.55	25.24	0.00	25.24	25.24	25.24	0.00
6	5	5	2555.25	0.70	57.10	48.55	8.55	47.10	7.93	58.34	41.45	49.93	8.41

APPENDIX D

DYNAMIC MODELLING

Dynamics is the part of mechanics which deals with the study of both motion of material bodies and the forces that bring about the motion. Dynamic modelling is the mathematical representation of such behaviour. In this appendix a simple system in motion is described and its mathematical equation is given.

In Figure D1 a body of mass, m, is fixed to a spring with stiffness, k, and damper with damping coefficient, ρ. The system possesses only one degree of freedom since its motion is described by a single coordinate, x. If the body is acted upon by a restoring force k per unit displacement from the equilibrium position and by a damping force ρ per unit velocity, the force equilibrium according to Newton's second law of motion is given by the following equation.

$$ m \, \frac{d^2 x}{dt^2} = - kx - \rho \, \frac{dx}{dt} \qquad \text{(D1)} $$

The equation is called the equation of motion of the system and is mathematically defined as a homogeneous second-order differential equation. It can be seen that the restoring force and the damping force is negative since its direction is opposite to that of the displacement and velocity respectively.

In some cases the body may be subjected to a disturbing force due to the movement, y, of the spring and damper support. In this instance the equation of motion becomes

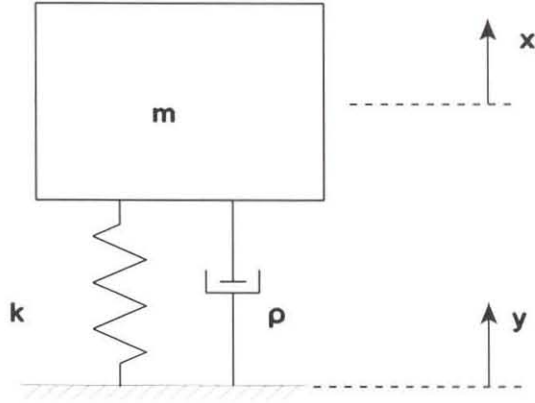$$m \frac{d^2x}{dt^2} = -k(x - y) - \rho\left(\frac{dx}{dt} - \frac{dy}{dt}\right) \qquad (D2)$$

Figure D1: One degree-of-freedom model.

REFERENCES

Ahlbeck, D.R. and Hadden, J.A. 1985. Measurement and prediction of impact loads from worn railroad wheel and rail surface profiles. *Journal of Engineering for Industry*. Transactions of the ASME, May 1985.

Ahlbeck, D.R. 1995. Effects of track dynamic impedance on vehicle-track interactions. Interaction of railway vehicles with the track and its substructure. Edited by Knothe, K., Grassie, S.L. and Elkins, J.A.: Swets & Zeitlinger. Supplement to: *Vehicle System Dynamics: International Journal of Vehicle Mechanics and Mobility*, Volume 24.

Anon. 1961. Automatische Auswertmethode zur Bestimmung der Wagenlaufgüte. *Glasers Annalen*, December 1961.

Becker, K. 1978. Evaluation of the ride quality in vehicles. *High Speed Ground Transportation Journal*. Volume 12, No. 3.

Bendat, J.S. and Piersol, A.G. 1971. *Random data: Analysis and measurement procedures*. Wiley Interscience.

Berg, H., Gößling, G. and Zück, H. 1996. Radsatzwelle und Radscheibe - die richtige Kombination zur Messung der Kräfte zwischen Rad und Schiene. *ZEV + DET Glasers Annalen 120*. Nr 2, February 1996.

Bhatti, M.H. and Garg, V.K. 1984. A review of railway vehicle performance and design criteria. *International Journal of Vehicle Design*. Volume 5, Nos 1/2.

Botwright, K. 1979. Interaction of vehicle and track. *Railway Engineer Journal*. IMechE, January/February 1979.

Chang, C.S., Adegoke, C.W. and Selig, E.T. 1980. GEOTRACK model for railroad track performance. *Journal of the Geotechnical Engineering Division*. Proceedings of the American Society of Civil Engineers. Volume 106, No. GT11, November 1980.

Chrismer, S. and Selig, E.T. 1993. Computer model for ballast maintenance planning. *Proceedings of the 5th International Heavy Haul Conference.* Beijing, China, June 1993.

Clark, R.A.P. 1984. Rail corrugations - recent theories. *Track Technology.* Thomas Teleford Ltd., London.

Cohen, A. and Hutchens, W.A. 1970. Methods for the reconstruction of rail geometry from mid-chord offset data. *ASME, 70-Tran-24.*

Cox, S.J. and Grassie, S.L. 1986. Understanding dynamics as an aid to developing track. *Proceedings of the 3rd International Heavy Haul Conference.* Vancouver, B.C., Canada, October 1986.

Dahlberg, T., Akesson, B. and Westberg, S. 1993. Modelling the dynamic interaction between train and track. *Railway Gazette International.* June 1993.

Dong, R.G., Sankar, S. and Dukkipati, R.V. 1994. A finite element model of railway track and its application to the wheel flat problem. *Proceedings Institution Mechanical Engineers.* Volume 208, IMechE.

Ebersöhn, W., Trevizo, M.C. and Selig, E.T. 1993. Effect of low track modulus on track performance. *Proceedings of the 5th International Heavy Haul Conference.* Beijing, China, June 1993.

Ebersöhn, W. and Selig, E.T. 1994. Track modulus measurement on a heavy haul line. Paper No 940538. *Transportation Research Board.* 73rd Annual Meeting, Washington, D.C., January 1994.

Ebersöhn, W. 1995. *Substructure Influence on Track Maintenance Requirements.* Ph.D. Dissertation, Department of Civil and Environmental Engineering, University of Massachusetts at Amherst.

Eisenmann, J. 1972. Germans gain a better understanding of track structure. *Railway Gazette International.* August 1972.

Eisenmann, J., Leykauf, G. and Mattner, L. 1993. Deflection and settlement behaviour of ballast. *Proceedings of the 5th International Heavy Haul Conference.* Beijing, China, June 1993.

Esveld, C. 1989. *Modern Railway Track.* MRT-Productions, Duisburg.

Fastenrath, F. 1977. *Die Eisenbahnschiene.* Verlag von Wilhelm Ernst & Sohn.

Ford, R. 1995. Differential ballast settlement, and consequent undulations in track, caused by vehicle-track interaction. Interaction of railway vehicles with the track and its substructure. Edited by Knothe, K., Grassie, S.L. and Elkins, J.A.: Swets & Zeitlinger. Supplement to: *Vehicle System Dynamics: International Journal of Vehicle Mechanics and Mobility*, Volume 24.

Frederich, F. and Hecht, M. 1986. Erfassung der Gleislage auf ÖPNV-Strecken. *Fortschritt-Berichte VDI Reihe 12: Verkehrstechnik /Fahrzeugtechnik.* Nr. 64, VDI Verlag, Düsseldorf.

Frederick, C.O. and Round, D.J. 1984. Vertical track loading. *Track Technology.* Thomas Teleford Ltd., London.

Fröhling, R.D. 1994. *Random Data Analysis* (Random Data Analysis Program (RDAP (Version 1.0 (b)))). June 1994.

Fröhling, R.D. 1995. Measurement, interpretation and classification of South African track geometry. Interaction of railway vehicles with the track and its substructure. Edited by Knothe, K., Grassie, S.L. and Elkins, J.A.: Swets & Zeitlinger. Supplement to: *Vehicle System Dynamics: International Journal of Vehicle Mechanics and Mobility*, Volume 24.

Fröhling, R.D., Scheffel, H. and Ebersöhn, W. 1996a. The vertical dynamic response of a rail vehicle caused by track stiffness variations along the track. The dynamics of vehicles on roads and on tracks: Proceedings of the 14th IAVSD Symposium, Ann Arbor, Michigan, USA, August 1995, Edited by Segel L., Swets & Zeitlinger. Supplement to: *Vehicle System Dynamics: International Journal of Vehicle Mechanics and Mobility*, Volume 25.

Fröhling, R.D., Howard, M.A. and Kayser, C.R. 1996b. Experimental and theoretical investigation into load sensitive damping in three-piece freight car bogies. Proceedings of the *Conference on Freight Car Trucks/Bogies* organised by the International Heavy Haul Association, Montreal, Canada, June 1996.

Fryba, L. 1987. Dynamic interaction of vehicles with tracks and roads. *Vehicle System Dynamics: International Journal of Vehicle Mechanics and Mobility*, Volume 16.

Garg, V. K. and Dukkipati, R. V. 1984. *Dynamics of railway vehicle systems.* Acedemic Press.

Girardi, L. and Recchia, P. 1991. Use of a computational model for assessing dynamical behaviour of a railway structure. *Proceedings of the 12th IAVSD Symposium*, Lyon.

Grassie, S.L. 1980. *The corrugation of railway track.* Ph.D. Dissertation, University of Cambridge.

Grassie, S.L., Gregory, R.W., Harrison, D. and Johnson, K.L. 1982. The dynamic response of railway track to high frequency vertical excitation. *Journal Mechanical Engineering Science.* Volume 24, No.2.

Grassie, S.L. and Cox, S.J. 1985. The dynamic response of railway track with unsupported sleepers. *Proceedings Institute Mechanical Engineers.* Volume 199, No D2, IMechE.

Grassie, S.L. 1989. Behaviour in track of concrete sleepers with resilient railpads. *Proceedings Institute Mechanical Engineers.* Volume 203, IMechE.

Grassie, S.L. 1993. Dynamic models of the track and their uses. Kalker J.J. *et al.* (eds.), *Rail Quality and Maintenance for Modern Railway Operation*, Kluwer Academic Publishers.

Guins, S.G. 1980. First order dynamic response of freight car to track irregularities. *Journal of Engineering for Industry.* Transactions of the ASME. Volume 102, August 1980.

Hecht, M. 1988. Gleislageuntersuchung aus fahrzeug- und oberbautechnischer Sicht: Entwicklung eines universellen dynamischen Meßverfahrens. *Fortschritt-Berichte VDI Reihe 12: Verkehrstechnik / Fahrzeugtechnik.* Nr. 104, VDI Verlag Düsseldorf.

Hempelmann, K. 1994. Short pitch corrugations on railway rails - A linear model for prediction. *Fortschritts-Berichte VDI Reihe 12: Verkehrstechnik / Fahrzeugtechnik.* Nr. 231, VDI Verlag, Düsseldorf.

Hetényi, M. 1946. *Beams on elastic foundation.* University of Michigan Press, Ann Arbor.

Hettler, A. 1984. Bleibende Setzung des Schotteroberbaus. *ETR Eisenbahntechnische Rundschau* 33, Volume 11.

Howard, M.A., Fröhling, R.D. and Kayser, C.R. 1997. Validation, simplification and application of a computer model of load sensitive damping in three piece bogies. *Proceedings of the 6th International Heavy Haul Conference*. Cape Town, April 1997.

Hunt, H.E.M. 1996. Track settlement adjacent to bridge abutments. Paper presented at the *Fourth Vehicle/Infrastructure Interaction Conference*. San Diego, California, USA, June 1996.

Ilias,H. and Müller S. 1994. A discrete-continuous track-model for wheelsets rolling over short wavelength sinusoidal rail irregularities. The dynamics of vehicles on roads and on tracks. Edited by Shen Z., Swets & Zeitlinger. *Proceedings of the 13th IAVSD Symposium*. Chengdu, P.R. China, August 1993.

International Standard ISO 2631/1. 1985. *Evaluation of human exposure to whole-body vibration, Part 1: General requirements.*

International Union of Railways, Office for Research and Experiments, Question C 116. 1977. *Interaction between vehicles and track, Report No. 8, Methods for assessing the comfort quality of passenger vehicles.* Utrecht, Holland, April 1977.

International Union of Railways, Office for Research and Experiments, Question D71 1965. *Stresses in the track, ballast and formation as a result of rolling loads, Stresses in rails, Part 2: Calibration and measuring procedures.* Report No. 1, Utrecht, Holland.

International Union of Railways, Office for Research and Experiments, Question D 71 1970. *Stresses in the rails, the ballast and in the formation resulting from traffic loads, Report No. 10, Deformation properties of ballast (Laboratory and track tests).* Volume 1 - Text and Appendices & Volume 2 - Tables and Figures, Utrecht, Holland, April 1970.

International Union of Railways, Office for Research and Experiments, Question D 117 1974. *Optimum adaption of the conventional track to future traffic, Report No. 5, Deformation of railway ballast under repeated loading (Triaxial Tests).* Utrecht, Holand, October 1974.

International Union of Railways, Office for Research and Experiments, Question D 161 1987. *Dynamic vehicle/track interaction phenomena, from the point of view of track maintenance, Report 1: General conditions for the study of the evolution of track geometry based on historical information.* Utrecht, Holland, April 1987.

Jeffs, T. 1994. *The influence of the critical train speed on vertical wheel-rail forces.* Minor Thesis, Department of Mechanical Engineering, Monash University, Australia, February 1994.

Jenkins, H.H., Stephenson, J.E., Clayton, G.A., Morland, G.W. and Lyon, D. 1974. The effect of track and vehicle parameters on wheel/rail vertical dynamic forces. *Railway Engineering Journal.* January 1974.

Kerr, A.D. 1964. Elastic and viscoelastic foundation models. *Journal of Applied Mechanics.* Transactions of the ASME. September 1964.

Knothe, K. and Ripke, B. 1989. The effects of the parameters of wheelset, track and running conditions on the growth rate of rail corrugations. The dynamics of vehicles on roads and on tracks. Edited by Anderson R.J., Swets & Zeitlinger. *Proceedings of the 11th IAVSD Symposium,* Kingston, Ontario.

Knothe, K. and Grassie, S.L. 1993. Modelling of railway track and vehicle/track interaction at high frequencies. *Vehicle System Dynamics: International Journal of Vehicle Mechanics and Mobility,* Volume 22.

Knothe, K., Grassie, S.L. and Elkins, J.A. 1995. Interaction of railway vehicles with the track and its substructure. Swets & Zeitlinger. Supplement to: *Vehicle System Dynamics: International Journal of Vehicle Mechanics and Mobility,* Volume 24.

Koffman, J.L. 1959. The effect of suspension design on rail stresses. *The Railway Gazette.* March 1959.

Kortüm, W. and Sharp, R. 1993. Multibody computer codes in vehicle system dynamics. Swets & Zeitlinger. Supplement to: *Vehicle System Dynamics: International Journal of Vehicle Mechanics and Mobility*, Volume 22.

Lane, G.S. 1982. The effects of track and traffic parameters on the development of track vertical roughness. *Proceedings of the 2nd International Heavy Haul Conference*. Colorado Springs, Colorado, September 1982.

Leshchinsky, D., Choros, J. and Reinschmidt, A.J. 1982. A simplified methodology to evaluate the effect of heavier axle loads on track substructure performance. *Proceedings of the 2nd International Heavy Haul Conference*. Colorado Springs, Colorado, September 1982.

Levy, S. and Wilkinson, J.P.D. 1976. *The component element method in dynamics*. McGraw-Hill.

Li, D. and Selig, E.T. 1995. Wheel/rail dynamic interaction: Track substructure perspective. Interaction of railway vehicles with the track and its substructure. Edited by Knothe, K., Grassie, S.L. and Elkins, J.A.: Swets & Zeitlinger. Supplement to: *Vehicle System Dynamics: International Journal of Vehicle Mechanics and Mobility*, Volume 24.

Lombard, P.C. 1978. Track structure - Optimisation and design. *Proceedings of the Heavy Haul Railways Conference*. Perth, Australia, September 1978.

Luo, R.K., Gabbitas, B.L. and Brickle, B.V. 1994. Fatigue life evaluation of a railway vehicle bogie using an integrated dynamic simulation. *Proceedings of the Institute of Mechanical Engineers*. Volume 208, Part F: Journal of Rail and Rapid Transit, IMechE.

Maree, J.S. 1989. Evaluation of track structure problems on the coal line. *Proceedings of the 4th International Heavy Haul Railway Conference*. Brisbane, September 1989.

Maree, J.S. 1993. Aspects of resilient rail pads. *Proceedings of the 5th International Heavy Haul Conference*. Beijing, China, June 1993.

Mauer, L. 1995. Determination of track irregularities and stiffness parameters with inverse transfer functions of track recording vehicles. Interaction of railway vehicles with the track and its substructure. Edited by Knothe, K., Grassie, S.L. and Elkins, J.A.: Swets & Zeitlinger. Supplement to: *Vehicle System Dynamics: International Journal of Vehicle Mechanics and Mobility*, Volume 24.

Moravčík, M. 1995. Response of railway track on nonlinear discrete supports. Interaction of railway vehicles with the track and its substructure. Edited by Knothe, K., Grassie, S.L. and Elkins, J.A.: Swets & Zeitlinger. Supplement to: *Vehicle System Dynamics: International Journal of Vehicle Mechanics and Mobility*, Volume 24.

Newland, D.E. and Cassidy, K.J. 1975. Some fundamental design considerations for railway vehicles. *REJ*. March 1975.

Nielsen, J.C.O. 1994. Dynamic interaction between wheel and track - A parametric search towards an optimal design of rail structures. *Vehicle System Dynamics: International Journal of Vehicle Mechanics and Mobility*, Volume 23.

Ostermeyer, M., Berg, H. and Zück, H.H. 1980. Der heutige Entwicklungsstand der Meßmethode "Radsatzwellenverfahren" zur Bestimmung der Kräfte zwischen Rad und Schiene. *Glasers Annalen*.

Parsons, K. C. and Whitham, E. M. 1979. Six axis vehicle vibration and its effects on comfort. *Ergonomics*. Volume 22, No. 2.

Permanent Way Instructions. 1984. South African Transport Services.

Radford, R.W. 1977. Wheel/Rail vertical forces in high speed railway operation. *Journal of Engineering for Industry*. Transactions of the ASME. November 1977.

Riessberger, K. and Wenty, R. 1993. Track quality - Key to load bearing capacity and efficient maintenance. *Proceedings of the 5th International Heavy Haul Conference*. Beijing, China, June 1993.

Sato, Y. 1995. Japanese studies on deterioration of ballasted track. Interaction of railway vehicles with the track and its substructure. Edited by Knothe, K., Grassie, S.L. and Elkins, J.A.: Swets & Zeitlinger. Supplement to: *Vehicle System Dynamics: International Journal of Vehicle Mechanics and Mobility*, Volume 24.

Schielen, W. 1990. *Multibody Systems Handbook*. Springer-Verlag.

Schwab, C. A. and Mauer, L. 1989. An interactive track/train dynamics model for investigating system limits in high speed track. The dynamics of vehicles on roads and on tracks. Edited by Anderson R.J., Swets & Zeitlinger. *Proceedings of the 11th IAVSD Symposium*, Kingston, Ontario.

Selig, E.T. and Alva-Hurtado, J.E. 1982. Predicting effects of repeated wheel loading on track settlement. *Proceedings of the 2nd International Heavy Haul Conference*. Colorado Springs, Colorado, September 1982.

Selig, E.T. and Waters, J.M. 1994. *Track geotechnology and substructure management*. Thomas Telford.

Shenton, M.J. 1985. Ballast deformation and track deterioration. *Track Technology*. Thomas Teleford Ltd., London.

Stewart, H.E. and Selig, E.T. 1982. Prediction of track settlement under traffic loading. *Proceedings of the 2nd International Heavy Haul Conference*. Colorado Springs, Colorado, September 1982.

Talbot, A.N. 1980. *Stresses in railroad track - The Talbot reports*. The reports presented for the AREA bulletins of the Special Committee on Stress in Railroad Track, 1918 to 1940, American Railway Engineering Association.

Timoshenko, S. 1926. Methods of analysis of statical and dynamical stresses in rail. Proceedings of the *Second International Congress for Applied Mechanics*. Zürich.

Uetake, Y. 1980. Standards of riding quality in foreign railways. *Permanent Way*. Volume 22, No. 1, March 1980.

Urban, C.L. 1991a. *Suspension wear and truck performance: A case study*. AAR Report R-785, August 1991.

Urban, C.L. 1991b. *125-ton freight car vertical performance: A case study*. AAR Report R-792, October 1991.

Wangqing, W., Geming, Z., Kaiming, Z. and Lin, L. 1997. Development of inspection car for measuring railway track elasticity. *Proceedings of the 6th International Heavy Haul Conference*. Cape Town, April 1997.

Winkler, E. 1867. *Die Lehre von der Elastizität und Festigkeit*. Prag: Verlag H. Dominicus.

Winkler, E. 1875. *Der Eisenbahnoberbau* (3rd edition), Prag: Verlag H. Dominikus.

Yabuto, K., Hidaka, K. and Fukushima, N. 1981. Influence of suspension friction on riding comfort. The dynamics of vehicles on roads and on tracks. Edited by Shen Z., Swets & Zeitlinger. *Proceedings of the 7th IAVSD-Symposium*. Cambridge University, Cambridge, UK.

Yamazaki, M. and Hara, S. 1980. JNR's standards for riding comfort. *Permanent Way*. Volume 22, No. 1, March 1980.

Zeilhofer, M., Sühsmuth, G. and Piwenitzky, G. 1972. Ermittelung der Kräfte zwischen Rad und Schiene aus den Biegedehnungen der Radsatzwelle. *Glasers Annalen, ZEV*, Jahrgang 96, Heft 12.

Zhai, W. and Sun, X. 1993. A detailed model for investigating vertical interaction between railway vehicle and track. The dynamics of vehicles on roads and on tracks. Edited by Shen Z., Swets & Zeitlinger. *Proceedings of the 13th IAVSD Symposium*. Chengdu, P.R. China, August 1993.